MAX PLANCK INSTITUTE FOR HUMAN COGNITIVE AND BRAIN SCIENCES LEIPZIG

Jens Brauer: Functional Development and Structural Maturation in the Brain's Neural Network Underlying Language Comprehension. Leipzig: Max Planck Institute for Human Cognitive and Brain Sciences, 2009 (MPI Series in Human Cognitive and Brain Sciences; 105)

Functional development and structural maturation in the brain's neural network underlying language comprehension

Functional development and structural maturation in the brain's neural network underlying language comprehension

Von der Fakultät für Biowissenschaften, Pharmazie und Psychologie

der Universität Leipzig

genehmigte

DISSERTATION

zur Erlangung des akademischen Grades

doctor rerum naturalium

Dr. rer. nat.

vorgelegt von

Jens Brauer, Dipl.-Psych.

geboren am 20. März 1973 in Jena

Dekan:	Professor Dr. Matthias Müller
Gutachter:	Professor Dr. Angela D. Friederici
	Professor Dr. Erich Schröger
	Professor Tomáš Paus M.D., Ph.D.

Tag der Verteidigung: 30. 10. 2008

Acknowledgements

I want to thank all the people who helped to accomplish the present work. I am predominantly grateful to Professor Angela Friederici for providing me with the opportunity to conduct this work and for her continuous support during discussions and beyond.

It's impossible to list all friends and colleagues for encouragement and support to improve the present work. They are warmly appreciated for their considerable contributions, substantially and personally.

Last not least, I am particularly thankful to Professor Friederici, Professor Schröger, and Professor Paus for reviewing this thesis.

Contents

1 Introduction

The functional organization of the human brain has been a research question for hundreds of years. Especially the faculty of language became a main focus in this domain. This was, first, because the elaborated human faculty of language is probably the most distinguished feature that discriminates human beings from any other beings we know. Second, among the early most influencing works in the field of functional neuroanatomy were those of Paul Broca (1863) and Carl Wernicke (1874) concerning the human brain areas responsible for language processing. The Broca-Wernicke model of language organization in the human brain has been persistently influential in cognitive neuroscience since the 19th century. Even nowadays, it serves as a useful heuristic to characterize language processing, but also lesions and syndromes in the clinical context. Nevertheless, modern accounts for the functional neuroanatomy of language are far more detailed and precise in their elaboration of the variety of linguistic domains, such as phonology, syntax, semantics, and speech prosody (Grodzinsky, 2000). Recent advances in neurocognitive methods like functional and anatomical brain imaging allowed formulating increasingly comprehensive models of language processing (e.g., Friederici, 2002; Hickok and Poeppel, 2007).

Here, the term of language processing is meant to refer to any process that involves the cognitive perception, recognition, or production of human language. Language comprehension can rely on auditory (speech) or visual (reading) input. Auditory language comprehension goes beyond mere speech perception which in turn can take place at even the syllable or phonetic (i.e., sublexical) level. Rather, auditory language comprehension involves recognition of sounds that allow a mapping of sound to meaning.

Information about the functional brain organization can help to achieve deeper knowledge about the subprocesses involved in language processing. A thorough understanding, however, of how language in organized in the human brain needs a deeper insight not only in its functional organization. Moreover, the link between the structural prerequisites of the brain and the functional network of the variety of subprocesses that we in sum describe as language comprehension delivers a broader basis for a profound under-

standing of the nature of the unique human faculty of language. Hence, a combined view on structure and function might help to provide more comprehensive information. In the field of human development, answers to the question about concurrent structural maturation may possibly be especially useful in order to gain deeper insight into the unfolding of particular cognitive functions such as the ability to handle a complex information processing task like language comprehension.

The present work is supposed to provide an insight in the development of the organization of language in the human brain. An investigation in functional neural networks of language comprehension in children compared to adults will discuss how the implementation of language is achieved during development. Furthermore, a study in more basic neurophysiologic underpinnings of the brain regions that participate in the language comprehension network will expand the view towards more basic properties of the development of language processing. Finally, information on the neural fiber tracts in the white matter of the brain that connect the cortical regions where the actual processing of language takes place, will help to understand how the maturation of the brain network for language assembles with the development of the faculty of language.

1.1 The adult network of language comprehension

Functional brain imaging has facilitated the study of on-line language processing in vivo in the brain, and an increasing body of empirical data has been collected. The investigation of language comprehension on the sentential level allows to extract information on lexical-semantic processing, i.e., the content that a sentence conveys, but also information on the processing of sentence structure, i.e., its syntax.

There are generally two main approaches towards the examination of syntactic processing in sentences. Thereby, the experimental manipulation of sentence materials presented to listeners or readers employs for instance a variation of syntactic complexity. This might be achieved by the variation of argument hierarchies with e.g., object-initial sentences such as in the following example.

1 “Der Junge schenkt der Mutter die Blumen”

The boy$_{NOM}$ presents to the mother$_{DAT}$ the flowers$_{ACC}$,

2 “Die Blumen schenkt der Mutter der Junge”

The flowers$_{ACC}$ presents to the mother$_{DAT}$ the boy$_{NOM}$

where NOM denotes nominative, DAT denotes dative, and ACC denotes accusative case. Here, (1) is an example of a canonical sentence with subject-initial word order, while (2) exemplifies an object-initial sentence. Such object-initial structures are syntactically more complex, but still correct sentences in many free word-order languages like for instance German. Many studies have successfully applied the variation of syntactic complexity to identify syntax-relevant cortical language areas in the brain (Bornkessel, Zysset, Friederici, von Cramon, & Schlesewsky, 2005; Friederici, Fiebach, Schlesewsky, Bornkessel, & von Cramon, 2006). Other kind of complexity manipulations used e.g., subject relative clauses vs. object relative clauses where object relative clauses are described to be syntactically more complex (Caplan et al., 2008; Just et al., 1996).

On the other hand, violation paradigms have been implemented in which the brain response to the violation of any syntactic rule within a sentence was observed. Several studies have made use of syntactic and/or semantic violation paradigms in order to identify the essential neural substrates for syntactic and semantic processes in the brain. As in syntactic complexity paradigms, also in violation paradigms specific syntactic information can be manipulated experimentally (Friederici & Alter, 2004). The core idea behind syntactic violation and complexity paradigms is a need for augmented processing demands within those brain structures that are responsible for syntactic processing as soon as the system encounters a violation of a syntactic rule or as syntactic complexity is increased.

However, there has also been a discussion about differences in the processing between syntactic violation and complexity. Some forms of complexity variation were argued to manipulate short term memory demands as well, especially when the syntactic function of a word is not yet clear at the position where the word is encountered, but only in a later position in the sentence. Hence, there is a gap between the two positions. Such filler-gap dependencies might require a stronger role of short term memory with increasing distances being reflected in higher transformation

costs (Gibson, 1998). The investigation of these transformation operations in syntactic complexity was helpful to specify the role of Broca's area in syntactic processing and syntactic working memory (Ben-Shachar, Hendler, Kahn, Ben-Bashat, & Grodzinsky, 2003; Fiebach, Schlesewsky, & Friederici, 2001).

Syntactic manipulations in violation paradigms made, for instance, use of word order violations in sentences, such as *'*Mary asked question a about theorem the in class*'[1] (Embick, Marantz, Miyashita, O'Neil, & Sakai, 2000), or tense violations as *'*Trees can grew*' (Ni, et al., 2000), or made use of pseudowords in sentences without semantic-lexical content (Moro, et al., 2001). Other syntactic violation paradigms implemented phrase structure violations by omitting words. One such paradigm applied sentences with a missing noun after a preposition as in the following example.

- "Das Baby wurde gefüttert"

  The baby was fed

- *"Die Gans wurde im gefüttert"

  **The goose was in-the fed*

- "Die Kuh wurde im Stall gefüttert"

  The cow was fed in the barn

where (1) represents a correct sentence, (2) represents a syntactically violated sentence with an incorrect phrase structure since the preposition is followed by a verb, and (3) represents a correct sentence with an intact prepositional phrase. With this kind of sentence, it is also easily possible to manipulate lexical semantics of the sentence as the following example illustrates:

- "Das Lineal wurde gefüttert"

  The rule was fed

where (4) represents a semantically incongruous sentence with a violation of the verb's selectional restriction. This paradigm of syntactic and semantic violations has been successfully applied in a number of electrophysiological and functional imaging studies (e.g., Friederici et al., 2003; Hahne

[1] The asterisk * denotes ungrammaticality of the subsequent sentence.

et al., 2004; Hahne and Friederici, 2002; Sabisch et al., 2006). Also for such lexical-semantic violations, increased processing demands are expected in those brain regions being responsible for semantic processing.

As for the investigation of syntax, empirical work in the processing of semantic information has been conducted at several processing levels, from the sentential level (as the studies cited above) or text discourse level (Ferstl, Rinck, & von Cramon, 2005) down to the word level (Noppeney & Price, 2004; Raettig & Kotz, 2008). There seems to be a differentiation in the brain between long-term storage of semantic information in posterior temporal, inferior parietal, and hippocampal regions and its more strategic and goal-directed retrieval in prefrontal regions (Binder and Price, 2001; Bookheimer, 2002).

Semantic processing in adults has been investigated also at the sentential level, repeatedly by violation paradigms that presented semantically incongruous and semantically correct sentences (Friederici et al., 2003; Kuperberg et al., 2008; Newman et al., 2001). In comparison to semantic incongruence at the word level, semantic violations at the sentence level are generally reported to activate more extended semantic networks (Kiehl, Laurens, & Liddle, 2002; A. J. Newman, Pancheva, Ozawa, Neville, & Ullman, 2001).

The neural networks subserving adult language comprehension have been described quite well over the past years. Different parts of the inferior frontal cortex as well as the temporal and parietal cortex of the left and right hemispheres are known to be responsible for particular subprocesses during auditory language comprehension (for reviews see Bookheimer, 2002; Friederici, 2002; Friederici and Alter, 2004; Hagoort, 2005; Hickok and Poeppel, 2007).

In summary, experimental data suggest an entire network of brain areas to participate in language comprehension in the adult brain. Syntactic processes are subserved by the left superior temporal gyrus (STG) and the inferior frontal gyrus (IFG), in particular by Brodmann Area (BA) 44 and the frontal operculum (FO) (Bornkessel et al., 2005; Friederici et al., 2000; Friederici et al., 2003; Just et al., 1996; Moro et al., 2001; Stromswold et al., 1996). Semantic processes, in contrast, are supported by the left middle temporal gyrus (MTG), the supramarginal gyrus (SMG), and BA 45 and 47 in the IFG (Fiez, 1997; Kotz et al., 2002; Poldrack et al., 1999;

Thompson-Schill et al., 1997). The particular function of left inferior frontal region in semantic and syntactic networks appears to be correlated with increased processing demands. For semantic processes, BA 45/47 seems to come into play whenever strategic processes are required (e.g., semantic categorization) (Fiez, 1997; Thompson-Schill, D'Esposito, Aguirre, & Farah, 1997). For syntactic processes, BA 44 is recruited when syntactic processing demands increase, i.e. when processing non-canonical sentences (for a review see Grodzinsky & Friederici, 2006), but not during local phrase structure processing (Friederici, Bahlmann, Heim, Schubotz, & Anwander, 2006).

For auditory language comprehension in adults, specialized left and right hemispheric involvement has been reported, with the left hemispheric (LH) perisylvian cortex supporting the processing of semantic and syntactic information (Friederici, 2002), while the perisylvian cortex of the right hemisphere (RH), in particular the posterior STG and the FO, has been shown to be responsible for the processing prosodic information (e.g. Meyer, Alter, Friederici, Lohmann, & von Cramon, 2002; Meyer, Steinhauer, Alter, Friederici, & von Cramon, 2004; Zatorre, Belin, & Penhune, 2002). The right hemispheric lateralization of prosodic interpretation, however, appears to be dependent not only on input parameters, but, moreover, on task demands (e.g. Plante, Creusere, & Sabin, 2002). Combined experimental data suggest a model for adult language comprehension that assumes segmental information (semantic and syntactic information) to be processed predominantly in the left hemisphere (LH) and suprasegmental information (prosody) to be processed primarily in RH (Friederici & Alter, 2004).

In conclusion, results from a broad range of empirical data support the view that a temporo-frontal network of brain areas in the perisylvian cortex subserves the processing of sentence comprehension, including the different aspects of language domains. Specific regions can be identified that hold responsible for specific processes during language comprehension. However, the data do also show that language processing generally involves an entire network of brain areas, and only selected contrasts in experimental designs isolate the brain basis for a particular processing.

1.2 The developing network of language comprehension

The brain basis of language in the developing brain and specific processing of certain aspects of language such as syntax and semantics still remain an open issue. So far, we know little about the neural network of language comprehension during childhood. In the domain of language production, a number of fMRI studies using verbal fluency tasks have reported activation in the left inferior frontal gyrus, dorslateral prefrontal and midfrontal gyri as well as activation in the temporal regions (for a review see Sachs & Gaillard, 2003). Imaging studies investigating language comprehension in children have focused primarily on the issue of functional language lateralization. Functional lateralization has been claimed to be evident as early as 3 months of age (Dehaene-Lambertz, Dehaene, & Hertz-Pannier, 2002). This claim, however, was based on the finding that the summed activation of forward and backward speech compared to baseline revealed a left hemispheric dominance, and not on a direct comparison between forward and backward speech which would have allowed more specific claims. Forward and backward speech both contain segmental information, i.e., information about phonemes as the sounds of language. Thus, the reported finding could be interpreted to show that nascent lateralization for speech sounds is evident early during life. A near-infrared spectroscopy study in 3-month-olds supports this view by indicating that prosodic information is mainly processed by the RH (Homae, Watanabe, Nakano, Asakawa, & Taga, 2006). In this study, normal speech was compared to speech lacking any prosodic information, thus allowing a specific claim about the involvement of the RH with respect to prosodic processes in infants. An ERP study indicates that specific prosodic cues in the speech input that signal the onset and offset of syntactic phrases are processed by 9 months, i.e., long before syntactic knowledge is present in the infant (Pannekamp, Weber, & Friederici, 2006). These results are in line with theories of language acquisition which assume that early language processing during development strongly relies on prosodic information to uncover syntactic structures (Weissenborn & Höhle, 2001). That is, once children have learned to use those prosodic cues which mark phrase boundaries (Snow & Balog, 2002), their identification of syntactic phrase boundaries and thereby of syntactic constituents is eased, as each prosodic phrase boundary is a syntactic

phrase boundary. This in turn allows to uncover the grammatical structure of a given language (Jusczyk, 2002).

Those fMRI studies in older children which compared spoken language input (texts and sentences) to resting baseline, reported bilateral activation in the STG and Heschl's gyrus as well as in frontal and parietal regions either with no hemispheric dominance (Ulualp, Biswal, Yetkin, & Kidder, 1998) or some dominance of the left hemisphere (Balsamo, et al., 2002). A more left-lateralized pattern was found for verb generation and story comprehension (Wilke, et al., 2005) and when speech was compared to reversed-speech (Ahmad, Balsamo, Sachs, Xu, & Gaillard, 2003). It appears that there is larger involvement of the RH in children compared to adults, but further studies will have to specify the exact developmental pattern with respect to LH and RH functions during language comprehension.

Another open question with respect to the neural basis of language development concerns whether and at what age children demonstrate specific networks for semantic and syntactic processes within the LH. The present work presents a study (Study 1) which is the first fMRI experiment with children investigating syntactic and semantic aspects of language processing at the sentential level. There have been, however, a few fMRI studies with children investigating semantic processes at the word level. Using a semantic judgment task requiring the evaluation of the semantic relatedness of two auditory words, a study with 9 to 15-year-old children revealed activation in the temporal gyri bilaterally (BA 22), in the left middle temporal gyrus (BA 21) and in the inferior frontal gyri bilaterally (BA 47/45) (Chou, et al., 2006). Correlations with age were observed for the left middle temporal (BA 21) and the right inferior frontal gyrus (BA 47). The increased frontal activation in this study was interpreted to reflect a broader semantic search, and the temporal activation was interpreted to be related to more efficient access to lexical-semantic representations. Using a semantic categorization task, an fMRI study with 5 to 10-year-old children found activation in similar inferior frontal and temporal regions of the left hemisphere and in the left fusiform gyrus (BA 37, BA 20), suggesting language to be left-lateralized by at least 5 years (Balsamo, Xu, & Gaillard, 2006).

1.3 The timing of language comprehension

The main body of brain imaging research has been utilized fMRI generally to identify specific functional areas in the brain. That also applies for brain imaging studies that investigate the processing of human language areas. Thereby we have progressively learned about the involvement of the perisylvian region of the human cortex in language processing and respective contributions of frontal, temporal, and parietal brain areas in different linguistic aspects such as syntax, semantics, and phonology (see the previous sections).

The focus of brain imaging studies is generally the spatial pattern of cortical and subcortical activation in the context of a specific perception or behavior. But the brain response also follows a specific time course. This time course of brain activation has been usually examined by means of event-related brain potentials (ERPs) or event-related fields (ERFs). While temporal information in ERP and ERF data is of high precision, spatial information is unfortunately rather imprecise. Conversely, very high spatial resolution about brain areas involved in cognitive processing can be gained from fMRI. As the underlying physiology also contains information about temporal dynamics of brain activation (Friston, Frith, Turner, & Frackowiak, 1995), the temporal dynamics of functionally identified brain areas can also be obtained from fMRI data in addition to the spatial information.

Several methods have been developed to extract and investigate temporal information from hemodynamic brain responses. For example, spectral analysis using measures of coherence and phase of the blood oxygenation level-dependent (BOLD) signal have been administered to human brain data (Dehaene-Lambertz et al., 2006a; Müller et al., 2003; Sun et al., 2005). With these approaches, sequences of fMRI brain activation were separated at temporal resolutions down to about 100 milliseconds (Sigman, Jobert, LeBihan, & Dehaene, 2007). Also time-to-peak and other parameters have been extracted from the BOLD time course to describe its temporal behaviour (Bellgowan et al., 2003; Neumann et al., 2003; Thierry et al., 1999). Both measures of hemodynamic latency, i.e., spectral phase shift and time-to-peak of the BOLD time course, were confirmed to highly correlate with each other, in particular for short stimulation times up to several seconds (Müller, Neumann, Lohmann, Mildner, & von Cramon,

2005). Other approaches have employed independent component analysis (Duann et al., 2002) or nonlinear regression analysis (Kruggel & von Cramon, 2001) to model the BOLD response under specific assumptions.

It was shown that the time course of the BOLD response varies between different brain areas (Anemueller et al., 2006; Duann et al., 2002; Thierry et al., 1999). Moreover, the latency of the BOLD response can even be selectively affected in specific brain regions by cognitive demands such as verbal working memory load (Thierry, Ibarrola, Demonet, & Cardebat, 2003), by stimulus repetition (Dehaene-Lambertz et al., 2006a), or lexical decision (Henson et al., 2002). While temporal activation (Wernicke's area) appears earlier than inferior frontal activation (Broca's area) in language comprehension, language production, in contrast, is characterized by an opposite pattern of peak activation with temporal primacy for Broca's over Wernicke's area (Heim & Friederici, 2003).

For written language comprehension, subregions within the IFG could be functionally differentiated on the basis of their temporal signature (Haller, Klarhoefer, Schwarzbach, Radue, & Indefrey, 2007). For auditory language comprehension, fastest hemodynamic responses were found in primary auditory cortices bilaterally and later responses in inferior frontal cortex, particularly in the left hemisphere (Dehaene-Lambertz et al., 2006a). Data of BOLD response delays between temporal and frontal areas were also reported for 3-month-old infants (Dehaene-Lambertz et al., 2006b). These results were interpreted to reflect an adults-like timing structure showing a complex, hierarchical organization of language-relevant brain areas, although the comparison was only qualitative in nature.

Apparently, temporal properties of the hemodynamic brain response deliver additive information on functional processing. The more profound analysis of temporal parameters of the BOLD response seems to be promising for an advanced understanding of language development in the human brain. In the present work, Study 2 will present a deeper analysis of children's brain responses during auditory language comprehension. An evaluation of their functional activation time course in direct comparison to the adult time course pattern shall provide a developmental perspective on temporal hemodynamics. In order to gain a more fine-grained insight into the temporal dynamics' development of language-related brain recruitment in the

perisylvian cortex, time-to-peak information extracted from the hemodynamic response function was contrasted.

1.4 The structural basis of the language network in the human brain

A comprehensive investigation of the human brain is incomplete when being restricted to its functional processing and psychophysiology alone. Moreover, the structural underpinnings that physically enable these processes should be considered as well. Anatomical MRI data can be investigated by several morphometric approaches. Morphometry refers to the description of brain structure and can be applied in vivo to quantify and characterize MRI data according to several research questions (Tittgemeyer & von Cramon, 2004). Brain morphometry methods allow to examine structural aspects that help to better understand how the variety of functional processes executed in the brain are compiled and organized. The human gray matter, i.e., the neurons in the cortical layers of the brain where the actual processing of functions takes place, can be investigated with respect to its thickness, density, size, gyrification, and structural adaptation. Likewise, the underlying white matter provides information on the connection between these cortical regions. Early approaches to better understand the human brain utilized post-mortem methods to investigate white and gray matter anatomy. Nowadays, the exact location and extent of individual fiber tracts within the human white matter can be identified in vivo by means of diffusion tensor imaging (DTI) and by fiber tracking. These methods have revolutionalized research in human white matter mapping during the last decade (Assaf & Pasternak, 2008). They will be introduced comprehensively in chapter 2. So far, it might be sufficient to mention that DTI offers measures on the directionality of water diffusion e.g., fractional anisotropy (FA), which in turn allow inferring information about fiber pathways. The relationship between structural brain variation in gray matter and/or white matter has been reported for various psychometric measures of performance or behavior, such as intelligence (Haier, Jung, Yeo, Head, & Alkire, 2004), response times (Madden, et al., 2004), or memory (Persson, et al., 2006).

Haier and colleagues (2004) investigated regional gray and white matter volumes by means of voxel-based morphometry and assessed their association with measures of general intelligence. There results suggested that more gray matter was associated with higher intelligence in a variety of cortical areas in frontal, temporal, parietal, and occipital lobes. Likewise, a study on visual processing revealed lower levels of integrity in white matter of corpus callosum (CC) and internal capsule, as indicated by smaller fractional anisotropy values, being associated with longer response times (Madden, et al., 2004). Hippocampus volume and FA values in anterior CC were positively correlated to episodic memory performance in elder adults (Persson, et al., 2006). These data indicate the impact of cortical and subcortical area volumes and white matter integrity on psychometric performance.

1.5 Structural maturation of the language network

Concerning human development, change and adaptation are permanently ongoing processes that alter brain morphometry during the brain's entire dynamic life course. However, early brain maturation during fetal development and childhood are most remarkable and significant (Dubois, et al., 2008; Provenzale, Liang, DeLong, & White, 2007). At the same time, human development during infancy, childhood, and adolescence provides some major changes in motor, sensory, executive, and cognitive functions, among them increasing skills in language comprehension and production. These developmental changes of brain functions on the one hand and maturation of the brain's physical underpinnings, specifically its gray and white matter structures, on the other hand, are simultaneous processes accompanying each other.

Maturation of the human brain is a complex process characterized by some distinguished changes over time, including progressive and regressive adjustments. These processes of change can be described for cortical as well as subcortical brain structures (Toga, Thompson, & Sowell, 2006), and multiple imaging techniques have been administered for noninvasive evaluations of brain maturation. Gray matter maturation shows on average significant overall reduction of cortical thickness during childhood, espe-

cially in frontal and parieto-occipital regions (Sowell, et al., 2003). Likewise, changes in gray matter density have been described following a similar pattern (Giedd, et al., 1999). Moreover, the cortical changes were suggested to be nonlinear in nature with an initial increase and later decrease during childhood and adolescence (Sowell, et al., 2004), while the exact age of the gray matter volume peak is still controversial. The time course of gray matter maturation, however, has been confirmed to be heterogeneous across brain lobes and regions. Conversely to the gray matter loss in frontal and parieto-occipital regions, there are other regions that show ongoing slight gray matter thickening during childhood (age 5 to 11), such as the perisylvian region (Whitford, et al., 2007). Though, in these regions the gray matter loss might only be shifted in time, an interpretation that seems to be supported by longitudinal surveys investigating cortical development until early adulthood (de Graaf-Peters & Hadders-Algra, 2006). In their study, differentiated time courses of cortical development were revealed for earlier maturing somatosensory and visual cortices and later maturing higher-order association cortices. Furthermore, these results suggested phylogenetically older brain areas to mature earlier than phylogenetically newer areas.

The overall loss of gray matter during childhood and adolescence occurs probably due to programmed pruning out of synapses and their associated neuropil, i.e., axon terminals, dendrites, and dentritic spines, rather than due to neuron loss (Staudt, Krageloh-Mann, & Grodd, 2000), while programmed cell death seems to be more a matter of very early maturation during fetal gestation (Pujol, et al., 2006).

The white matter undergoes major changes during infancy and early childhood, indicated by diffusion data with an increase in fractional anisotropy by about 200 percent and a decrease in mean diffusivity by about 40 percent until about 5 years of age (Dubois et al., 2006; Hermoye et al., 2006; Mukherjee et al., 2001). Albeit less pronounced, these maturation processes continue and last until adulthood where they reach a plateaus level (Barnea-Goraly et al., 2005; Ben Bashat et al., 2005; Lebel et al., 2008). Structural maturation of fiber pathways in the brain is particularly characterized by increasing myelination of the fibers. Myelination refers to formation and progression of myelin sheaths which originate from extended plasma membranes of oligodendrocytes wrapping around portions of an

axon. Thereby, the speed of electric impulses along the axon are increased and hence information transport in neuronal networks as well. Concerning development, the process of initial myelination is most pronounced until the second year of life, roughly preceding from occipital to frontal regions in inferior-to-superior and posterior-to-anterior directions, but further condensation and agglomeration occurs during the entire childhood (Boujraf et al., 2002; Lenroot and Giedd, 2006). During early childhood, the volume increase in myelinated white matter shows a very similar time course in frontal and temporal (i.e., language-related) regions which is, moreover, later in time than the volume increase in the (sensorimotor) central region (Pujol, et al., 2006).

White matter maturation can be explicitly assessed by means of diffusion tensor imaging. Diffusion measures of tensor anisotropy ratio and tensor volume ratio in fiber tracts indicate white matter maturation on the basis of diffusion anisotropy (Zhang, et al., 2007). Consistent with three-dimensional MRI data (Barnea-Goraly, et al., 2005), a DTI investigation of the superior longitudinal fasciculus (SLF, connecting temporal and inferior frontal language-related brain regions) showed that the SLF is among the very late fiber tracts to mature (Giorgio, et al., 2008). Changes in fractional anisotropy and white matter density reflect maturation of fiber pathways even until late adolescence (Herschkowitz, 2000; Nagy et al., 2004; Niogi and McCandliss, 2006; Sowell et al., 2001). Intriguingly, the increase in white matter FA during adolescence was shown to be correlated to the age-related decrease in directly connected gray matter regions (Hallett & Proctor, 1996).

Associations between the level of functioning or behavioral records on the one hand and physical dimensions of the brain on the other have been reported in children and adolescents for several cognitive domains such as intelligence, working memory, reading, and word production (Beaulieu et al., 2005; Deutsch et al., 2005; Nagy et al., 2004; Niogi and McCandliss, 2006; Olesen et al., 2003; Pujol et al., 2006; Qiu et al., 2008).

A thorough assessment of the maturation of white matter fiber tracts that constitute the networking basis of language comprehension would assist in acquiring a comprehensive understanding of functional processing within that system. Study 3 of the present work will provide data to address these issues.

1.6 Hypotheses and perspectives

The present research on language development is supposed to present a combined view on the functional and structural neuroanatomical underpinnings of language comprehension in the human brain. The research presented in the following chapters shall provide a neuroscientific view on the brain basis of language development with a focus on sentence comprehension. In that context, the research will first focus on developmental aspects of syntax and semantics in auditory language comprehension. Furthermore, a deeper investigation in the brain's hemodynamic BOLD response in the context of language comprehension will enlighten developmental issues on the human brain's neurophysiology underlying brain imaging in the domain of developmental neuroscience. Finally, besides the method of functional brain imaging for answering questions on language development, an investigation in the underlying white matter anatomy of the developing brain will help to better understand how the faculty of language is incorporated in the architecture of the human brain and how it evolves. A comparison of white matter pathways between adults and children will evaluate structural parameters in language-related perisylvian fasciculi on the basis of functional activation in perisylvian cortical areas during language processing.

Based on the current knowledge in the field of developmental neurosciences in general and language development in particular, the developing language comprehension network of children is expected to differ from the mature network of adults in several respects. Children can be assumed to require more resources for the processing of different aspects of language such as syntax or semantics. Especially brain areas that are known to be recruited in adults during more complex processing demands such as Broca's area might be stronger involved in children. The faculty of language develops very fast in humans during ontogenesis. Nevertheless, it takes years until it progresses to a mature state. The underlying neurophysiology of the perisylvian language areas can be expected to coincide with this development and possibly even to serve as an essential precondition to evolve language to its full-fledged quality. Therefore, the case of BOLD latencies is selected to investigate the neurophysiology underlying language comprehension in the developing human brain. Differences in the neurophysiology such as hemodynamic parameters like BOLD latencies might

reflect not only a general immature state of the developing language system, but even a distinction in the processing characteristics of language. Temporal hemodynamics are expected to differentiate the developing language processing system from the mature system, first, in a general sense, but, moreover, also in a more sophisticated sense such that differences in BOLD latencies might shed light on specific processing demands that distinguish the immature from the mature language system. Finally, on an even more basic level, brain maturation is assumed to coincide with functional processing capacities such as language comprehension. The still developing brain of children is expected to provide immature means for language processing which in turn might require alternative or supplementary processing strategies within the not fully developed network of the language system in the human brain.

A deeper understanding of how maturation and development enable higher-order cognitive processes such as language comprehension might open new insight in the nature of the unique organ called brain. Newly developed methods in neurosciences, especially in the field of brain imaging to investigate structure and function and their interface in the human brain will open new fields in cognitive neuroscience and answer future question that will help to expand our current understanding of the intersection between maturation of structure and development of functions.

Taken together, the research questions of the present investigations can be summarized as follows:

1. Are there differences in the processing of syntactic and semantic aspects of auditory sentence comprehension in the developing brain compared to the mature brain which support the assumption of augmented processing demands in the developing language system?

2. Can neurophysiologic parameters of the hemodynamic BOLD response such as the BOLD time course provide a perspective on the development of language processing in the brain? If so, is this informative for the immature brain in general only or can it provide a profounder insight into particular processing needs with respect to language comprehension?

3. What is the role of anatomical underpinnings such as the white matter anatomy of the brain in the context of language processing in

the brain's perisylvian language areas? Do anatomical means of the immature brain coincide with functional processing characteristics of the developing language system?

2 Methods

The aim of this chapter is to describe the backgrounds of experimental methods utilized in the following experiments. A concise primer on behavioral measurements will be followed by the introduction of nuclear magnetic resonance imaging and some of its manifold applications in cognitive neuroscience, particularly functional magnetic resonance imaging (fMRI) and diffusion tensor imaging (DTI).

2.1 Behavioral measurements

Behavioral data in neuropsychology subsume any performance measurements associated with brain-behavior interactions. This includes the results of all tasks that can be related to functional measurements of the brain. Such tasks might be judgment tasks about a certain stimulus. In language research, judgment tasks are commonly acceptability judgments, i.e., whether a word or sentence is adequate with respect to e.g., syntactic, semantic, or some other properties. Typically, a measure of percent correctly judged items will be computed to evaluate responses. Moreover, the data can be used to assess and categorize associated functional brain data. The task might simply involve some behavior that is simultaneously or subsequently categorized e.g., correct/error. If the judgment is given via button press or comparably, reaction times can be obtained as well. Judgments as much as reaction times can be employed as measures during an experiment and assist to construe functional brain data.

In developmental neuroscience, some tasks are not possible to be realized, especially if they require more than an age-appropriate amount of cognitive requirement or effort. Still, tasks can often be adapted to the special needs of children. Children do not only need an easy-to-perform task, moreover, the task should include at least a basic level of enjoyment to execute it. One such adaptation is the acting-out paradigm. In this paradigm, the child is typically involved in some kind of object manipulation task designed as whether a game to play. Some critical behavior is supposed to indicate the child's internal representation or decision about the issue

under investigation and is registered. One such adaptation of a task to the special needs of children will be described in more detail in Study 1.

2.2 Nuclear magnetic resonance imaging

In the following, the core principles of the physics of nuclear magnetic resonance (NMR) are introduced and an overview of the methods of MRI is given. The biochemical and physiological principles underlying functional MRI are outlined and the way it can be utilized for investigations in cognitive neurosciences. Furthermore, the technique of diffusion-weighted imaging (DWI) and its value in anatomical investigations is introduced.

2.2.1 Nuclear magnetic resonance

The physics of NMR was first described by Felix Bloch and Edward Purcell (Bloch, Hansen, & Packard, 1946; Purcell, Torrey, & Pound, 1946). NMR is based upon the existence of a spin property in the nuclei of hydrogen atoms. Hydrogen (^{1}H) nuclei contain only one single proton. That proton possesses a spin angular momentum – an implication from the theory of quantum mechanics, according to which a nucleus containing an odd-numbered quantity of protons or neutrons possesses an intrinsic magnetic moment and angular momentum. The ratio of the magnetic dipole moment to its angular momentum is denoted as the gyromagnetic ratio γ which for ^{1}H equals 42.58 MHz.

The spin itself is a core property of elementary particles that cannot be influenced or altered. However, the vector direction of the spin can be influenced instead. Any magnetic moment placed in an external magnetic field B_0 produces a precession movement, or torque, of the magnetic dipole. The precession vector of the angular momentum precesses along the external field axis at a particular frequency (the *Larmor* frequency). This frequency is directly proportionally dependent on the field strength of the external magnetic field B_0 (and on the gyromagnetic ratio γ of the proton) in a way that the *Lamor* frequency $\omega_0 = \gamma * B_0$. For instance, in a 3 Tesla MR Scanner, the precession frequency of ^{1}H equals 127.73 MHz (42.58 MHz * 3T). Thus, if not the spin by itself can be influenced, the precession frequency can so by external factors, such as the field strength. This fact can

be utilized for many purposes (for example to obtain images of a probe placed into the magnetic field, as we will see in the next chapter).

The rather stabilized spin system within an external magnetic field can be changed by application of an electromagnetic radiation at a certain frequency – the resonance frequency. This is the so-called excitation of the spin system and can be achieved by applying an alternating magnetic field B_1 transversal to the static magnetic field B_0. Assuming B_0 to be present in longitudinal Z direction (B_Z), the transversal B_1 can be notated as B_{XY}. Now, the precession vectors of the protons' spins have changed from B_Z to the B_{XY} plane. As a consequence, resonant absorption of energy has occurred. Removing the temporary B_1 radiofrequency pulse will gradually return the spinning protons to B_Z direction. Simultaneously, the protons will release the energy that they absorbed and induce a signal in a receiver coil as long as a vector component exists away from the B_0 direction. The gradual process of decreasing signal induction while returning to B_0 is called *free induction decay* (FID). The induced signal energy can be detected and recorded e.g., to make it visible by assigning grey values to signal values. In that sense, any probe placed in a magnetic field, excited, then admitted to return to the static field, and finally recorded, would produce a certain grey value according to tissue properties and to its internal number of freely spinning protons.

So far, an overview of NMR physics as a basis for MRI, an exhaustive introduction to NMR can for instance be found in Levitt (2008).

2.2.2 Magnetic resonance imaging

The potential to make water molecules visible is usually not a value by itself, but the MR signal serves as an indicator for structures and events in certain tissues, as for instance the human body or brain.

Upon the physical basis introduced above taken for granted, it is easily conceivable to create an image from the recorded MR signals by mapping color values on signal values. By means of a spatial coding for the detected MR signal, the image can be produced in two, three, or four dimensions (defining time as the fourth dimension, changes in signal strength on a time series of signal values can be illustrated). The first images based on

proton NMR i.e., magnetic resonance images, were produced in the 1970s (Lauterbur, 1973).

In order to get into the details, the above introduced excitation of the spin system does not only affect the precession vector of each single proton, rather they now spin in parallel – or in phase – and produce a temporary single spin vector based on this phase coherence. The precession in B_{XY} is also called *transversal magnetization* (M_{XY}). It was already mentioned that a signal is induced in the receiver coil as long as magnetization exists away from B_0. Since the excitation is usually only generated by a short frequency impulse, the transversal magnetization (and the signal) will decay and the spin system will return to B_0 and simultaneously regain *longitudinal magnetization* (M_Z). So, the signal decay is based on the longitudinal relaxation of the magnetization, or *spin-lattice relaxation*. The time constant of this relaxation is *T1*. However, signal decay happens to be faster than predicted on the basis of *T1* alone. That's the case because there is additional signal decay based on the loss of phase coherence between spins. Loss of coherence does not emit energy. Rather spins interchange energy among each other and thereby destroy the single spin vector. The time constant of this *spin-spin interaction* is *T2*. In reality, further inhomogeneities of the external magnetic field B_0 as well as tissue properties and geometry of the measured object entail an even yet faster signal decay, described by the time constant *T2**. It is important to note that the relaxation processes expressed by *T1* on the one hand and by *T2*, *T2** on the other are mutually independent and concurrent. In general, the MR signal has collapsed already after 100 to 300 ms by phase coherence loss (*T2*), long before M_Z has been re-established (*T1*) after 0.5 to 5 seconds.

So far, the induction and detection of the MR signal has been explicated. In order to obtain an MR image in more than one dimension, a spatial coding of the detected signal is necessary. A three-dimensional image needs some sort of selective coding for each dimension.

First, there is a *slice selection* for signal values in an MR image, being obtained by basically one of the fundamental principles of precession frequency introduced in section 2.2.1 i.e., its dependency on the external magnetic field B_0. As outlined above, the excitation of the spin system is based on the resonance frequency of the excitation impulse. When implementing a field gradient along B_0, the resonance frequency is individually

different for certain *XY* planes along B_Z. Therefore, by frequency selection for the excitation pulse along *Z* direction (head-foot), only one selected slice in the *XY* plane that meets the resonance criterion gets excited.

Second, a *phase coding* is realized along M_Y immediately after the excitation of the selected slice by means of a phase gradient. Basically, an implemented field gradient in *Y* direction (top-down) produces a phase shift along the lines in the selected slice. Since that field gradient is implemented only for a very short period, the spins will afterwards go on to rotate with the same *Lamor* frequency, but now shifted in phase.

Third, the coding in the third spatial direction is accomplished by *frequency coding*. A frequency gradient in *X* direction (right-left) causes different continuously differentiable *Lamor* frequencies for each *X* line in the selected slice.

A three-dimensional dataset in a certain field of view can be achieved if this procedure is repeated for several slices along the *Z* direction. Now, each single volume element, or voxel, is uniquely coded by frequency and phase. However, the MR signal detected is not a single frequency anymore, rather an entire frequency spectrum that is mathematically represented in the *k*-space. The data matrix in the *k*-space is then to be decomposed by analyzing the signal spectrum using a *Fourier transformation* to obtain an image (see Figure 2.1).

Finally, the fourth (temporal) dimension is easily completed by measuring the total field of view at different time points, e.g., continuously throughout an experiment or before and after brain surgery or during development and aging etc.

The contrast of the signal depends on several characteristics of the probe that is measured. There are tissue properties like proton density i.e., the number of spins that can be excited. Other properties that are characteristic for particular tissues are *T1* and *T2* time constants of the tissue. They also determine the image contrast. In fact, tissue distinctions can be visualized in MR images according to the choice of imaging parameters. Accentuation of *T1* is crucially manipulated by the *repetition time* (TR) that describes the time between two successive excitations of the same slice. A short TR admits fast relaxing tissue to emit a massive signal after being re-excited while slow relaxing tissue gains only little longitudinal relaxation

and becomes saturated. Hence, it emits only a small signal. Images accentuating the *T1* contrast are labeled *T1*-weighted.

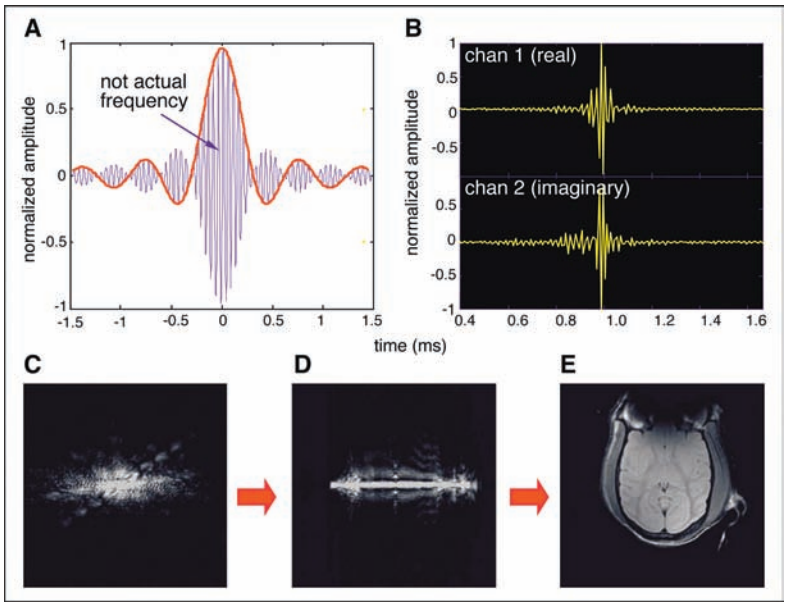

Figure 2.1 MR image acquisition and reconstruction. A radiofrequency pulse (sinc function) excites the spin system at resonance frequency of 127.73 MHz at 3 Tesla (A). Note that the sinus wave illustrates this at a much lower frequency for display purposes. The spin echo measured at two orthogonal channels is produced by an inversion pulse of 180° (B, represented as combination of the real and imaginary part of a complex number). Each row in the k-space (C) consists of a sequence of complex numbers and represents echoes with the same frequency composition but different phase coding. Top and bottom rows have the strongest phase coding gradient and hence the largest dephasing (weakest signal); the strongest echo is in the center of the k-space. The result of the first Fourier transformation along the readout direction is shown in D. The second Fourier transformation along the phase coding direction results in the actual image (E). Figure adopted from Logothetis (2002).

Comparably, images can be acquired *T2*-weighted. This is obtained by manipulating the *echo time* (TE) which is the time between excitation of the spin system and signal detection. The longer TE is, the more dephasing has occurred between the spins (depending on tissue properties). Consequently, given a sufficiently long TE, fast dephasing tissue emits a smaller signal compared to slowly dephasing tissue. *T2*-weighted images are characterized by a long TE.

The entire method of MRI is very suitable to acquire images of living tissue, e.g., the human body. Water is the most common molecule in the human body and brain. Thus, the spin property of ^{1}H molecules is available. Furthermore, imaging by MR does not require the body to be exposed to any externally applied radiation as in X-ray radiograph or computed tomography (CT) nor radioactive tracer as in positron emission tomography (PET). Rapid MR imaging strategies have reduced measurement time immensely. For example, echo-planar imaging (EPI) obtains a complete image from only one excitation, or: a single "shot", in only about 100 ms (Mansfield, 1977; Turner, et al., 1990). Other important MR protocols are for instance the magnetization-prepared rapid gradient echo, MP-RAGE, a *T1*-weighted 3D sequence that is especially appropriate for anatomical images (Mugler & Brookeman, 1990). Another one is the *T1*-weighted modified driven equilibrium Fourier transform (MDEFT) sequence, an anatomical imaging technique that bridges the gap to functional image slices (Ugurbil, et al., 1993).

A more comprehensive overview on MRI can e.g. be found in Vlaardingerbroek and den Boer (2002).

2.2.3 Blood oxygenation level dependent contrast and functional magnetic resonance imaging

The principles of MRI introduced so far are useful to acquire anatomical images of the human body (or any other object containing a certain amount of atoms with spinning nuclei). However, the physiology of the human body provides a characteristic feature that interacts with signal intensity emitted by ^{1}H protons. Ogawa et al. (1990) were the first ones who took advantage of these effects to image a brain's microvasculature (at that time, it was a

cat brain) and already suggested it's value to measure regional neural activity.

2.2.3.1 Physiological and metabolic prerequisites

The basic source behind the effect that enables functional MR imaging is the presence of iron (Fe^{2+}) ions in hemoglobin molecules (red blood cells). Hemoglobin (Hb) is the main carrier for oxygen O_2 in the human body. By means of the blood circuit, Hb supplies the entire body with oxygen that is necessary for all aerobic metabolic processes. Oxygen is transported by Hb, more exactly, by the heme compound of Hb that uses four oxygen binding sites with each of them containing one Fe^{2+} ion as core unit. Thus, the Hb molecule can be found either with O_2 bound to it (Hb_{OXY}) or without (Hb_{DEOXY}, when having supplied O_2 to some body part and returning to the lung now carrying carbon dioxide, CO_2). This means for the aerobic metabolism that whenever some energy consuming process goes on (muscular, neuronal, or any other), the regional ratio of Hb_{OXY} to Hb_{DEOXY} increases (while consequently the ratio of Hb_{DEOXY} to Hb_{OXY} decreases).

Since, first, the MR imaging technique relies on the magnetic properties of spinning protons, and since, second, Fe^{2+} ions (i.e., iron) do also contain magnetic properties, it seem reasonable that the presence of iron in the vicinity of ^1H atoms alters the magnetic effects of spinning protons in a magnetic field. And that's exactly the case. The effect is called magnetic susceptibility, an index for the distortion of an applied magnetic field when it interacts with any material. However, the influence of Hb on the MR signal depends on whether it is in the state of Hb_{OXY} or Hb_{DEOXY}. Because in the case of Hb_{OXY} O_2 molecules are bound to the Fe^{2+} ions, the oxygen acts like an insulator. Therefore, Hb_{OXY} is said to be diamagnetic (while Hb_{DEOXY} is paramagnetic): The oxygen shields the magnetic influence of the iron ion on the ^1H protons to a certain degree – enough to yield measurable effects. This means in the context of MR measurement that the magnetization effect of an external field on the ^1H protons is larger and more stable if the surrounding Hb is diamagnetic, and a larger signal is obtained in the receiver coil.

Brain activation entails an increase in cerebral blood flow (CBF), and in metabolic rate of oxygen ($CMRO_2$) in engaged brain areas (Ginsberg, Dietrich, & Busto, 1987). Thereby, the rate of changes in CBF is more pro-

nounced than the rate of changes in oxygen metabolism. Nonetheless, as a consequence the venous blood oxygenation increases (Ogawa, et al., 1990). A massive change in CBF is mandatory to support just a small increase in $CMRO_2$ (R. B. Buxton & Frank, 1997), and changes in CBF relative to changes in $CMRO_2$ are reflected in the blood oxygenation level dependent (BOLD) response (Richard B. Buxton, Uludag, Dubowitz, & Liu, 2004). The inference is that changes in the BOLD response reflect cognitive processes mirrored in neural activity. Indeed, this BOLD contrast mechanism is considered to reflect neural activation (Logothetis, Pauls, Augath, Trinath, & Oeltermann, 2001). In that way, the regional metabolic and blood flow changes in active neurons and glia and surrounding tissue in a particular brain area that is involved in a certain cognitive process affects the MR signal measured in voxels at corresponding locations in the field of view (see Figure 2.2).

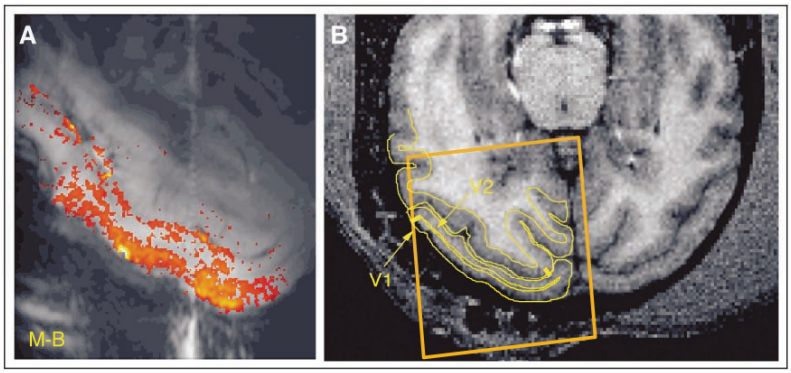

Figure 2.2 Significant BOLD response in the human cortex in response to visual stimulation (Figure A), shown as a contrast between moving stimulus (M) vs. blank screen (B). The activation shown in Figure A corresponds to the primary (V1) and secondary visual cortices (V2) of the human brain (delineated in Figure B). Figure adopted from Logothetis (2002).

2.2.3.2 Temporal properties of the BOLD response

Even though the hemodynamic response is considered to reflect neural activity, it is characterized by a certain amount of temporal delay. Neural responses of the brain can be observed by means of electroencephalography (EEG) or by magnetencephalography (MEG) within a few tens to hundreds of milliseconds. BOLD fMRI deals with a much lower temporal resolution than those methods. The hemodynamic response increases only after seconds and reaches its peak after 5 to 8 seconds on average (time to peak) (see Figure 2.3). But also times to peak of less than 3 seconds to more than 10 seconds are possible – according to stimulus parameters and to the specific brain regions under investigation. That's because, first, the onset time and duration of the BOLD response correlates closely with stimulus onset time (R. S. Menon, Luknowsky, & Gati, 1998) and stimulus duration. For stimulus duration up to 4 seconds, the physical parameters of the stimulus are critical for the hemodynamic time to peak. Beyond 4 seconds, the neural response and thereby the BOLD signal saturates, then only resulting in increasing width of the signal peak (Ravi S. Menon & Kim, 1999). However, the width of the response can be used as a measure of processing time (Richter, Andersen, Georgopoulos, & Kim, 1997). Second, the exact mechanisms behind the varying temporal behavior of the BOLD signal in different brain regions still remains unclear, but it was speculated that differences in vasculature might be responsible for those observations (Miezin, Maccotta, Ollinger, Petersen, & Buckner, 2000).

The technique of functional MRI has been meanwhile applied in a broad spectrum of research issues in cognitive neurosciences. An extensive overview on fMRI is provided e.g. by Jezzard et al. (2001).

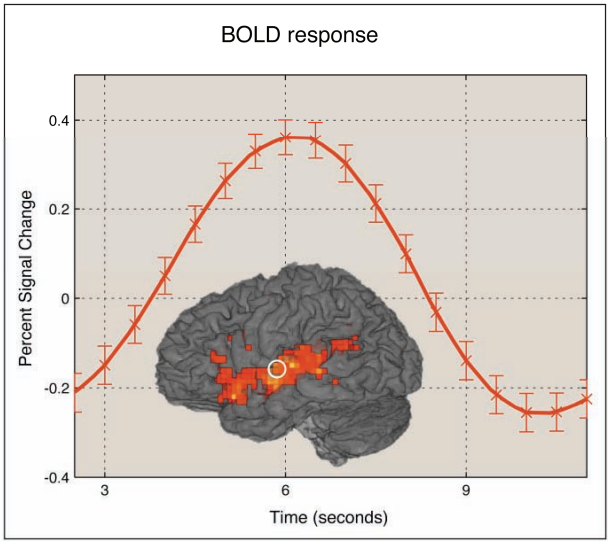

Figure 2.3 Blood oxygenation level dependent (BOLD) response example from human primary auditory cortex during speech perception. The graph illustrates the averaged BOLD time course of one voxel of interest in Heschl's gyrus, indicated by the white circle on the inset image. Crosses represent measured data with standard error bars, and the line graph shows a linear interpolation of data points. The hemodynamic response peaks at about 6 seconds and undershoots after 9 seconds.

2.2.4 Diffusion-weighted imaging and diffusion tensor imaging

The principles of MRI introduced in chapter 2.2.2 are a useful basis also for alternative image contrasts. In the basic model of MRI, protons are assumed to be stationary during measurement. Thus, a particular ^{1}H molecule being excited is expected to be measured in the very same voxel location during signal detection. Any movement of spins like diffusive motion interacts with signal detection. These diffusive processes are a drawback for spatial resolution in MR imaging. Generally, the limitation of spatial resolution is about 10 µm, based on the diffusion of water molecules during the measurement time (typically 10 to 100 ms).

Spin motion along a magnetic field gradient (regardless whether slice selection gradient, phase coding gradient, or frequency gradient) results in phase shifting. But knowledge about the particular phase of each spin is necessary for correct spatial coding. Molecular displacement by reason of blood supply, cellular transportation, diffusion etc. does not converge with the assumption of stationary spins and therefore increases the error variance of the measured signal. But on the other hand, molecular motion can also be used as a parameter of investigation by itself.

Water molecules follow, as any molecules, the law of Brownian molecular motion. Brownian motion is basically the thermally driven random mobility of molecules. It can be characterized by the diffusion coefficient *D*, a physical constant being related to the root mean square of translational displacement of molecules in a given time (see Figure 2.4A). In many media or tissues, molecular mobility is not equal in all directions (i.e., isotropic). Rather, according to tissue microstructure, diffusive mobility is more or less directed (i.e., anisotropic). An example for anisotropic diffusion is depicted in Figure 2.4B.

Like in basic MRI, it is predominantly the hydrogen molecule, better: its diffusivity, that is used for anatomical diffusion-weighted MRI because of the abundant availability of water in the human body. In the human brain, particularly the white matter entails anisotropy of hydrogen diffusion due to its arranged orientation of cellular microstructure (protein filaments, cell membranes, myelin). The white matter is formed by axonal fibers that connect cortical (and also subcortical) regions of grey matter. The grey matter of the human brain also includes these cellular microstructures, however, they are not as aligned, at least on the macroscopic level detectable by MR scanning.

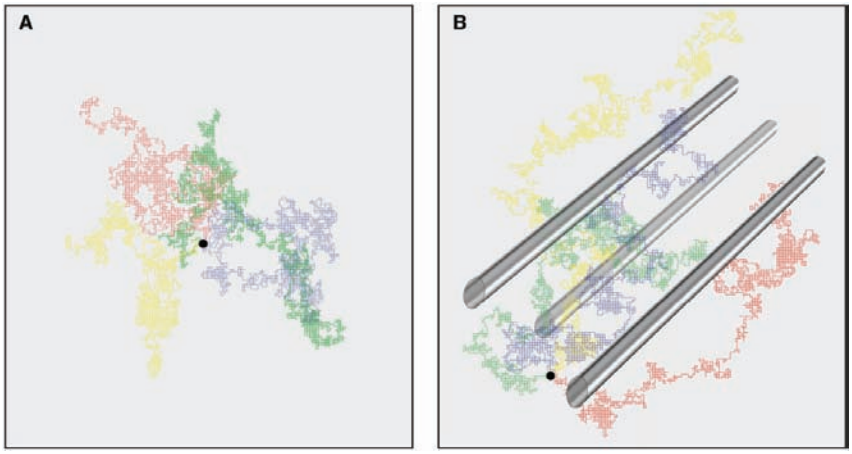

Figure 2.4 Simulation of molecular diffusion based on a randomization algorithm (random walk) with 5000 iteration steps. The images represent instances of diffusive trajectories of four different particles depicted in four different colors. Likewise, the colors can be read as possible diffusive trajectories of a single particle; each color then represents a random trajectory of equal probability. The black dot indicates the seed point. Figure A illustrates isotropic diffusion with no preferred direction of the diffusion process. Figure B illustrates anisotropic diffusion. Anisotropy can for instance be determined by ordered structures – like for instance fiber bundles in the brain's white matter (symbolized by cylindrical formations). The random walk illustrating anisotropic diffusion involves unequal probabilities for the directions at each step with a preferred diffusion direction from lower left to upper right due to hinderance and restriction caused by the presence of ordered structures in the medium. In the example, it is confined to only one direction (upper right) as a result of e.g., media flow in the tissue to the upper right direction. Otherwise, diffusion to the opposite direction (lower left) would have equal probability.

Note: For the simulation examples illustrated above, the figures are simplified to 2D space. Biological diffusion, however, takes place in all 3 spatial dimensions.

In biological diffusion MRI, the diffusion coefficient of interest is the *apparent diffusion coefficient* (ADC) rather than *D*. ADC takes into account that in anatomical diffusion imaging not pure physical diffusion is measured, but diffusion of hydrogen in a specified time span that is hindered and re-

stricted by molecular interactions with cellular structures (Douek, Turner, Pekar, Patronas, & Le Bihan, 1991). Biological diffusion in the brain covers about 10 µm within the typical MR measurement time of 10 to 100 ms (S. Mori & Zhang, 2006). There is a direct association of the anisotropy of diffusion in the brain's white matter and fiber geometry: diffusion parallel to the main fiber direction ($ADC_{\parallel}$) is faster and greater than diffusion perpendicular to it ($ADC_{\perp}$) (Moseley, et al., 1990). The diffusion ratio ($ADC_{\parallel}/ADC_{\perp}$) quantifies the overall amount of anisotropy. Focused investigations in selected directional diffusivity, i.e., either parallel or perpendicular to the main fiber direction, is even able to distinguish between myelin vs. axonal contributions to the anisotropy of diffusion (S. K. Song, et al., 2002).

The measurement of diffusion in an MR scanner is accomplished by the application of different gradient direction. For traditional diffusion-weighted imaging (DWI), the three main directions in space are used as directions for the pulsed magnetic field gradient (cf. chapter 2.2.2). Like in conventional MRI, a spin echo of the original FID is created after excitation along one of the gradient directions. However, due to diffusive motion of the molecules, the rephasing will not result in a perfect spin echo for those protons that have diffused along the field gradient during TE. Since they have changed precession frequency, the rephasing pulse they now experience is not equivalent to the original phasing pulse. Hence, the imperfectly dephased signal detected from those protons will be reduced (A. W. Song, Wong, Tan, & Hyde, 1996). Accordingly, the longer the time between the two gradient pulses, the more diffusive motion has occurred and hence the greater the signal loss is. This time span is described by the *b* value.

DWI provides basic information about average diffusivity, the so-called *trace*. The problem with DWI is that only diffusive motion along the applied gradient axis can be measured. In order to detect natural fiber orientations, an almost infinite number of field gradients would have to be applied. A simplification can be obtained by using the tensor model (Basser, Mattiello, & Lebihan, 1994). If more than three directions of diffusion are measured by using more directions of applied gradient vectors, at least six, a tensor model can be computed for each voxel. Accordingly, this method is then called diffusion tensor imaging or DTI. The tensor is simply a symmetric matrix of diffusion values. The values within the matrix describe the

direction and distance of diffusion. This implies for white matter DTI that the fiber direction is described by the main eigenvector of the matrix. Conversely, the *trace* mentioned above is basically the scalar measure of the total diffusion within a voxel and provides information on mean diffusivity in the voxel. More specific information on actual white matter tracts can be obtained by measures of directional diffusivity, such as axial diffusivity (parallel to the tract) or radial diffusivity (perpendicular to the tract). They are assumed to represent specific information on biological processes as changes within axons or in myelin sheaths (S. K. Song, et al., 2002). Another very useful index of diffusion is fractional anisotropy (FA) which gives information about the shape of the tensor and hence the degree of diffusion anisotropy (Pierpaoli & Basser, 1996). Graphically, the tensor matrix can be represented by a 3-dimensional diffusion ellipsoid (see Figure 2.5).

In current diffusion modeling, alternative approaches to the meanwhile classical tensor model have been proposed and are under evaluation (Frank, 2001; Tournier, Calamante, Gadian, & Connelly, 2004; Tuch, Reese, Wiegell, & Van, 2003; Wedeen, Hagmann, Tseng, Reese, & Weisskoff, 2005). For a more comprehensive introduction to DTI, see e.g., Mori (2007).

DTI gives rich information about the orientation of fiber structures, it does not, however, provide information about the directionality of axonal connections, either one way or the other. Though, further information can be extracted from and models and can be applied to DTI data once they have been acquired. For instance by applying color schemes, orientation information of the longest vector from the tensor model can be illustrated and also utilized to render 2- or 3-dimensional visualizations of brain white matter (Pajevic & Pierpaoli, 1999) (see also Figure 2.5). Additionally, a more sophisticated method is fiber tract mapping on the basis of DTI data. Within this framework, local fiber orientation inside one voxel represented by magnitude and orientation of the diffusion tensor is modeled and connected to proximate voxels in eigenvector directions by a 3D streamlining algorithm applied to the tensor field. Accordingly, when starting at a seed point and mathematically propagating, an illustration of the anatomical structure of fiber tracts can be obtained (e.g. Susumu Mori & van Zijl, 2002).

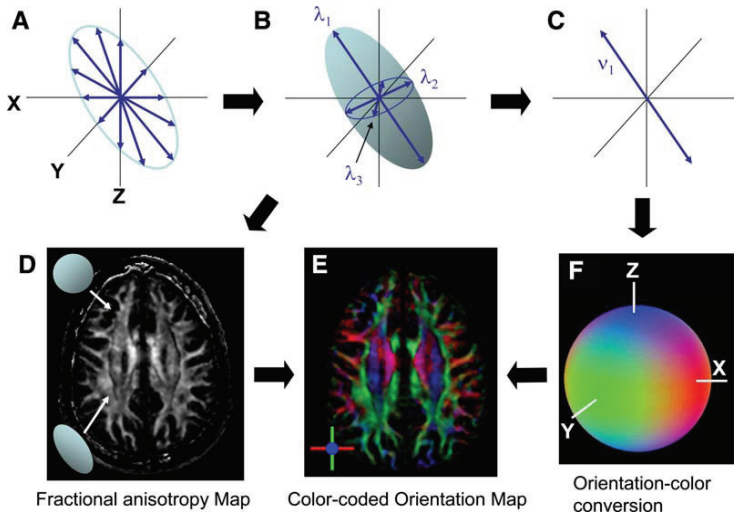

Figure 2.5 Measurements of diffusion along multiple axes (A) are fitted to a single 3D ellipsoid model of average diffusion distances (B). The eigenvalues λ_1, λ_2, λ_3 of the tensor matrix describe the length of the three ellipsoid axes. The eigenvectors v_1, v_2, v_3 describe their orientation (C). The orientation of the longest axis is assumed to represent the local fiber orientation. The shape of each voxels ellipsoid model can be illustrated by grey values in an anisotropy map with black (spherical) to white (most elongated) color coding (D). Moreover, the orientation information obtained from the eigenvector v_1 can be color-coded in an orientation map to illustrate the fibers in the brain (E,F). The Figure is adopted from Mori and Zhang (2006).

2.3 Statistical data analysis

The following section will summarize statistical measures and methods to analyze behavioral, functional, and anatomical data. The main emphasis of the explanations rests upon those implementations of techniques and procedures that will be relevant for the experiments described in detail in subsequent chapters.

2.3.1 Behavioral data

Behavioral measurements implemented in the present experiments comprise mainly acceptability judgments on speech stimuli given by button presses. Hence, response correctness and reaction times are of particular interest. If not stated otherwise, statistical analysis comprised analyses of variance (ANOVA) in a repeated-measures design. Exact description of the statistical approach to behavioral data is provided in the method sections of each experiment.

2.3.2 Functional MR data

2.3.2.1 Pre-processing of raw data

The dataset acquired in the MR scanner has to be prepared for statistical treatment by a chain of pre-processing steps. These steps comprise motion correction, slice time correction, and spatial as well as temporal filtering. Below, each step is explicated in detail.

Motion correction

The acquisition of images in a scanner is based on the assumption of a static probe that is mapped onto the scanners internal coordinate system. However, if the probe is a human participant, its immobility is imperfect. Reasons for head motion are diverse: from pulsation or involuntary tiny muscle twitches to even stimulus or task dependent movement. Even on the scale of less than one millimeter, head motion can become a problematic source of error. The assumption in data analysis is to record the exactly identical brain region in a certain voxel during the entire time series of the dataset. If this assumption is violated by head motion, the data will be incorrect. The implication for functional datasets is that especially when head motion correlates with an experimental manipulation, signal changes in a voxel due to motion cannot be differentiated from signal changes associated with the experiment.

In order to prevent motion-related artifacts in the data, it is necessary to correct the time series of fMRI data for motion-related misalignment. This is achieved by realigning all images acquired in a functional MR session to make them geometrically compatible. A simple but effective realignment is

based on image-similarities (Friston, Williams, Howard, Frackowiak, & Turner, 1996). This approach relies on changes in global image intensity distribution between two successive images in the time series of the data-set. A vector of a set of three translational and three rotational motion parameters can be used to numerically minimize the sum of squares of image differences. The algorithm is fast and valid and can be applied iteratively.

Slice time correction

Functional MR volumes of a 3-dimensional image of the brain are assumed to represent a single point in time. However, MR images are acquired slice by slice (i.e., 2D images), one after the other. Therefore, even those slice that form an instantaneous 3D image of the brain are captured serially – not simultaneously – which can take up to a few seconds. This is no problem for anatomical images. For functional images, though, that are considered to reflect the hemodynamic brain response, this time delay among slices would cause problems in the statistical evaluation of the data.

The slice time correction provides an adjustment for these acquisition timing differences by applying a phase shifting of the time series at each voxel (on the basis of Fourier transformation). It employs a cubic-spline-interpolation to virtually move backwards the voxel values in time which results in a data file that contains data values as if all slices of one time step had been acquired simultaneously. The correction applied is identical for all voxels in a single slice.

Spatial filtering

The application of a spatial filter has basically two consequences. First, the signal to noise ration (SNR) increases. Second, inter-subject variability gets reduced. Otherwise, statistical group analysis, when relying on spatially unsmoothed data, will almost certainly yield artifacts. However, noise in data can be reduced by averaging over a local region. The blurring function of the spatial filter will reduce signal noise, since noise values tend to become mutually negated. In consequence, SNR is increased.

A standard method for spatial filtering is to apply a Gaussian kernel on the data with a filter size of several millimeters FWHM (Full Width at Half Maximum). Greater width of kernel results in greater smoothing. However,

it is important to note that general image intensity remains unaffected by the filter.

Temporal filtering

The temporal filter works on the time series of each individual voxel and is also known as high-pass or low-pass filtering. High-pass filtering removes low frequency drifts in the time series that can result e.g., from breathing or from scanner-induced drift artifacts in the data. In order to apply a suitable cutoff frequency, it is necessary to know the frequency of experimental stimulation. This is important not only for general stimulation frequency. In experiments with more than one condition, it is, moreover, necessary to concern each individual condition's frequency for filter selection. Otherwise, condition specific variance (the signal of interest) in the data will be corrupted.

Low-pass filtering is generally applied in block designs only, or sometimes in cases of very long event-related trial. Thereby, high-frequent noise can be removed from the data. The temporal low-pass filter is typically a linear convolution with a Gaussian kernel like in spatial filtering, but this time in the temporal domain, and results in data smoothing.

Finally, it is labeled band-pass filter if both high-pass as well as low-pass filters are applied on the same data. A band-stop filter is a reversed band-pass filter because it suppresses only the specified frequency window between them.

2.3.2.2 Registration and normalization

In order to refer from functional MR data to specific brain areas, the functional EPI volume needs to be mapped onto the anatomical MR dataset. Routinely, prior to the acquisition of an experimental fMRI time series, an anatomical *T1* image (MDEFT) of the head is captured in the same session. This anatomical *T1* image is geometrically aligned with the slices of the functional EPI volume. The co-registration of the functional data with the individual high-resolution *T1*-image (MP-RAGE) is performed in two steps: First, a transformation matrix is computed that registers the 2D slices of the MDEFT with the 3D MP-RAGE. This transformation method is validly and reliably employed being rigid and affine linear by means of six parameters, three translational and three rotational ones (Lohmann, et al.,

2001). The second step is to apply the obtained matrix to the functional EPI volume and the high-resolution *T1* anatomical volume. In case no MDEFT *T1* image was obtained during the experimental session, it is also possible to register the functional EPI time series directly on the 3D MP-RAGE.

In a group study, the transformation is to be accomplished onto the same anatomical image for all individual datasets. This enables the implementation of group statistics across participants. Data normalization converges individual datasets into a common reference space. This is typically implemented by rotating and shifting the functional data into a standard stereotactic coordinate space. There are two major reference spaces commonly used in cognitive neuroscience, the Talairach space (Talairach & Tournoux, 1988) and the MNI space (Collins, Neelin, Peters, & Evans, 1994). The studies described in the following chapters consistently utilized the Talairach space.

2.3.2.3 Statistical modeling and analysis

Experimental design

The design of the experiment is certainly to be determined before any data acquisition. However, certain peculiar features of experiments to be conducted as an fMRI experiment shall be mentioned at this point, since the nature of the magnetic measurement requires some thoughtfulness of data acquisition and data modeling in order to obtain valid results. The type of design used in the experiment affects data modeling as well as statistical analysis.

The classical and still most commonly implemented experimental fMRI design is the block design. In a block design, a longer period of several trials (e.g., 20 to 60 seconds) belonging to one condition are followed by a period of trial belonging to another condition. Typically, these periods, or blocks, will alternate between several conditions. Because of these rather rigid prerequisites, the block design technique inevitably confines experimental alternatives, especially in psychological research.

A more advanced technique that allows randomized presentation of trials belonging to different conditions is the event-related design (ER-MRI). Within this approach, trials can be presented jittered and also randomized. Given the temporal resolution of the hemodynamic response, event-related

paradigms seem challenging to implement. But image acquisition technique has improved and fastened (cf. EPI, section 2.2.2). Moreover, even very short neural activity results in measurable BOLD effects (Savoy, et al., 1995), and transient signal increase can be measured even during isolated trials (Buckner, et al., 1996). It is, as a consequence, feasible to acquire and evaluate functional MR data event-related. A resultant advantage is a much higher temporal resolution of the signal than of signals obtained in block designs. In addition, the hemodynamic response to stimuli that are presented rapidly with only few seconds in-between adds up almost linearly (Dale & Buckner, 1997), a fact that facilitates statistical linear modeling of accelerated ER-MRI data. The introduction of ER-MRI was a major step to open the method of functional MR imaging to broader research questions (Raichle, Arthur, & John, 2000).

Statistical parametric mapping

Although statistical analysis of fMRI data can also be implemented by model-free methods, (e.g. McKeown, et al., 1998), the most common method is to use a model-based approach (e.g. Friston, et al., 1994). Within this framework, a General Linear Model (GLM) fits a model of hemodynamic responses within one voxel (i.e., univariate) into the observed data time series of the voxel. The computational basis is a mathematical approximation to the hemodynamic response that can be modeled by a simple gamma function (Lange, 1996) or by a convolution of two gamma functions (Friston, et al., 1998). The GLM delivers a model of the fMRI time series by a linear combinatorial equation of independent variables (e.g., conditions) – plus constant and error term. The impact of each model (condition) is described by parameter estimates (beta values). The higher the beta value of a certain independent variable, the stronger the relation between the respective model condition and the observed fMRI time series of the voxel.

The parameter estimates can then be converted into *t*- or *z*-statistics with corresponding *p*-values – a central description of the goodness of fit of the data to the model. Similarly, parameter estimates can also be subtracted from each other to obtain direct comparisons between conditions. These *t*-, *z*-, or *p*-values for each voxel can also be visualized on a statistic map.

However, to obtain a suitable statistic out of the single-voxel statistic, the data need thresholding to deal with the multiple-comparison problem.

Since each of the thousands of voxels measured is modeled univariate, a significant number of voxels will show activation by chance, even at a quite conservative significance level. Bonferroni correction approaches were suggested, even though they suffer from being too stringent and somehow over-conservative. Several other approaches have been developed to solve this problem, e.g., to implement Gaussian Random Field (GRF) theory. The application of a cluster-based threshold can assist to avoid too stringent thresholding: only those voxels are considered that show activation in a cluster of e.g., 5 or 10 active voxels (according to spatial resolution of the data). The idea behind is that false positive values are supposed to be randomly distributed over the voxel space while reliably activated voxels should cluster at certain regions (for a practical implementation, see Forman, et al., 1995).

A higher level inference on the data by e.g., random-effects analysis will allow to model, on a second level, between-subject and subsequently between-group comparisons.

2.3.3 Diffusion MR data

Once diffusion data of the brain are acquired as outlined in chapter 2.2.4, they might be evaluated according to several research issues. FA values are computed voxelwisely and can be used for statistical comparison across individuals or groups. Since FA represents scalar values (cf. chapter 2.2.4), it does not rely on fiber orientation what facilitates its application to between-subject statistics. Previous approaches to deal with spatially local comparisons across individuals have implemented solutions derived from voxel-based morphometry (VBM). VBM was originally created to compare anatomical *T1* datasets for investigations in grey matter structure (Ashburner & Friston, 2000). The VBM method registers individual images into one common standard coordinate space and executes voxelwise statistical comparison. The challenging intricacy with this kind of data approach is settled in the fact that its results strongly depend on the validity of registration. Any local misalignment during registration of the datasets might easily generate statistical differences (Bookstein, 2001). Moreover, arbitrary selection of the image smoothing kernel and/or significance level can be further sources of artifacts (Derek K. Jones, Symms, Cercignani, & Howard, 2005). Therefore, the potential ambiguity as to whether observed

differences can be attributed to real anatomical structure or simply to registration deficits might hamper reliable inferences. Though, careful application and validation of VBM can yield valid conclusions (Ashburner & Friston, 2001; Watkins, et al., 2002).

A VBM guided analysis of DTI data could for instance compare the white matter structures between two groups and correlate possible differences to some covariate of interest. But the registration problems remain the same as for *T1* datasets and, even worse, might be amplified given the filigreed structure of white matter. For that reason, a registration based on only the fiber tracts without considering grey matter structure could be anticipated to be much more efficient and suitable to the statistical comparison of DTI data across individuals. And in fact, this approach has been recently developed and established (Stephen M. Smith, et al., 2006). The method implements several processing stages to DTI raw data as well as statistical comparison and is referred to as tract-based spatial statistics (TBSS) (see Figure 2.6).

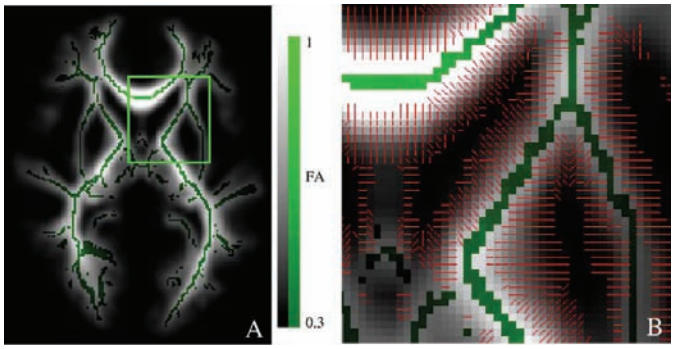

Figure 2.6 The methodological underpinning of tract-based spatial statistics (TBSS). Example of a multi-subject mean FA skeleton axial slice of the human brain (A). Individual fiber tracts are clearly discriminated and easy to identify. Figure B shows a magnification including local FA centers-of-gravity to identify tract perpendiculars. The Figure is adopted from Smith et al. (2006).

The TBSS approach elaborates a series of data processing steps. First, by means of a nonlinear registration to a common target, all individual FA images undergo an initial approximate registration. Second, a mean FA image out of all aligned images is generated. This image is then reduced to the core white matter structure by a non-maximum-suppression perpendicular to the local fiber direction. This image is referred to as the mean FA skeleton (see Figure 2.3). Third, all individually aligned FA images from step one get projected onto the skeleton utilizing a voxel-by-voxel search space perpendicular to the local skeleton structure. Fourth, at this point voxelwise statistics across subjects can be calculated on the skeleton space (Stephen M. Smith, et al., 2006). TBSS has been successfully implemented in several studies, among them also studies concerning developmental issues (Giorgio, et al., 2008; Lebel, Walker, Leemans, Phillips, & Beaulieu, 2008).

With respect to connectivity information between brain areas, it was until recently mostly animal models that have helped to understand the exact location and direction of fiber tracts. Thereby, the tissue is treated invasively by lesions or injection of active tracers that degenerate neurons so that the animal's brain can be inspected afterwards (Passingham, Stephan, & Kotter, 2002). Because of their invasive nature, these methods are not suitable for humans. Some tracers are possible to be applied to human brains post mortem, but only for small distances up to about 10 mm (Mufson, Brady, & Kordower, 1990). To obtain information on long-range connectivity is much harder in humans, only possible by less exact methods such as dissection (Klingler & Gloor, 1960). However, modern diffusion imaging techniques enable noninvasive in vivo quantification of fiber connections in the human brain by white matter tractography. Tractography uses information on local fiber orientation to trace fiber bundles throughout the brain (Susumu Mori & van Zijl, 2002). The method has been confirmed to faithfully reconstruct anatomical white matter fasciculi (Catani, Howard, Pajevic, & Jones, 2002; S. Mori, et al., 2002).

There are basically two major approaches for fiber tracking which are on the one hand deterministic and on the other probabilistic white matter tractography. Both of them attempt to reconstruct a fiber bundle trajectory from a predefined seed point. Deterministic approaches use a maximum-likelihood computation to find the best solution for the tracking algorithm

(e.g. Conturo, et al., 1999; S. Mori, Crain, Chacko, & van Zijl, 1999). This algorithm generates a reconstructing trajectory by following the direction corresponding to the eigenvector with the largest eigenvalue of the diffusion tensors. Though, probabilistic tractography has its shortcomings. First, it might fail in regions with merging, crossing, or splitting fiber bundles, and rather produces only one solution for a reconstructed trajectory. Second, no confidence indicator can give information about the reliability of the solution (D. K. Jones & Pierpaoli, 2005).

For a more realistic assessment of anatomical connectivity between arbitrary regions, an algorithm which differentiates between trajectories in highly aligned bundles on the one hand and paths through almost isotropic matter on the other is needed. This can be achieved by probabilistic tractography which considers multiple pathways emanating from the predefined seed point (e.g., Behrens, et al., 2003; Tuch, et al., 2003). The idea behind probabilistic tractography is to take into account the uncertainty of the trajectory direction information within the voxel. This results in a local probability density function, based on a model of local diffusivity, such as the diffusion tensor model introduced in chapter 2.2.4 (Basser, et al., 1994). Within the probabilistic tractography approach, each reconstructed pathway is assigned a certain level of confidence, or probability. In order to find a numerical measure meeting the confidence requirements, several ways of the computational procedure can be implemented that result in probabilistic tracking algorithms. The probability can be obtained for instance by the number of times it is reconstructed in a Monte Carlo random walk simulation which relies on the diffusion tensor properties within each voxel (Koch, Norris, & Hund-Georgiadis, 2002).

The implementation of white matter tractography can be very helpful to subdivide white matter into its compartments (Catani, et al., 2002), to yield information on anatomical connectivity between certain cortical areas by underlying fiber pathways (Behrens, et al., 2003; Koch, et al., 2002), or to conduct a connectivity-based parcellation of the cortex (Anwander, Tittgemeyer, von Cramon, Friederici, & Knosche, 2007; Johansen-Berg, et al., 2004; Klein, et al., 2007).

3 Study 1 – Functional networks of auditory sentence comprehension in adults and children

The present experiment examines auditory language comprehension in adults and 6-year-old children. The functional neuroanatomy of language in the adult brain separates semantic and syntactic processes in the superior temporal gyrus (STG) and in the inferior frontal gyrus (IFG). It is presently, however, unknown whether a similar specialization exists in the developing brain. The goal of this fMRI study is to specify the neural basis of semantic and syntactic processes at the sentential level in young children aged 5 to 6 years. The central results and conclusion of this study have been published in Brauer & Friederici (2007).

The present experiment applied a violation paradigm that has been used successfully in event-related brain potential (ERP) studies with young children (Hahne, Eckstein, & Friederici, 2004; Oberecker, Friedrich, & Friederici, 2005). In this paradigm, correct sentences and sentences containing either a semantic or a syntactic violation were presented auditorily. These previous ERP studies reported an adult-like ERP pattern for semantic violations (N400) in 1 and 2-year-olds (Friedrich & Friederici, 2005). An adult-like though still delayed ERP pattern for syntactic violations (ELAN-P600) was not observed before the age of 2 (Oberecker & Friederici, 2006; Oberecker, et al., 2005). Here, we chose to test 5 to 6-year-olds because the ERP studies cited above as well as behavioral studies suggest that by this age the major semantic and syntactic aspects of the mother tongue have been acquired (e.g. Gleitman & Wanner, 1982; Pinker, 1984). Psycholinguistic theories of language acquisition, however, differ with respect to their view of how dependent or independent semantic and syntactic processes during this developmental stage are (Gleitman & Wanner, 1982). Behavioral studies in children are not decisive as they report data in support of interactive processes throughout development (Tyler & Marslen-Wilson, 1981), but they also report results for an independence of syntactic processes in older children (after the age of 7 years) though not in younger children (Friederici, 1983). So far, no ERP studies with children on the interaction of semantic and syntactic factors are available. The different

ERP components observed for the processing of semantic violations (N400) and for syntactic violations (ELAN-P600) in children approaching the age of 3 years, however, could be interpreted to indicate independent neural networks for semantic and syntactic processes. If children at the age of 5 to 6 years base their semantic and syntactic processes on independent neural networks similarly to adults, we expect semantic processes to engage mainly the left STG's mid-portion (mid STG) and posterior portion (post STG) and syntactic processes to activate in particular the left anterior STG (ant STG) and the frontal operculum (FO). An overlap of the activation pattern for semantic and syntactic processes would rather be predicted by theories assuming a higher interdependence of these processes during development. Another possible difference between language processing in adulthood and childhood that might lead to different activation patterns could be related to the finding of increased processing costs during sentence comprehension in children. All behavioral reaction time studies (Friederici, 1983) as well as all ERP studies (Hahne, et al., 2004; Oberecker, et al., 2005) indicate slower and less automatic semantic and syntactic processes in children than in adults, a result which is construed to reflect higher processing demands. In second language learners, such higher processing demands are associated with an involvement of BA 44/45 compared to native listeners (Rüschemeyer, Fiebach, Kempe, & Friederici, 2005). Thus, it is likely that children, for whom processing demands are higher than for native speaking adults, might show a larger involvement of the IFG.

3.1 Methods

3.1.1 Data acquisition

The experiment was carried out on a 3 Tesla scanner (Siemens TRIO, Germany). For functional measurements, a gradient-echo EPI sequence was used with TE 30 ms, flip angle 90 degrees, TR 2 s, acquisition bandwidth 100 kHz. The matrix acquired was 64 × 64 voxels, FOV 192 mm, in-plane resolution 3 × 3 mm. 20 slices were recorded, slice thickness was 4 mm with an interslice gap of 1 mm.

For registration, T1-weighted modified driven equilibrium Fourier transform (MDEFT) images (Ugurbil, et al., 1993), data matrix 256 × 256, TR 1.3 s, TE 7.4 ms, were obtained with a non slice-selective inversion pulse followed by a single excitation of each slice (Norris, 2000). Additionally, a set of T1-weighted spin-echo EPI images, TE 14 ms, TR 3 s, was taken with the same geometrical parameters (slices, resolution) and the same bandwidth as used for the fMRI data. A slice-selective inversion pulse was applied with an inversion time of 1.2 s. For anatomical data, a T1-weighted 3D magnetization-prepared rapid gradient echo (MP-RAGE) sequence was obtained with magnetization preparation consisting of a non-selective inversion pulse and the following imaging parameters: TI 650 ms, repetition time of the total sequence cycle 1.3 s, repetition time of the gradient-echo kernel (snapshot FLASH) 10 ms, TE 3.97 ms, alpha 10°, bandwidth 130 Hz/pixel (i.e., 67 kHz total), image matrix 256 × 240, FOV 256 × 240 mm, slab thickness 192 mm, 128 partitions, 95% slice resolution, sagittal orientation, spatial resolution 1 × 1 × 1.5 mm. To avoid aliasing, oversampling was performed in the read direction (head-foot).

3.1.2 Participants

The study was approved by the Research Ethics Committee of the University of Leipzig (Germany). Five to six-year-old children, recruited through letter announcements in local Kindergartens, participated in the study. Interested parents were invited for education and clarification of facts about the experiment and procedures. They gave written, informed consent. Children gave verbal assent prior assessment and scanning.

Children underwent psychological diagnostics, including expressive and receptive language skill assessment: four subscales of the Heidelberger Sprachentwicklungstest (HSET, Grimm & Schöler, 1991) and a non-word repetition task selected from Sprachentwicklungstest SETK 3-5 (Grimm et al., 2001). Non-verbal IQ was assessed by Kaufman Assessment Battery for Children (K-ABC, Kaufman et al., 2001). Handedness was evaluated by an adopted version of the Edinburgh handedness inventory (Oldfield, 1971). Parents completed a questionnaire about the child's developmental and medical history as well as a checklist about the child's behavior (CBCL, 1998). Hearing was examined by otoacoustic emission (OAE) measurement.

All children had normal intelligence and language skills. Exclusionary criteria comprised (i) non-German or bilingual background; (ii) neurological diseases or seizures; (iii) known neurological or psychiatric disorder; (iv) medical treatment affecting the central nervous system; (v) significant head injury with loss of consciousness; (vi) body weight or size at birth or head circumference at birth out of normal range (below 3rd or above 97th percentile); (vii) hearing problems; (viii) handedness laterality quotient below 60.

Twenty-three children were assessed psychologically, five had to be excluded on basis of their language, intelligence, or behavior test results. Hence, eighteen children were invited for functional MRI scanning. Three children had to be excluded from the study for too little compliance during an initial mock session (see below), three additional children had to be excluded from further data analysis for too much movement during the scanning session. Thus, data of 12 children (8 girls) were obtained for data analysis (mean age 6.2 years, SD 0.7, range 5.1 to 6.9).

Additionally, 13 adult native speakers of German (7 female, mean age 25.9 years, SD, 2.7, range 21.9 to 30.5) participated in the study after informed consent. None of them had any history of neurological or psychiatric disorders. All participants were right-handed and German native speakers.

3.1.3 Materials

The stimulus material consisted of short sentences in active voice intelligible for children at the accordant age. There were three critical conditions: a correct basic condition (COR), a syntactically incorrect condition (SYN), and a semantically incongruous condition (SEM). Furthermore, a filler condition (FIL) with a correct prepositional phrase was included to match the syntactically incorrect condition in which the prepositional phrase was incomplete (see Table 3.1).

In syntactically incorrect sentences, the preposition was immediately followed by a verb, thus entailing a phrase structure error as the preposition requires a noun phrase to follow up. In semantically incongruous sentences, the verb could not satisfactorily be integrated into the preceding context due to its selectional restrictions. Correct prepositional sentences containing a prepositional phrase, which were not included in the final

fMRI analysis, provided a filler condition to avoid prediction of a syntactically incorrect sentence by simply the appearance of the preposition.

Table 3.1 Stimulus Examples for experimental conditions employed in the present study. The three critical conditions and the filler condition are shown in their original German wording and in English translation. Sentences were presented auditorily via headphones and participants performed an acceptability judgment.

Correct condition (COR)	'Der Frosch quakt' The frog croaks
Syntactic violation condition (SYN)	'Der Joghurt im schmeckt' The yoghurt in-the tastes good
Semantic violation condition (SEM)	'Der Stein blutet' The stone bleeds
Correct filler condition (FIL)	'Das Eis am Stiel schmilzt' The iced-lolly melts

This material had been evaluated previously to the experiment. Purpose of this pre-study was to confirm children's familiarity with vocabulary and sentence structure. Four-year-old children from local kindergartens participated in a behavioral experiment that included an acting-out paradigm. A set of entirely 440 items (110 per condition) was created. For the behavioral study, the sentences from the SEM and the FIL condition were selected. The rational behind was that SYN and COR conditions were based on the FIL condition. In the SYN condition, the second noun phrase, excluding the preposition, was absent. In the COR condition, the entire second noun phrase (including the preposition) was absent. Thus, a set of 220 sentences was evaluated. The acting-out paradigm required the children to help a hand puppy, sitting down on the experimenters' lap, to allocate statements to two stacks: either intelligible ones (those "… that can be said") or unintelligible one (those "… that cannot be said"). The puppy selected a small piece of paper from a messy cluster and requested the experimenter to read the statement written on it. The child received it and had to allocate it to

one of the stacks. The experiment was videotaped and children's judgments were assessed subsequently on the videotape basis by the experimenter. The experiment for each child was stopped when the child refrained to continue. Every item was required to be processed by at least 4 children to be regarded as reliably assessed.

On average, 29 sentences (range 14 to 51 items) were presented to each child. Thirty-eight children participated in the pre-study (mean age 4.5 years, range 4.1 to 4.8), resulting in 965 reliable item judgments. Items with less than four judgments were removed as well as items that were refuse to be intelligible by more than one child. Whether unintelligibility of items was based on missing vocabulary or on sentence structure was not distinguished. Rather, any item that did not fulfill the criteria of intelligibility was removed. Out of the 220 items evaluated, 72 were removed from further processing. The remaining 148 sentences constituted the basis for 66 items per condition. Finally, a set of 50 items per condition was selected for the experiment, the remaining items were used as preparation and practice items for the mock session (see below).

For the purpose of auditory presentation during the actual experiment, items were spoken by a trained female native speaker in a well pronounced and child-directed manner. All sentences were recorded and digitized at 44.1 kHz, 16 bit mono. For the syntactic violation, the speaker produced an entire phrase with a filler word after the preposition that was later spliced out of the speech signal by means of a speech-editing tool (Adobe Audition) to avoid possible prosodic or other acoustic cues that would differentiate conditions. To guarantee a natural sound of the sentences, they were listened to and confirmed by three independent experts. As mentioned above, the final item pool consisted of 50 items per condition. Conditions differed slightly in average length (correct condition = 1,769 ms, syntactically incorrect condition = 2,053 ms, semantically incongruous condition = 1,755 ms, and filler condition = 2,764 ms).

3.1.4 Procedure

Out of the 200 sentences, together with 25 null events, in which no stimulus was presented, two different stimulus sequences were pseudo-randomized from the material with constrains on consecutive trials for

different stimulus conditions and target verbs. These constrains comprised that (i) no more than 3 consecutive trials belonged to the same stimulus condition, (ii) no more than 4 consecutive trials contained either correct or incorrect/incongruous stimuli, (iii) repetition of the same noun or verb in another trial was only permitted after a gap of at least 15 items, and (iv) within 45 trials each of the condition should have occurred 10 times (null events 5 times). The two sequences were then reversed. Thus, four different lists of items resulted, which were pseudo-randomly assigned across participants, matched for gender and right hand/ left hand button allocation for behavioral responses.

Children participated in a mock MRI scanner session few days before the actual measurement to familiarize them with experimental setting, task, and scanner noise. Each child underwent a simulated scanner session including the task with stimuli similar but not identical to those presented during the actual fMRI measurement. To practice lying still in the scanner, the child got verbal feedback via headphones during the session. Children with too much movement or other problems during the mock session were excluded from the further study.

For the adult sample, each session contained 4 × 50 critical trials – plus 25 null events, in which the blood oxygenation level dependent (BOLD) response was allowed to return to a baseline state (Burock, Buckner, Woldorff, Rosen, & Dale, 1998). For children, one session contained 4 x 30 critical trials plus 15 null events, otherwise the procedure was the very same as the one used for adults.

Trials took 8 s each i.e., 4 scans of TR 2 s. Onset of every stimulus presentation relative to the beginning of the first scan was randomly jittered between 0, 500, 1,000, and 1,500 ms to get measurements at numerous time points along the BOLD signal curve, thus providing a higher resolution of the BOLD response (Miezin, et al., 2000). While listening to stimuli and during the entire measurement, participants could see an aquarium screensaver with fishes swimming calmly across the scene. Immediately after hearing a sentence, participants were required to judge the correctness of each stimulus. Maximum response time allowed was 2.7 s, identifying the type of error was not required. Participants indicated their responses by pressing buttons on two response boxes in their right and left hands, respectively. Right/left allocation of correct/incorrect judgments

was balanced between participants. Only correctly answered trials were included in subsequent analyses.

3.1.5 Data analysis

Data processing was performed by means of the software package LIPSIA (Lohmann, et al., 2001). Functional data were motion-corrected offline with the Siemens motion correction protocol (Siemens, Germany). Movement correction was allowed up to 3 mm (one voxel). Because of too much movement, datasets of three children had to be excluded from further analyses, another three datasets of children had to be cut after 376, 460, and 532 of 540 repetitions. To correct for the temporal offset between the slices acquired in one scan, a cubic-spline-interpolation was applied. A temporal highpass filter with a cutoff frequency of 1/60 Hz was used for baseline correction of the signal and a spatial gaussian filter with 4.239 mm full with at half maximum (FWHM) was applied. To align functional data slices with a 3D stereotactic coordinate reference system, a rigid linear registration with six degrees of freedom (3 rotational, 3 translational) was performed. Rotational and translational parameters were acquired on the basis of the MDEFT (Norris, 2000; Ugurbil et al., 1993) and EPI-T1 slices to achieve an optimal match between these slices and the individual 3D reference data set. The rotational and translational parameters were subsequently transformed by linear scaling to a standard size (Talairach & Tournoux, 1988). This linear normalization process was followed by a subsequent processing step that performed an additional nonlinear normalization (Thirion, 1998).

To test for the feasibility of a direct comparison between the two groups, anatomical data of both samples were inspected statistically. The extent of nonlinear normalization to a common adult stereotactic standard space was extracted for each dataset. A 2 (Group) × 3 (Dimension) repeated measures general linear model (GLM) revealed a main effect of Group, $F(1, 23) = 9.16$, $p < .01$. Because of this result and based on concerns in the literature regarding a common stereotactic space for adults and children younger than 7 years of age (Kang, Burgund, Lugar, Petersen, & Schlaggar, 2003), we refrained from a direct comparison between the two groups. A greater value of spatial normalization in children could have produced significant artifacts (Muzik, Chugani, Juhasz, Shen, & Chugani, 2000).

Therefore, adults and children were aligned to separate stereotactic spaces based on group averages.

Statistical evaluation of functional data was based on a least-squares estimation using the general linear model for serially autocorrelated observations (Friston, 1994; K.J. Friston, et al., 1995). The design matrix was generated with a synthetic hemodynamic response function (Friston, et al., 1998; Josephs, Turner, & Friston, 1997) and its first and second derivative. The model equation, including the observation data, the design matrix, and the error term, was convolved with a Gaussian kernel of 4 s FWHM dispersion to deal with the temporal autocorrelation (K.J. Worsley & Friston, 1995). Movement correction parameters were included as regressors into the model. For each participant, three contrast images were generated to represent the main effects of correct basic condition, syntactically incorrect condition, and semantically incongruous condition. Each individual functional dataset was aligned with the stereotactic group reference space.

Single-participant contrast images for each condition compared to baseline (null events) were entered into a second-level random-effects analysis for each of the contrasts. The random-effects model for group analysis consisted of a one-sample *t*-test across the contrast images of all subjects that indicated whether observed differences between conditions were significantly distinct from zero. Subsequently, *t*-values were transformed into *z*-scores. Group maps were thresholded at $z > 3.09$ ($p < .001$, uncorrected). In order to control for cumulating alpha errors, only clusters with a volume greater than 270 mm^3 (equivalent to 10 voxels) were considered.

Blobs of activation were analyzed in more detail by extracting clusters around local maxima of activity. Local maxima were defined by a peak activation within a search diameter of 4 voxels (12 mm) in any direction. Primary regions of interest (ROIs) were defined for further investigation: these regions were the STG and the IFG bilaterally to get a more fine-grained insight in their activation patterns. An epoch-averaged waveform for each subject and ROI was calculated and the time point of maximal BOLD change across all conditions was determined. Then, for each condition, the amplitude of the mean response within a 3 seconds time window, centered on the BOLD peak, was determined (Huettel, Song, & McCarthy, 2005). ROIs were analyzed by direct statistical comparison between conditions. To do so, contrast values of the selected local maxima were extracted

for each participant and entered in a repeated measures GLM (Bosch, 2000). ROIs that yielded a significant condition effect were further investigated by post-hoc test to evaluate the specific contrast between the three conditions. Post-hoc tests were Bonferroni corrected for multiple comparisons.

We also tested both groups for hemispheric lateralization. Firstly, we compared cluster sizes of cortical activation within temporal language areas between the two hemispheres. Clusters were extracted from individual fixed-effects *z*-maps, thresholded at $z > 3.09$. Only clusters greater than 162 mm³ (equivalent to 6 voxels) were considered. Data were analyzed by a 2 (Group) × 2 (Hemisphere) × 3 (Condition) repeated measures GLM. Additionally, these data were also analyzed by extracting a lateralization index (LI) by size of activated areas of the left (L) and the right (R) hemisphere for each participant by the formula [$LI = (L - R) / (L + R)$], that covers a co-domain of $-1 \leq LI \leq 1$. Positive values denote a more extended activation to LH, negative values a more extended activation to RH. Only values of at least ± .15 are considered to represent a significant lateralization, whereas values around 0 are considered to represent a bilateral activation pattern. Secondly, as an additional approach, we compared BOLD response amplitudes between both hemispheres. For that purpose, local maxima from the ROI analyses were selected for corresponding brain areas in the left and the right hemisphere. Equivalent contra-hemispheric local maxima were compared with each other. Statistical comparison by a repeated measures GLM indicated whether there was a significant lateralization effect for cortical activation or not.

In all GLMs, the Greenhouse-Geisser correction of degrees of freedom was applied (Greenhouse & Geisser, 1959).

3.2 Results

Results are presented for both groups consecutively. Behavioural results are followed by functional imaging data which in turn are subdivided into, first, the presentation of the sentence comprehension network and brain areas that participate in it and, second, an investigation or functional language lateralization.

3.2.1 Behavioural results

Response accuracy rates for adults and children are summarized in Figure 3.1. A 2 (Group) × 3 (Condition) repeated measures GLM revealed no significant main effect of Group [$F(1, 23) = 1.64$, $p = .21$] or Condition [$F(2, 46) = 1.07$, $p = .35$], nor a significant Group × Condition interaction [$F(2, 46) = 1.82$, $p = .18$].

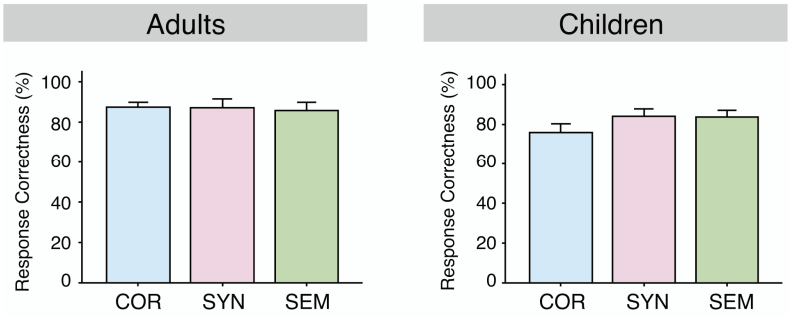

Figure 3.1 Behavioral data: Means and standard errors of response correctness for both groups in the correct condition (COR), syntactically incorrect condition (SYN), and semantically incongruous condition (SEM), with no main effect of condition or group and no interaction.

Participants were not instructed to respond as fast as possible, still the data were scrutinized for reaction times. Adults were faster than children, and produced an average reaction time of 448.5 ms (SD = 181.8), while the average reaction time in children was 1148.8 ms (SD = 299.6), resulting in main effects of Group [$F(1, 23) = 52.50$, $p < .0001$] and also Condition [$F(2, 46) = 3.29$, $p < .05$], but with no Group × Condition interaction [$F(2, 46) = 1.78$, $p = .18$].

3.2.2 Functional imaging results

3.2.2.1 The language network

BOLD contrast main effects of increased activation are reported per group for each of the experimental conditions compared to baseline. Subsequently, direct statistical comparison between conditions is provided to evaluate the extent of activation increase based on a specific violation condition. The data from the two groups are presented in succession.

Adults

Activation main effects for each condition, COR, SYN, and SEM, are displayed in Figure 3.2. In baseline comparison, correct sentences activated the STG bilaterally, most pronounced in mid STG and ant STG. Syntactically incorrect sentences involved areas along the entire STG including ant STG, mid STG, and post STG as well as the left anterior frontal operculum (aFO). Semantically incongruous sentences elicited stronger activation of mid STG and post STG bilaterally and the left posterior frontal operculum (pFO). For all conditions, some involvement of cingulate cortex (CC) and basal ganglia (BG) as well as cerebellum and thalamus was observed. Activation clusters of the adult group are listed in Table 3.2.

Direct comparisons between the three different conditions for different ROIs revealed the following results. The SYN condition showed selectively enhanced activation along the STG at the left ant STG [(-56, 3, -6), $F(2, 24) = 7.88$, $p < .005$], the left mid STG [(-50, -12, 3), $F(2, 24) = 12.79$, $p < .001$], and left post STG [(-56, -39, 12), $F(2, 24) = 19.57$, $p < .001$] as well as the right post STG [(40, -33, 9), $F(2, 24) = 13.36$, $p < .001$]. Additionally, the aFO (-32, 27, 0) was selectively recruited [$F(2, 24) = 7.42$, $p < .01$] for the SYN condition. For the SEM condition, a more medial and posterior region in the pFO (-35, 18, 0) showed a significant condition effect [$F(2, 24) = 6.15$, $p < .05$]. As revealed by post-hoc analysis, the effect was based on a SEM vs. COR contrast ($p < .05$) only. For SEM condition, no specific enhancement of activation was observed in the STG, suggesting a large overlap of activation for the three conditions with only enhanced activation observed for the SYN condition. Local maxima of activation in defined ROIs are added in Table 3.2.

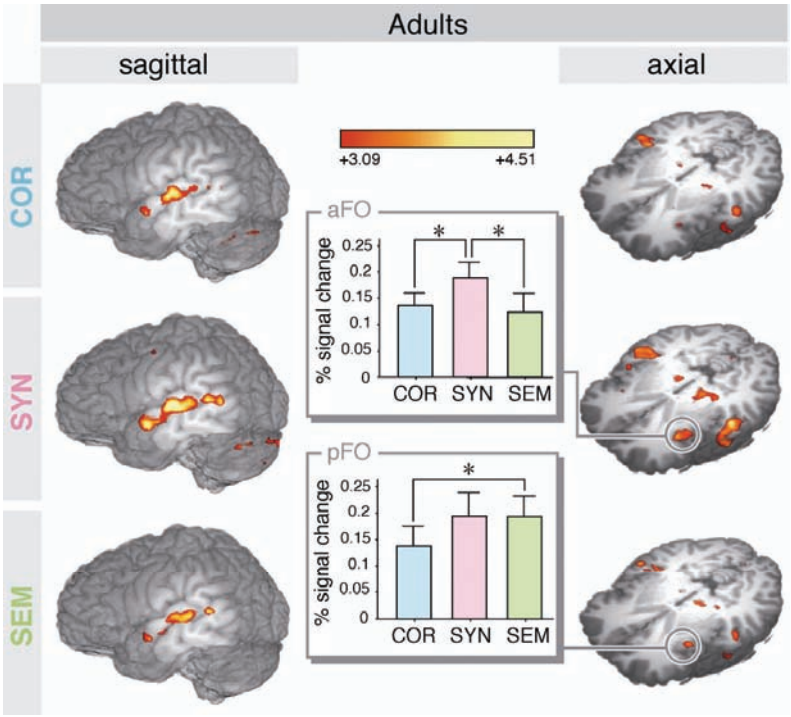

Figure 3.2 BOLD contrast main effects for the adult group in the three critical conditions, mapped on a 3D rendered reference brain in sagittal and axial sections. Bar graphs illustrate condition effects in the anterior frontal operculum (aFO) at -32, 27, 0 for the syntactic violation (SYN) and the posterior frontal operculum (pFO) at -35, 18, 0 for the semantic violation (SEM).

Table 3.2 Gray matter brain regions reliably activated in adults with cluster size in mm³, Talairach coordinates, and maximum z-value. Data are shown for the three critical conditions against resting baseline (null events). The size column indicates total size of activated clusters and incorporates subregions in ROIs. The Location column indicates location (x, y, z) of activation clusters and of local maxima within the ROIs.

COR = correct condition, SYN = syntactic violation, SEM = semantic violation; BG = basal ganglia, CC = cingulate cortex, IFG = inferior frontal gyrus, FO = frontal operculum, STG = superior temporal gyrus, ant = anterior, mid = mid-portion, post = posterior.

	Left Hemisphere			**Right Hemisphere**		
	Size	**Location**	**Z-max**	**Size**	**Location**	**Z-max**
COR vs. Baseline						
Perisylvian Cortex	4,617			3,969		
ant STG		-59 0 -6	3.58		49 0 -6	3.60
mid STG		-44 -21 15	3.80		43 -15 6	4.03
mid STG		-56 -12 6	3.89			
mid STG		-62 -27 9	3.49			
CC	648	-5 6 42	3.47			
CC	270	-8 -27 30	3.87			
BG	486	-23 24 6	3.81			
Precuneus				297	28 -54 48	3.73
Cerebellum	10,611	-35 -54 -21	4.62	12,177	28 -60 -21	4.65
Cerebellum	378	-20 -78 -39	3.56			
SYN vs. Baseline						
Perisylvian Cortex	13,581			12,933		
ant STG		-56 3 -6	3.99		46 3 -6	3.58
mid STG		-50 -12 3	4.32		40 -18 6	4.21
mid STG					55 -24 6	3.71
post STG		-56 -39 12	3.75		40 -33 9	4.08
post STG		-62 -48 12	3.78			
FO	1,728	-32 27 0	3.80			
CC	621	-5 9 42	3.36			
Precuneus				1,836	28 -54 45	3.90
Cerebellum	17,604	-41 -63 -18	4.40	15,525	34 -69 -21	4.49

	Left Hemisphere			Right Hemisphere		
Cerebellum	729	-8 -54 -21	3.57			
	Size	**Location**	**Z-max**	**Size**	**Location**	**Z-max**
SEM vs. Baseline						
Perisylvian Cortex	2,484			3,969		
mid STG		-50 -15 6	3.87		40 -18 6	3.88
mid STG		-62 -27 9	3.82			
post STG		-59 -39 12	3.71		40 -33 9	3.85
FO	378	-35 18 0	3.59			
CC	540	-5 18 39	3.88	405	1 24 33	3.82
Cerebellum	297	-8 -54 -24	3.74	270	1 -51 -12	3.34
Cerebellum	6,939	-23 -84 -18	4.16	6,426	22 -75 -33	4.11

The inferior frontal activation in the FO was scrutinized in more detail in order to clarify its exact location. The deep frontal operculum is very closely located to the anterior insular cortex which in turn has been reported in several studies to participate in a variety of cognitive functions including language processing (Augustine, 1996). Therefore, it is important to differentiate inferior frontal activation in the FO from activation in the anterior insula in order to draw valid conclusions on the network of activated cortical areas involved in sentence comprehension. The analysis was conducted by selecting assorted voxels of interest in the very vicinity of the activation found in the study, especially of the posterior activation observed in the SEM condition which was closest located to the insular cortex. These voxels were selected in the axial plane (z = 0) in anterior lateral (FO) and posterior medial (insula) direction surrounding the observed activation. Voxels were in the FO: A. -38, 23, 0; B. -41, 19, 0; C. -40, 15, 0, and in the insula: D. -28, 17, 0; E. -32, 12, 0; F. -36, 6, 0. The analysis of nearby voxels aimed to designate the activation to one of the cortices by inspection of the hemodynamic response in those voxels in close proximity even if the activation was too weak to show up in the overall statistics. The differences in activation are assumed to be informative. If one of the cortices was involved in sentence processing and not the other, differences in the activation time course should be found in these voxels.

A 2 (Cortex: FO vs. insula) × 3 (Subregion: 3 subregions within each cortex) × 3 (Condition: COR, SYN, SEM) within-subject GLM revealed a significant

effect for factor Cortex of $F(1, 12) = 22.54$, $p < .001$ and a three-way interaction of Cortex × Subregion × Condition, but no other significant effect. This result leads to the conclusion that it is the frontal operculum rather than the insula which is involved in sentence comprehension (see Figure 3.3).

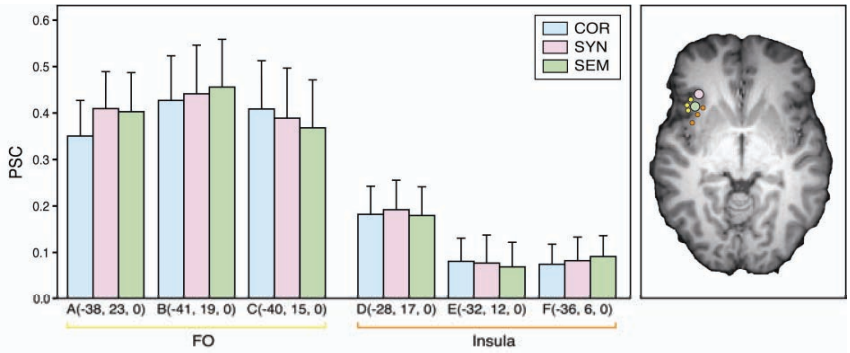

Figure 3.3 Activation in voxels closely located to the inferior frontal activation observed for the SYN and the SEM conditions. On he right-hand brain map, activation areas for SYN (pink) and SEM (green) conditions are indicated by big spots. The smaller spots indicate voxels selected for the analysis of activation in the inferior frontal cortex. The data points indicate coordinates of three voxels in the inferior frontal cortex (yellow: A. -38, 23, 0; B. -41, 19, 0; C. -40, 15, 0) and three voxels in the insular cortex (orange: D. -28, 17, 0; E. -32, 12, 0; F. -36, 6, 0) located closely to the observed frontal opercular activation.

Bar graphs on the left show extracted values of percent signal change (PSC) in these voxels for all three conditions (COR - correct, SYN – syntactic violation, and SEM – semantic violation). Statistical comparison revealed a strong main effect for factor Cortex (FO vs. insula, see text for details).

Children

Children showed an overall broader distribution of activation for all conditions compared to baseline (see Figure 3.4). For correct sentences, the entire left STG (anterior, mid, and posterior) showed extended involvement, whereas in the right hemisphere especially the ant STG and mid STG were activated. Further regions of enhanced activity for the correct condition were found in lateral IFG, FO, and SMG. Both, in the SYN and in the SEM

conditions, again the entire STG was solidly activated bilaterally (anterior, mid, posterior) together with lateral IFG, FO, and SMG. All three conditions also showed some involvement of CC, BG, cerebellum, and thalamus. See Table 3.3 for a comprehensive list of activated brain areas.

Direct comparisons between the different conditions were performed for selected ROIs in more detail. For the SYN condition, only one area (-50, 17, 21), located in the left IFG (Broca's area), was selectively recruited, $F(2, 22) = 5.41$, $p < .05$, see Figure 3.4. There was no exclusively activated region in any other conditions. Thus, a large overlap between the three conditions was confirmed statistically. Local maxima of activation in defined ROIs are listed in Table 3.3.

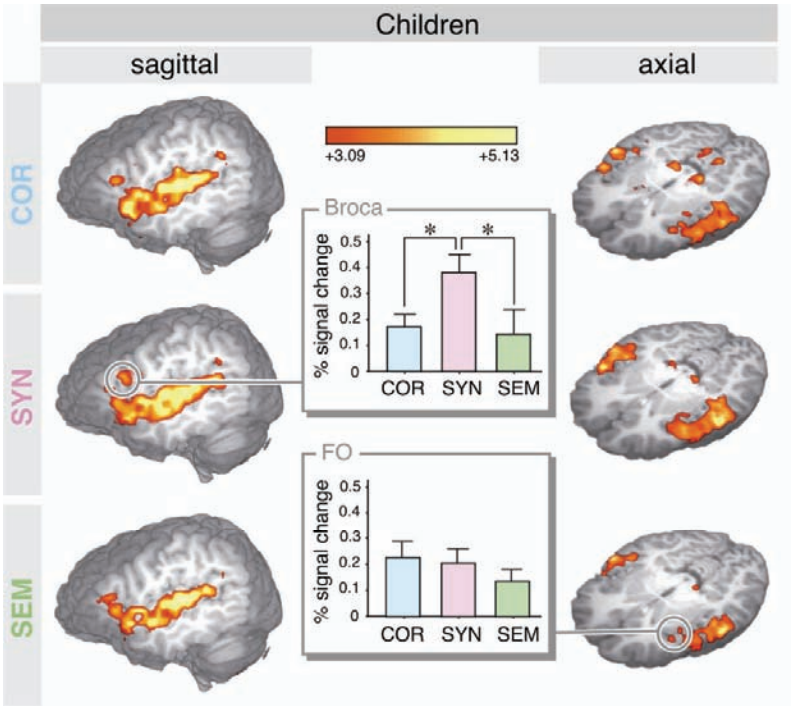

Figure 3.4 BOLD contrast main effects for the children's group in the three critical conditions, mapped on a 3D rendered reference brain in sagittal and axial sections. Bar graphs illustrate a condition effect in Broca's area (-50, 17, 21) and no differentiation between conditions in the frontal operculum (FO) (-32, 14, -3).

Table 3.3 Gray matter brain regions reliably activated in children with cluster size in mm^3, Talairach coordinates, and maximum z-value. Data are shown for the three critical conditions against resting baseline (null events). The size column indicates total size of activated clusters and incorporates subregions in ROIs. The Location column indicates location (x, y, z) of activation clusters and of local maxima within the ROIs.

COR = correct condition, SYN = syntactic violation, SEM = semantic violation; BG = basal ganglia, CC = cingulate cortex, FG = frontal gyrus, FO = frontal operculum, IFG = inferior frontal gyrus, MFG = middle frontal gyrus, PG = precentral gyrus, SMG = supramarginal gyrus, STG = superior temporal gyrus, ant = anterior, mid = mid-portion, post = posterior, TC = temporal cortex.

	Left Hemisphere			**Right Hemisphere**		
	Size	**Location**	**Z-max**	**Size**	**Location**	**Z-max**
COR vs. Baseline						
Perisylvian Cortex	46,170			20,520		
ant STG		-44 14 -9	4.93		52 14 -9	3.45
ant STG					46 2 3	4.57
mid STG		-59 -7 9	5.12		58 -1 3	4.95
mid STG		-41 -19 9	5.44		49 -13 9	4.90
mid STG		-50 -7 9	5.17			
mid STG		-47 -19 0	4.05			
mid STG		-44 -4 -6	4.42			
post STG		-50 -31 15	5.12			
post STG		-62 -43 18	3.54			
post STG		-50 -55 15	3.21			
IFG		-50 8 3	4.27		49 8 3	4.31
IFG		-44 14 24	4.20		49 20 0	4.52
IFG		-53 20 15	3.99		40 20 -9	3.65
FO		-35 29 3	4.09		28 23 6	4.51
SMG		-47 -49 30	4.02			
MFG	648	-35 35 36	3.83	270	46 41 18	3.72
MFG				351	40 2 48	3.61
CC				4,212	7 17 21	4.32
CC				2,025	4 -25 30	4.59
BG	540	-5 20 3	3.65	1,080	1 11 3	4.28
BG				567	19 11 -12	3.97
Mesial TC				324	25 -10 -12	3.70

	Left Hemisphere			Right Hemisphere		
	Size	**Location**	**Z-max**	**Size**	**Location**	**Z-max**
Precuneus				324	13 -58 42	3.52
PG	378	-41 -10 45	3.57	837	13 -10 15	3.72
Cerebellum	270	-8 -52 -21	4.19	2,754	10 -52 -6	4.75
Cerebellum				324	31 -49 -18	3.69
SYN vs. Baseline						
Perisylvian Cortex	35,478			37,827		
ant STG		-44 14 -9	5.15		52 8 -6	4.82
ant STG		-47 2 3	5.13			
mid STG		-44 -19 -3	4.46		43 -4 -3	5.58
mid STG		-59 -7 6	5.77		52 -4 9	5.33
mid STG		-56 -16 9	5.27		52 -19 6	5.31
mid STG					37 -25 15	5.21
post STG		-62 -31 6	4.63			
post STG		-59 -40 9	4.31			
post STG		-50 -43 18	4.72			
IFG		-50 17 21	3.91		46 17 21	4.82
IFG		-44 8 15	3.88		49 17 0	4.94
IFG		-41 11 24	4.29			
FO		-41 23 -9	4.17		31 17 9	4.21
FO					37 23 15	4.98
SMG		-47 -46 33	3.70	675	52 -43 27	3.91
CC	729	-5 17 24	4.12	270	1 35 18	3.75
CC	1,836	-8 14 42	3.87	648	4 -25 30	4.33
CC	1,323	-11 -40 24	3.89	270	4 -40 21	3.43
CC	405	-20 -64 12	3.97			
Medial FG	270	-11 47 24	3.86	513	1 53 18	4.29
PG				702	46 -7 45	4.34
SEM vs. Baseline						
Perisylvian Cortex	21,843			13,041		
ant STG		-44 17 -18	3.29			
ant STG		-47 11 -6	4.52		52 8 -6	4.02
mid STG		-59 -10 9	5.46		58 -1 0	4.66
mid STG		-44 -4 -6	4.45		46 -1 -3	4.14
mid STG		-44 -16 9	5.05		49 -16 3	4.67

	Left Hemisphere			Right Hemisphere		
	Size	**Location**	**Z-max**	**Size**	**Location**	**Z-max**
mid STG					34 -22 12	4.78
post STG		-53 -43 15	5.05		58 -28 9	4.37
post STG		-41 -40 21	4.30			
IFG		-47 8 3	4.55			
FO		-41 14 6	3.62			
FO		-32 14 -3	3.71			
FO		-35 11 12	3.87			
SMG		-56 -52 24	3.84			
CC	1,350	-5 20 42	4.53	1,944	10 2 39	3.95
BG	351	-20 -1 9	3.66			
PG	378	-32 5 33	3.51			
Cerebellum				486	4 -70 18	3.83
Cerebellum				351	10 -58 -39	3.59

3.2.2.2 Language lateralization

To investigate language lateralization in adults and children, we also compared the recruitment of language-related brain areas between both hemispheres in an analysis with the factors Condition (COR, SEM, SYN) × Group (adults, children) × Hemisphere (left, right). This lateralization analysis according to cluster sizes in temporal activation areas revealed a significant main effect for Condition [$F(2, 30) = 4.70$, $p = .035$], a marginal main effect for Group [$F(1, 15) = 3.51$, $p = .081$], and a marginal effect for a Hemisphere × Group interaction [$F(1, 15) = 3.27$, $p = .091$], which statistically endorse the observed lateralization differences between both groups. Other main effects or interactions were not significant.

A reliable lateralization (LI of at least ± .15) to the left was observed in 4 adults (mean LI = .39, SD = .14), none was lateralized to the right, and 8 were bilateral (mean LI = .01, SD = .08) (one missing for too small activation clusters). In children, only one was lateralized to the left (LI = .22), five to the right (mean LI = -.21, SD = .04), and 6 were bilateral (mean LI = .03, SD = .06).

According to a ROI approach of BOLD response size, cortical activation in adults was lateralized to the left within the ant STG for SYN and COR condition, within the mid STG for COR condition, and within the post STG

for SEM condition. A bilaterally equivalent activation was found for both the SEM and SYN conditions within the mid STG and for the SYN condition within the post STG. Moreover, the FO was reliably activated in LH only. In children, cortical activation was less left-lateralized. Bilateral activation was observed within the temporal cortex in the ant STG for all three conditions and in the mid STG for COR and SEM condition, within the lateral IFG for the SYN condition and within the FO for SYN and COR condition. A left-lateralization, however, was seen in the mid STG for the SYN condition and in the lateral IFG for the COR condition. Right-lateralized activation was found within the post STG for the SEM condition and within the SMG for the SYN condition. There were also several areas reliably recruited only in LH: post STG in COR and SYN condition, lateral IFG and FO in the SEM condition, and SMG in COR and SEM condition (see Table 3.4).

3.3 Discussion

The findings of the present fMRI experiment indicate that children by the age of 6 years have not reached the mature stage with respect to specification of semantic and syntactic processes in the language network. At this developmental stage the neural substrates for semantic and syntactic processes are less specialized than in the mature brain. While the adult language comprehension network differentiates aspects of language such as semantic and syntactic processes, the developing language system in 6-year-olds activates the entire comprehension network largely disregarding the particular requirements currently to be met. Adults demonstrated function specific activations in the STG and the frontal operculum of the IFG, conversely, children showed a large activation overlap for these two language aspects in the STG. Compared to adults, they engaged additional areas in the left and right IFG which are known to support resource demanding processes. The only functional-neuroanatomically already specialized brain area was found in the left lateral IFG, specifically in Broca's area, for the processing of syntactic information. Thus, the language networks for semantic and syntactic processes are not yet specialized similarly to adults in the developing brain at age 6. Both semantic and syntactic processes demand a higher involvement of the entire IFG at this age than in adulthood.

Table 3.4 Language lateralization according to BOLD response size for both groups. The table lists the results of a direct comparison between local maxima in contra-hemispheric equivalent brain regions ($p < .05$). Only areas with significant activation on both hemispheres are contrasted against each other.
L = left-lateralized, R = right-lateralized, Bi = no significant lateralization (bilateral), LH = reliable activation exist only in the left hemisphere for the specified structure; COR = correct condition, SYN = syntactic violation, SEM = semantic violation; lat. IFG = lateral inferior frontal gyrus, FO = frontal operculum, ant STG = anterior part of superior temporal gyrus, mid STG = mid portion of superior temporal gyrus, post STG = posterior part of superior temporal gyrus.
In adults, 67 % of activated language areas are lateralized to the left, none to the right, and 33 % are bilaterally involved. In children, 44 % of activated language areas are lateralized to the left, 11 % to the right, and 44 % are bilaterally involved.

Brain region	**Adults**			**Children**		
	COR	**SYN**	**SEM**	**COR**	**SYN**	**SEM**
ant STG	L	L	-	Bi	Bi	Bi
mid STG	L	Bi	Bi	Bi	L	Bi
post STG	-	Bi	L	LH	LH	R
lat. IFG	-	-	-	L	Bi	LH
FO	-	LH	LH	Bi	Bi	LH
SMG	-	-	-	LH	R	LH

A possible confound for broader activation in children could have been due to the fact that children performed less critical trials than adults, resulting in more noise in their data. Hence, we tested for that possibility. We simulated a shorter experiment in adults equivalent to that in children by cancelling timesteps at the end of the recorded datasets. However, the total number of active voxels did not increase, rather it decreased slightly. This proves that the broader activation in children cannot be attributed to experiment length. We observed a greater value of movement correction in

children, this could be a possible source of more noise in the children's data. However, we controlled for movement by (i) excluding children with too much movement, (ii) inspecting each single dataset for movement artifacts, (iii) applying a movement correction algorithm, and (iv) including movement correction parameters into the general linear model. Hence, if at all, movement-related noise should contribute only little to the observed group differences. Another possible confound for the group differences could be a practice effect, since children practiced the task in a mock-scanner session and adults did not. However, there are two arguments against such an interpretation. First, children are supposed to have overall less experience and practice with auditory language processing than adults. Second, if children had experienced a practice effect, they should have shown less activation than adults (Bergerbest et al., 2004; Hasson et al., 2006; Meister et al., 2005). Instead, they show more activation. Thus, the mock-scanner session is unlikely contributing to the observed group differences.

We observed lower differentiation in children between syntactic and semantic processes indicated by the larger overlap in functional brain activation compared to adults. This observation corresponds to behavioral studies on language development in children between the ages of 5 years to 11 years which implied stronger interrelation of syntax and semantics during early childhood with syntactic processing becoming more and more independent of semantic processing with increasing age (Friederici, 1983). In contrast to those earlier results, children in our study did not commit more errors during syntactic and semantic processing than adults. This was not surprising and rather expected given the straightforward material constructed to be easy to process by children in order to enable a direct contrast of processing costs for syntactic and semantic processes of auditory language comprehension without interfering processing demands that would make group comparisons more difficult to interpret. However, despite the equal response correctness, we observed longer reaction times for children. This is in agreement with previous findings on reactions times where even 11-year-olds have not yet reached an adults level of reaction times during sentence processing, probably due to still ongoing development of their ability to process structural information like adult listeners (Friederici, 1983).

The present study demonstrated that children at the age of 6 years make use of the same perisylvian language comprehension network as adults during auditory sentence processing. However, they also show differences in activation patterns with an overall broader activation, less differentiation between certain aspects of language such as syntax and semantics, stronger involvement of the IFG, especially for syntactic processes, and less functional lateralization to the left hemisphere. While the network in adults comprises the STG and the FO, children make supplementary use of Broca's area. Studies in adults have shown that Broca's area is known to participate in language processing when syntactic processing costs increase (Bornkessel, et al., 2005; Friederici, Fiebach, et al., 2006; Stromswold, Caplan, Alpert, & Rauch, 1996). Hence, the present data support the conclusion of higher processing costs for children compared to adults during auditory sentence comprehension.

4 Study 2 – Temporal organization of the functional auditory language comprehension network

The present study is not a separate experiment by itself. Rather, it is a novel reanalysis of previously presented data (cf. Study 1). However, for reason of the entirely different approach to the data, this study was conceded a chapter on its own.

The present research extended on the initial work on children's language comprehension as elaborated in the previous chapter by focusing on the time course of activation in language-related brain regions. Specifically, here we investigated temporal dynamics of the BOLD signal within brain areas involved in language comprehension.

As elaborated in the previous chapter, the perisylvian region of the human cortex plays a major role in language processing, especially the STG and the IFG. As presented so far, syntactic and semantic processing during language comprehension require higher involvement of the perisylvian language areas in 6-year-old children compared to adults. Crucial areas of activation were primarily Broca's area, its right-hemispheric homologue and the FO bilaterally in the IFG as well as the STG bilaterally. In adults, IFG and STG were also involved, but IFG activation was limited to the left hemispheric FO, whereas activation of the more lateral part of IFG (Broca's area) was lower than in children and remained below threshold. Interestingly, adults showed differentiation between semantic and syntactic processes in the FO and along the STG, whereas children only showed such a functional differentiation in Broca's area.

In the present research, the timing of recruitment of these language-related brain areas in both hemispheres was examined as a function of age using functional imaging data of 6-year-old children and adults with a special focus on BOLD response time courses. In order to gain a more fine-grained insight into the temporal dynamics' development of language-related brain recruitment in IFG and STG, we analyzed the time course of the BOLD response during sentence processing in these regions. Time-to-peak information was extracted from the hemodynamic response. The time-to-peak

measure has been confirmed a very robust parameter along the BOLD time course (Neumann, Lohmann, Zysset, & von Cramon, 2003).

The results show that children's activation time courses differ from that of adults. First, children show an overall later peak of BOLD responses. Second, children's IFG responds much later than their STG, while in adults the difference between both regions is less pronounced. Within the STG, both groups show similar regionally U-shaped activation patterns with fastest peaks in voxels at the STG's mid-portion around Heschl's gyrus and longer latencies in anterior and posterior directions, suggesting a coarsely similar information flow in adults and children in the temporal region. Finally, children in contrast to adults, display a temporal primacy of right over left hemispheric activation. The observed overall latency differences between children and adults are in line with the assumption of ongoing maturation in perisylvian brain regions and the connections between them. A functional perspective on BOLD timing argues for a developmental change from higher processing costs in children compared to adults due to slower and less automatic language processes, in particular those located in the IFG. The observed hemispheric differences are discussed in the context of developmental models assuming a high reliance on right-hemisphere-based suprasegmental information processing during language comprehension in childhood.

The main results and conclusions of the present study were published in (Brauer, Neumann, & Friederici, 2008).

4.1 Methods

4.1.1 Participants and materials

Data of 13 adults (7 female mean age 25.9 years, SD = 2.7) and 12 children (8 girls, mean age 6.2 years, SD = 0.7) were available. Parents of the children and the adult participants themselves gave written, informed consent. Children gave verbal assent for attendance. All children had normal intelligence and language skills and no known neurological or psychiatric disease or disorder or medical treatment affecting the central nervous system. None of the adult participants had any history of neurological or psychiatric disorder. All participants were right-handed German native speakers

(Oldfield, 1971). The study was approved by the Research Ethics Committee of the University of Leipzig (Leipzig, Germany).

Stimulus material consisted of short sentences in active voice with age appropriate vocabulary. Items were spoken by a trained female native speaker in a well-pronounced, child-directed manner. All sentences were recorded and digitized at 44.1 kHz, 16 bit mono. They had an average length of about 2 seconds. For the adult sample, the session contained 200 trials plus 25 null events, in which the BOLD response was allowed to return to baseline state (Burock, et al., 1998). For children, the session contained 120 trials plus 15 null events. Otherwise the procedure was the same as that used for adults. Trials were presented every 8 seconds in a single session. Consequently, the experiment consisted of 30 min stimulation for adults, 18 min for children. While listening to stimuli and during the entire measurement, participants could see an aquarium screensaver with fishes swimming calmly across the scene. Onset of every stimulus presentation relative to the beginning of the first scan was randomly jittered between 0, 500, 1,000, and 1,500 ms to get measurements at numerous time points along the BOLD signal curve, thus providing a higher resolution of the BOLD response (Miezin, et al., 2000).

A comprehensive description of participants and materials can be found in Study 1 (chapter 3.1).

4.1.2 Scanning parameters

For functional measurements, a gradient-echo EPI sequence was used (TE 30 ms, flip angle 90°, TR 2 s, bandwidth 100 kHz, matrix 64 × 64 voxels, FOV 192 mm, in-plane resolution 3 × 3 mm,) at 3 T (Siemens TRIO, Germany) for 20 slices (slice thickness 4 mm, 1mm gap), covering a range of z = -40 mm to z = 60 mm from the AC-PC line. T1-weighted modified driven equilibrium Fourier transform (MDEFT) images (Ugurbil, et al., 1993), matrix 256 × 256, TR 1.3 s, TE 7.4 ms, with a non slice-selective inversion pulse followed by a single excitation of each slice (Norris, 2000) were used for registration. For anatomical data, a T1-weighted 3D magnetization-prepared rapid gradient echo (MP-RAGE) sequence was obtained with magnetization preparation consisting of a non-selective inversion pulse (TI 650 ms, TR 1.3 s, snapshot FLASH 10 ms, TE 3.97 ms, angle 10

degrees, bandwidth 67 kHz, matrix 256 × 240, slab thickness 192 mm, sagittal orientation, spatial resolution 1 × 1 × 1.5 mm). To avoid aliasing, oversampling was performed in read direction (head-foot). For further details, see chapter 3.1.

4.1.3 Data analysis

Since our main interest was the temporal dynamics of the BOLD response in general language comprehension, no distinction between syntactic and semantic information processing was made in order to increase signal-to-noise ratio. Rather, language stimulation in general was contrasted against resting baseline (null events). Data processing was conducted with the LIPSIA software package (Lohmann, et al., 2001) and included motion correction using three translational and three rotational parameters, slice time correction (cubic-spline-interpolation), highpass filtering (1/60 Hz), and spatial smoothing (4.24 mm full width at half maximum, FWHM). Motion correction was allowed up to 3 mm (one voxel). Three datasets of children were cut after 376, 460, and 532 of 540 repetitions for too much movement. Rotational and translational parameters of rigid linear registration were transformed to standard size by linear scaling (Talairach & Tournoux, 1988), followed by a nonlinear normalization (Thirion, 1998).

Statistical evaluation of functional activation was based on a general linear regression with pre-whitening (K. J. Worsley, et al., 2002). Specifically, autocorrelation parameters were estimated from the least squares residuals using the Yule-Walker equations. These parameters were subsequently used to whiten both data and design matrix. Finally, the linear model was re-estimated using least squares on the whitened data to produce estimates of effects and their standard errors. The design matrix was generated with a synthetic hemodynamic response function (Friston, et al., 1998; Josephs, et al., 1997) and its first and second derivatives. Movement correction parameters and stimulus duration were included as regressors. For each participant, one contrast image was generated to represent the main effect of sentence presentation vs. baseline. Individual functional datasets were aligned with the stereotactic group reference space.

Statistical evaluation of BOLD time course was based on the following procedure. Individual fixed-effects *z*-maps at $z > 2.33$ ($p < .01$, uncorrected)

were generated and used to mask individual preprocessed raw data. This was to guarantee that only reliably activated voxels would enter subsequent analysis where BOLD response information was obtained voxel-wisely from trial-averaged time courses for each subject by aligning the onsets for individual trials and averaging across these trials at a sampling rate of 5 Hz. Time points falling between measured data points due to jittering and the lower sampling rate for measuring were linearly interpolated from weighted values of their neighbors. Specifically, for two measured time points t1 and t2, the value x at a time point t0 between these two was calculated as

(Eq. 4.1) $$x_{t0} = (1-w_1) * x_{t1} + (1-w_2) * x_{t2},$$

where x_{ti} are the signal values of the time course at time point ti, and w_1 and w_2 are normalized distances of time points t1 and t2 to time point t0. Thus, the value of a time point closer to t0 gets a higher weight in the linear interpolation than the time point further away.

Trial averages obtained for null-events were subtracted from critical trial averages. Subsequently, maximum amplitude (in percent signal change, peak maximum minus preceding minimum) and the corresponding time-to-peak measures were determined for every time course within a time range from 3 to 12 seconds as described by Neumann et al. (2003). Finally, time course parameters were averaged for both groups separately and entered in group maps. Further analyses investigated the perisylvian language region more closely. The region was subdivided into subclusters of activation to examine their contributions in more detail. The IFG was subdivided into Broca's area and FO, the STG was subdivided along the *y*-axis in three subparts: anterior (ant STG), mid-portion (mid STG), and posterior STG (post STG). In order to acquire ROI time-to-peak values, voxel-wisely extracted time course information was averaged across subjects for each group and ROI, and obtained values were entered in repeated-measures GLM for statistical comparison.

Bonferroni correction for multiple comparisons of post-hoc analyses and Greenhouse-Geisser correction of degrees of freedom were applied as required (Greenhouse & Geisser, 1959; Shaffer, 1995).

4.2 Results

FMRI data on sentence comprehension in adults and children were analyzed with a focus on time courses of IFG and STG contributions to language processing in both groups. BOLD response parameters extracted voxel-wisely from individual preprocessed EPI maps were obtained. Only active voxels within IFG and STG were entered in subsequent analyses (see Figure 4.1).

We first tested contributions of the IFG in adults at the lower threshold. This preceding analysis should confirm a sufficient involvement of this area in adults, since strong activation within the IFG was found for both groups in the FO, but only for children in Broca's area at a higher threshold in a previous analysis (cf. chapter 3). Analysis revealed Broca's area activation in adults with a maximum *z*-value of 2.80 (children: 3.88). To get further evidence for a lower but significant involvement of Broca's area in adults, data were investigated for percent signal change (PSC) within the IFG. PSC values (incl. SD) for adults were 0.78 (0.23) in Broca's area and 0.84 (0.24) in Broca's homologue, 0.50 (0.10) in left FO and 0.53 (0.11) in right FO, for children 1.10 (0.47) in Broca and 0.97 (0.48) in Broca's homologue, 0.70 (0.22) in left FO and 0.74 (0.33) in right FO. Data were investigated by a 2 × 2 × 2 repeated-measures GLM with between-subject factor Group (children, adults) and within-subject factors Area (Broca, FO) and Hemisphere (left, right). A significantly lower PSC of Broca's area in adults would result in a Group × Area interaction. However, we found significant effects for Area, $F(1,23) = 38.12$, $p < .001$, and Group, $F(1,23) = 4.63$, $p < .05$, but no effect for hemisphere, $F(1,23) < 1$, and no significant interaction: Group × Area: $F(1,23) < 1$, Group × Hemisphere: $F(1,23) = 1.54$, $p = .23$, Area × Hemisphere: $F(1,23) = 1.40$, $p = .25$, Group × Area × Hemisphere: $F(1,23) = 2.65$, $p = .12$. Thus, children show higher PSC values than adults, and Broca's area higher PSC values than the FO. The main effect for Area without a Group × Area interaction indicates the same tendency for IFG recruitment in children and adults.

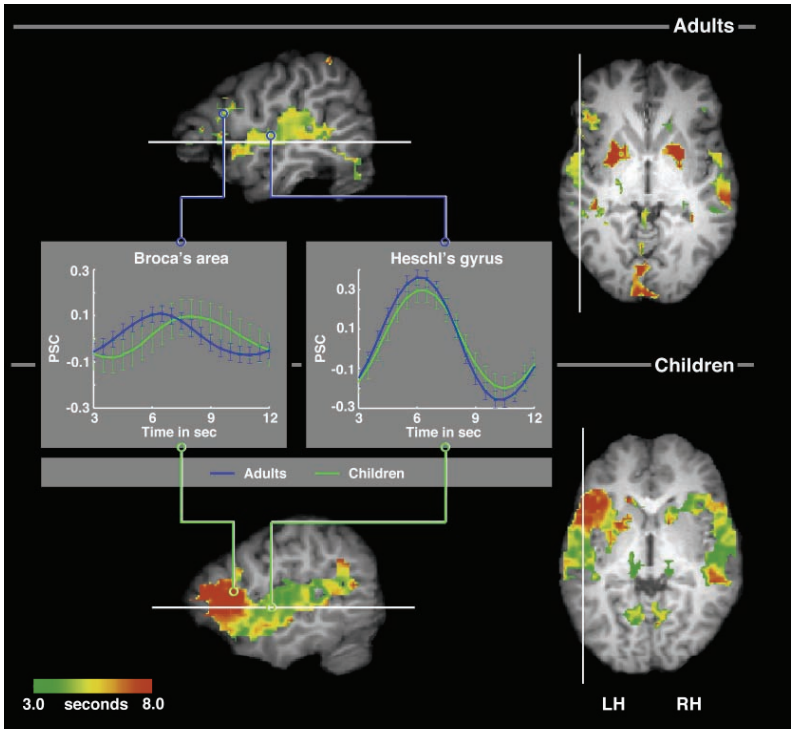

Figure 4.1 Temporal organization of cortical activation during sentence comprehension for adults and children in sagittal section (x = -50, left) and horizontal section (z = 2, right). Data are masked by random-effects activation maps at z > 2.33 and display a color coding for time-to-peak values in active voxels between 3.0 and 8.0 seconds. The lines indicate the cut for the corresponding section. Note the very late response in the inferior frontal cortex in children and their hemispheric differences in this region. Inserted diagrams demonstrate examples of BOLD responses to sentence comprehension in Broca's area (BA) and in Heschl's gyrus (HG) showing percent signal changes (PSC) between 3.0 and 12.0 seconds for adults and children. Talairach coordinates BA: adults -49 17 17, children -49 12 11, HG: adults -52 -10 8, children -46 -12 2. BOLD response information is obtained voxel-wisely from preprocessed raw data. Crosses and standard error bars indicate measured data points (TR 2 s with onset jitter of 0.5 s). Line graphs illustrate subsequent interpolation (resolution 0.2 s).

In order to investigate temporal dynamics of language-related brain activation in the perisylvian region, we investigated BOLD response time-to-peak latencies more closely in inferior frontal cortex and superior temporal cortex. Time-to-peak information was obtained and statistically compared between groups and hemispheres for Broca's area, FO, ant STG, mid STG, and post STG. Active voxels within these areas were entered in a 5 (Area) × 2 (Hemisphere) × 2 (Group) repeated-measures GLM. Analysis revealed a significant main effect for Group with time-to-peak mean values (incl. SD) of 5.8 s (0.4) for adults and 6.7 s (0.6) for children. There was also a significant main effect for Hemisphere, LH: 6.4 s (0.9), RH: 6.1 s (0.6), and a main effect for Area with fastest responses in the STG [mid STG: 5.7 s (0.6), ant STG: 6.2 s (0.8), post STG: 6.3 s (1.0)] and slower responses in the IFG [Broca: 6.6 s (0.9), FO: 6.6 s (1.0)]. Interactions were found for Group × Area and for Group × Hemisphere, and also the Group × Area × Hemisphere interaction yielded significance (see Figure 4.2 and Table 4.1). Consequently, post-hoc analyses were run for each level of factor Area with the following results. In the IFG, a Group main effect was found for Broca's area with BOLD latencies of 6.0 s (0.5) for adults and 7.2 s (0.8) for children. Also for the FO area, analysis yielded a significant Group effect [adults: 6.0 s (0.6), children: 7.2 s (0.9)], and, moreover, a Group × Hemisphere interaction, based on a significant hemispheric difference in children [LH: 7.8 s (1.3), RH: 6.6 s (0.7)], $F(1,11) = 8.37$, $p < .05$, while there was no such hemispheric effect in adults [LH: 5.8 s (0.6), RH: 6.1 s (0.8), $F(1,12) = 2.77$, $p = .37$]. In the STG, for mid STG and post STG, a significant Group effect was observed: mid STG 5.4 s (0.4) for adults and 6.0 s (0.6) for children, post STG 5.7 s (0.4) for adults and 6.8 s (1.2) for children, while no significant effect was observed for ant STG (see Table 4.2).

A post-hoc analysis of the overall Group × Hemisphere interaction from the initial 5 × 2 × 2 analysis revealed this effect to rely on hemispheric differences in children [LH: 7.0 s (0.8), RH: 6.4 (0.6), $F(1,11) = 8.27$, $p < .05$], not in adults [LH: 5.8 s (0.5), RH: 5.8 s (0.4), $F(1,12) < 1$].

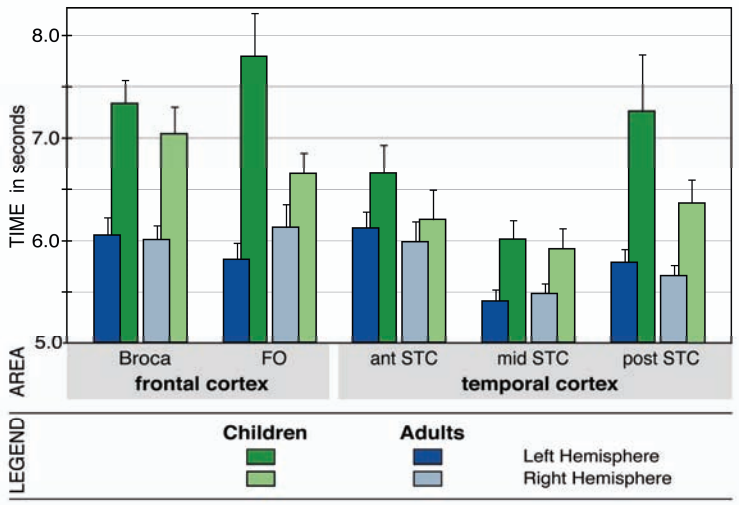

Figure 4.2 Bar graphs for time-to-peak latencies in seconds (+ standard error) in perisylvian language areas for children and adults within the left and the right hemisphere. In both groups, data show fastest responses in mid STG and shorter latencies in temporal cortex than in frontal cortex in both groups. However, children show overall longer latencies than adults and their fronto-temporal latency differences are much more pronounced than the fronto-temporal differences in adults. Furthermore, children, but not adults, demonstrate hemispheric differences with slower left than right hemispheric activation (cf. Figure 4.1).

Broca = Broca's area, FO = frontal operculum, STG = superior temporal cortex, ant = anterior, mid = mid-portion, post = posterior.

Results indicated a robust main effect of Group in the initial 5 × 2 × 2 GLM, confirmed by the same effect in nearly all areas in the post-hoc analysis. That indicates overall longer BOLD latencies in children than in adults. The Area effect in the initial analysis is based on an equivalent tendency in both groups with shortest latencies in the mid STG and longest latencies in the IFG. While in post-hoc analyses in the FO area of the IFG a significant Group × Hemisphere interaction was found, no such interaction was observed in STG areas. The overall main effect of Hemisphere was confirmed in the children's FO, and for both groups marginally ($p < .10$) in the STG (ant and post).

Table 4.1 Repeated-measures GLM results for BOLD time-to-peak. Factors are between-subject factor Group (adults, children) and within-subject factors Area (Broca, FO, ant STG, mid STG, post STG) and Hemisphere (left, right).

Broca = Broca's area, FO = frontal operculum, STG = superior temporal cortex.

Effect	***df***	***F*-value**	***p*-value**
Group	1,23	17.89	$p < .001$
Area	4,92	10.47	$p < .001$
Hemisphere	1,23	7.67	$p < .05$
Group × Area	4,92	3.15	$p < .05$
Group × Hemisphere	1,23	8.63	$p < .01$
Area × Hemisphere	4,92	1.90	$p = .16$
Group × Area × Hemisphere	4,92	3.56	$p < .05$

In a separate region analysis, the timing of inferior frontal and superior temporal contributions was contrasted. For that purpose, a 2 × 2 × 2 repeated-measures GLM was conducted with between-subject factor Group (children, adults) and within-subject factors Area (IFG, STG) and Hemisphere (left, right). Statistical comparison yielded significant main effects for all three factors as well as significant Group × Area, Group × Hemisphere, and Group × Area × Hemisphere interactions (see Table 4.3A). Interactions were further investigated by a follow-up analysis comparing each level of factor Group separately. Results revealed an Area main effect for adults with IFG: 6.0 s (0.5), STG: 5.7 s (0.4). For children, too, an Area main effect was observed, IFG: 7.2 s (0.8), STG: 6.4 s (0.6), and also the Hemisphere main effect in children was confirmed, LH: 7.0 s (0.8), RH: 6.4 (0.6) (see Table 4.3B). Theses results reveal the differences between children and adults with respect to the timing of inferior frontal and superior temporal contributions, as pointed out by the Group × Area interaction. Although both groups demonstrate later IFG than STG activation, this effect size was only moderate in adults ($\eta_p^2 = .41$), while the same effect was large in children ($\eta_p^2 = .65$).

Table 4.2 Repeated-measures GLM results for BOLD time-to-peak, post-hoc analysis for factor Area. There is a significant Group effect in Broca, FO, mid STG, and post STG, and a significant Group × Hemisphere interaction in the FO.

Broca = Broca's area, FO = frontal operculum, STG = superior temporal gyrus, ant = anterior, mid = mid-portion, post = posterior.

		Broca		**FO**		**ant STG**		**mid STG**		**post STG**	
Effect	***df***	***F*-value**	***p*-value**	***F*-value**	***p*-value**	***F*-value**	***p*-value**	***F*-value**	***p*-value**	***F*-value**	***p*-value**
Group	1,23	19.55	$p < .001$	16.81	$p < .001$	1.51	$p = .46$	6.75	$p < .05$	9.47	$p < .01$
Hemisphere	1,23	1.94	$p = .36$	3.72	$p = .13$	5.48	$p = .06$	< 1		4.90	$p = .07$
Group × Hemisphere	1,23	1.07	$p = .62$	11.65	$p < .01$	1.61	$p = .43$	1.80	$p = .39$	2.70	$p = .23$

Table 4.3 Contrast of IFG vs. STG BOLD time-to-peak measures (Table 4.3A). Factors are between-subject factor Group (adults, children) and within-subject factors Area (IFG, STG) and Hemisphere (left, right). The Group × Area and the Group × Hemisphere interactions reveal distinct patterns of frontal vs. temporal activation time courses for both groups. A follow-up analysis for both Groups separately reveals the Area effect for each Group, although lower effect size in adults (η_p^2 = .41) than in children (η_p^2 = .65). The Hemisphere effect is based on a hemispheric distinction in children, but not in adults (Table 4.3B).

IFG = inferior frontal gyrus, STG = superior temporal gyrus, LH = left hemisphere, RH = right hemisphere.

T**able 4.3A** BOLD time-to-peak contrast for IFG vs. STG areas

Effect	***df***	***F*-value**	***p*-value**
Group	1,23	18.98	p < .001
Area	1,23	29.52	p < .001
Hemisphere	1,23	7.21	p < .05
Group × Area	1,23	7.61	p < .05
Group × Hemisphere	1,23	9.24	p < .01
Area × Hemisphere	1,23	< 1	
Group × Area × Hemisphere	1,23	5.32	p < .05

Table 4.3B Post-hoc analysis for IFG vs. STG separated by levels of factor Group

Adults

Effect	***df***	***F*-value**	***p*-value**
Area	1,12	8.56	p < .05
Hemisphere	1,12	< 1	
Area × Hemisphere	1,12	3.00	p = .22

Children

Effect	***df***	***F*-value**	***p*-value**
Area	1,11	19.96	p < .05
Hemisphere	1,11	8.39	p < .05
Area × Hemisphere	1,11	2.42	p = .30

4.3 Discussion

This study examined temporal BOLD response properties in perisylvian language areas in 6-year-old children and adults. In both groups, similar brain regions in inferior frontal and superior temporal cortices were activated bilaterally. Analysis of BOLD amplitudes in Broca's area and FO revealed reliable involvement of Broca's area in adults albeit observable only at a lower threshold than in children.

Children as well as adults showed shortest BOLD latencies in the STG's mid-portion, i.e., within and close to the primary auditory cortex, and longer latencies in the anterior and the posterior STG as well as in the IFG. Although there was an overall equivalent time course pattern of perisylvian areas across the two groups, significant Group × Area and Group × Hemisphere interactions speak to the fact that the timing of activation in language area is different for the developing network of 6-year-olds than for the mature network. The time course pattern of children is characterized by much later involvement of the IFG as well as a marked hemispheric differentiation showing faster responses in the right compared with the left hemisphere.

We excluded a possible confound of experiment length on the group differences by an additional analysis. Since the experimental session for children was shorter than for adults (540 vs. 900 scanning repetitions), the effect for BOLD latencies could have been based on the longer experiment in adults. We simulated a shorter experiment in adults by truncating the adult datasets after 540 repetitions. Accordingly, we obtained a short and a long version of the experiment for adult participants. A repeated-measures GLM for these two versions yielded no effect of factor Length [$F(1,12) = 1.20$, $p = .29$] and no interaction of Length with any other factor: Length × Area [$F(4,48) < 1$], Length × Hemisphere [$F(1,12) < 1$], Length × Area × Hemisphere [$F(4,48) < 1$]. Hence, length of experiment cannot explain the observed group differences.

Based on findings from previous studies which reported delayed BOLD latencies as a function of cognitive demands such as e.g., verbal working memory (Thierry, et al., 2003), we conclude that prolonged BOLD latencies in children might be related to increased processing demand for language comprehension. This interpretation, moreover, seems to converge with the

result of stronger activation in children in perisylvian language areas. However, other factors cannot be excluded so far to contribute to the observed group differences in BOLD latency. These factors, such as properties of cerebral blood flow or the integrity of brain white matter fiber pathways connecting cortical areas, might not be directly linked to language processing, but to brain maturation and development in general.

Taken together, the present study presented evidence for particular properties of the developing language comprehension system beyond straightforward activation size differences as reported in Study 1. Rather, distinct hemodynamic response properties were revealed for those perisylvian brain areas involved in language processing and its development.

5 Study 3 – Anatomical networks of cortical connectivity in perisylvian language areas in adults and children

Diffusion-weighted imaging provides the opportunity to examine the white matter pathways in the human brain that connect cortical areas of functional interest. Investigations in the human brain by DTI rely for example on the white matter's fractional anisotropy (FA), i.e., the stronger directionality of water diffusion along fiber tracts. Moreover, anisotropy might be subject to systematic variation under certain circumstances. It was shown that reduction in anisotropy follows white matter degeneration after traumatic brain injury (Kraus, et al., 2007), cerebral ischemia and stroke (Sotak, 2002; Ulug, Beauchamp, Bryan, & Vanzijl, 1997), in multiple sclerosis (Terajima, Matsuzawa, Tanaka, Nishizawa, & Nakada, 2007), or amyotrophic lateral sclerosis (ALS) (Ellis, et al., 1999). Hence, sufficient integrity of fiber pathways in the brain appears to be a necessary precondition for a healthy level of functioning.

But differences in anisotropy do also exist aside from traumatic or pathological white matter degeneration. The brain undergoes functional and structural changes during development. Structural maturation affects the cortical surface and subcortical gray matter and, moreover, white matter fiber tracts. The main index of white matter maturation is its myelination with age. Pujol et al. (2006) investigated white matter myelination in human infants and children at 0 to 40 months of age. They reported increasing myelination in white matter with age. Particularly interesting was a later myelination increase in perisylvian language regions compared to sensorymotor regions. Furthermore, the maturation within language regions coincided with an increase in language abilities.

Also the increase in anisotropy after (and even already before) birth is likely to be a consequence of fiber myelination. However, myelination is not necessary for anisotropy, but it is a facilitating factor (Beaulieu & Allen, 1994). Increases in axonal density or axonal thickness are likewise conceivable factors.

In the present study, white matter fiber tracts in adults and 7-year-old children were investigated with a special focus on those pathways that presumably participate in the language network. Children were found to have smaller values of FA than adults, probably due to less myelination of fiber tracts in the immature brain. Direct comparison of white matter FA indicated that particularly perisylvian regions in superior temporal and left inferior frontal areas differed between adults and children. Especially the superior longitudinal fasciculus (SLF) showed prominent differences between groups, but also between hemispheres with higher FA on the language dominant left than on the right hemisphere. Comparison between fiber anatomy and functional activation during auditory language comprehension suggested adults and children to distinctly rely on pathways connecting perisylvian language areas. Children seem to support their not yet fully matured language network between IFG and STG by supplementary functional involvement of inferior frontal areas that connect the IFG with the STG via an inferior fronto-temporal connection that essentially involves the extreme capsule and the inferior fronto-occipital fasciculus (IFO).

5.1 Methods

5.1.1 Data acquisition

The experiment was carried out on a 3 Tesla scanner (Siemens TRIO, Germany). Diffusion-weighted data and high-resolution T1-weighted images were acquired on a whole-body 3 Tesla Magnetom Trio scanner (Siemens, Erlangen) equipped with an 8-channel head array coil. Written informed consent was obtained from all subjects in accordance with the ethical approval from the University of Leipzig. Diffusion-weighted images were acquired with twice-refocused spin echo echo-planar-imaging sequence (Reese, Heid, Weisskoff, & Wedeen, 2003), TE = 100 ms, TR = 12 s, 128 x 128 image matrix, NEX = 3, FOV = 220 × 220 mm^2, providing 60 diffusion-encoding gradient directions with a b-value of 1000 s/mm^2 (gradient duration: $delta_1$ = 12.03 ms, $delta_2$ = 19.88 ms, $delta_3$ = 21.76 ms, $delta_4$ = 10.15 ms). The herewith realized high angular resolution of diffusion directions improved reliability of probability estimation by reduced directional bias as well as increased signal-to-noise ratio per unit time. Seven

images without any diffusion weighting are obtained at the beginning of the scanning sequence and after each block of 10 diffusion-weighted images as anatomical reference for offline motion correction. The interleaved measurement of 72 axial slices with 1.7 mm thickness (no gap) covered the entire brain. Random noise in the data was reduced by averaging 3 acquisitions. Additionally, fat saturation was employed together with 6/8 partial Fourier imaging, Hanning window filtering and parallel acquisition (generalized auto-calibrating partially parallel acquisitions, GRAPPA, with reduction factor = 2). In order to limit the acquisition time, cardiac gating was not employed. For functional measurements, the same parameters were applied as in Study 1 and Study 2.

5.1.2 Participants

The study was approved by the Research Ethics Committee of the University of Leipzig (Germany). Seven-year-old children, recruited through letter announcements in local kindergartens, participated in the study. Data of 12 children were obtained, 2 of them had to be excluded from further analysis due to movement in the scanner during data acquisition. Thus, data of 10 children (5 girls) were available (mean age 7.0 years, SD 1.1, range 5.6 to 8.7). Five of the children had participated in Study 1. Interested parents were invited for education and clarification of facts about the experiment and procedures. They gave written, informed consent. Children gave verbal assent prior assessment and scanning.

Diagnostic measures obtained from all children. They underwent psychological diagnostics, including expressive and receptive language skill assessment as extensively described in Study 1. The same tests and criteria with identical requirements for participation as described in Study 1 where administered. Additionally, 10 adults (5 female, mean age 27.8 years, SD, 2.7, range 24.4 to 32.4) participated in the study after informed consent. Four of them had participated in Study 1. None had any history of neurological or psychiatric disorders. All participants were right-handed and German native speakers. Functional data on auditory language processing where available from all participants.

5.1.3 Materials

For the functional MRI part of the study, the same stimulus material as described in Studies 1 and 2 was applied, consisting of short sentences in active voice intelligible for children. Participants were asked to judge the correctness of the sentences while they were auditorily presented via headphones.

5.1.4 Data analysis

Data were processed using the software packages LIPSIA (Lohmann, et al., 2001) and FSL (S. M. Smith, et al., 2004). T1-weighted structural scans were used for skull-stripping, and the brain images were then co-registered into Talairach space (Talairach & Tournoux, 1988). The 21 images without diffusion weighting distributed in the whole sequence were used to estimate motion correction parameters using rigid-body transformations (Jenkinson, Bannister, Brady, & Smith, 2002). Motion correction for the 180 diffusion-weighted images was combined with a global registration to the T1 anatomy computed with the same method. The registered images were interpolated to the new reference frame with an isotropic voxel resolution of 1 mm and the three corresponding acquisitions and gradient directions were averaged. Finally, for each voxel, a diffusion tensor was fitted to the data. Voxel-wise analysis of diffusion data was performed by tract-based spatial statistics (TBSS) (Stephen M. Smith, et al., 2006), implementing the following steps. FA images of each individual were nonlinearly registered on the dataset that most closely approached the group mean anatomy. A skeletonization algorithm was applied that defined a group template for white matter tracts. Registered individual maps were projected onto the group template, and mean FA and diffusivity images were produced.

In order to test for white matter group differences between children and adults, we statistically compared the FA skeleton deformation for a joint co-registration including both groups. Deformation vector fields were obtained for a nonlinear registration on a common standard space. The target image for this procedure was selected on the basis of mutual alignment of every FA image on every other to identify the most representative FA image for the whole sample according to Smith et al. (2006). Values of image distortions for alignment were extracted for each voxel in each individual FA

image and compared on the basis of a repeated measures 2 (Group) × 3 (Dimension) GLM. Results revealed no main effect for Group [$F(1, 17) < 1$], nor Dimension [$F(2, 34) = 1.1$, $p = 0.33$], nor a significant interaction [$F(2, 34) < 1$]. Thus, there were no differences between groups in the amount of image distortion for nonlinear registration on a common source model. These results support the conclusion of low between-subject variance regarding FA images, even between children and adults. Accordingly, both groups were registered on a common standard space.

The anatomical connectivity and fiber orientation in human brain white matter was investigated by fiber tracking to compute the degree of connectivity between voxels in the diffusion tensor maps. The quantification of fiber connections in DTI maps was computed probabilistically based on the mathematical background of a Monte Carlo simulation in order to identify fiber orientation and connectivity. The transition of a modeled fiber tract direction from one voxel to a neighboring voxel is thereby described by the highest transition probability between a voxel and all its neighbors. A 3D extension of the random walk method as e.g., proposed by Koch et al. (2002) was applied on the whole white matter space with a predefined seed voxel.

Nonlinear registration was also compared for whole brain T1 images. Again, the same dataset as in the FA images registration which was closest to the entire group mean served as source image for the registration algorithm. Values of image distortion were extracted for each voxel and compared statistically on basis of a repeated measures 2 (Group) × 3 (Dimension) GLM. There was no main effect for Group [$F(1, 17) < 1$] and also no main effect for Dimension [$F(2, 34) < 1$], nor a significant interaction [$F(2, 34) < 1$]. Hence, EPI data of adults and children could be registered on a common source brain.

Statistical evaluation of functional activation was based on a general linear regression as described in detail for Study 2. Sentence comprehension was contrasted against resting baseline (null events). Data processing steps were identical to Study 1. Single-participant contrast images for sentence comprehension compared to baseline (null events) were entered into a second-level random-effects analysis consisting of a one-sample *t*-test across the contrast images of all subjects that indicated whether observed differences between conditions were significantly distinct from zero. Subse-

quently, *t*-values were transformed into *z*-scores. Group maps were thresholded at $z > 3.09$ ($p < .001$, uncorrected). In order to control for cumulating alpha errors, only clusters with a volume greater than 270 mm^3 (equivalent to 10 voxels) were considered.

Blobs of activation were analyzed in more detail by extracting clusters around local maxima of activity. Local maxima were defined by peak activation within a search diameter of 6 voxels (18 mm) in any direction. Broca's area was defined as a primary region of interest (ROI) for further investigation in order to define seed voxels for a connectivity analysis by tractography. For this ROI, a two-sample *t*-test was conducted across the two groups. For the smaller search space in a ROI with less false positives, threshold and cluster size were reduced compared a whole brain analysis. Threshold was set to $z > 2.58$ ($p < .005$, uncorrected). Controlling for cumulating alpha errors, only clusters greater than 81 mm^3 (equivalent to 3 voxels) were considered. The resulting contrast image was supposed to indicate whether observed differences between groups were significantly distinct from each other.

In all GLMs, Bonferroni correction of post-hoc analyses and the Greenhouse-Geisser correction of degrees of freedom was applied as required (Greenhouse & Geisser, 1959).

5.2 Results

In the following, results of a direct statistical comparison of FA between adults and children are presented, followed by a closer investigation of specific perisylvian fiber pathway connections. Finally, fMRI data on auditory language processing served as a basis to compare functional processing and underlying structural fiber pathways connecting cortical activation areas.

5.2.1 DTI and tractography results

This section will first refer TBSS results of FA for the whole brain white matter skeleton compared between groups. Afterwards, by means of fiber tractography, three main white matter tracts of the perisylvian region connecting inferior frontal and temporal areas are examined more closely,

i.e., a dorsal connection via the superior longitudinal fasciculus (SLF), a ventral fronto-temporal connection via the extreme capsule and the inferior fronto-occipital fasciculus (IFO), and the rostral connection between the inferior frontal and the anterior temporal region via the uncinate fasciculus (UNC).

5.2.1.1 Tract-based spatial statistics

Direct comparison of whole brain fractional anisotropy in white matter pathways was conducted between children and adults by tract-based spatial statistic. Adults showed overall higher FA than children. Regions with significant differences in FA were found in superior temporal, left inferior frontal, and premotor perisylvian areas (see Figure 5.1). Further regions of FA differences between groups were found in the corpus callosum and in inferior parietal areas. A comprehensive list of brain regions is presented in Table 5.1.

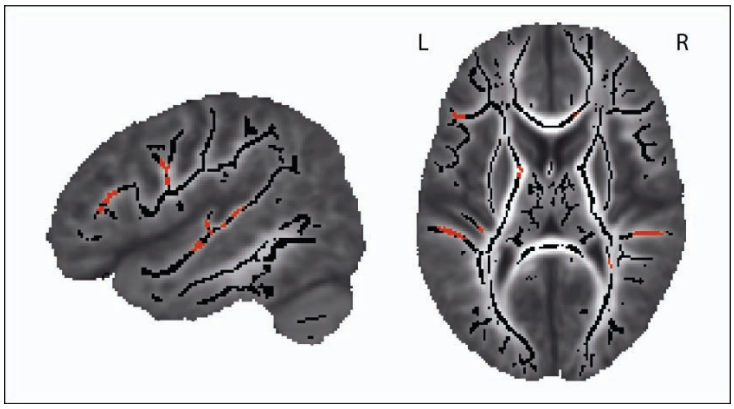

Figure 5.1 Tract-based spatial statistics across adults and children. The figure represents a mean FA image with the white matter skeleton superimposed (in black). Areas with significant differences between groups are highlighted in red. They indicate lower FA values in children compared to adults (p > .05, corrected). The brain is displayed in axial (z = 13) and sagittal slices (x = -44), featuring group differences in the left hemispheric perisylvian region.

Table 5.1 The table lists regions of sig. white matter differences ($p < .05$, corrected) in FA between adults and children including location (Talairach coord) and cluster size. All regions indicated lower FA values in children than in adults. ACR = ant corona radiata, CC = corp callosum, CST = corticospinal tract, IC = internal capsule, IFG = inf front gyrus, ILF = inf longitud fasciculus, L = left, R = right, SLF = sup longitud fasciculus, SMA = suppl motor area, STG = sup temp gyrus, PCG = precent gyrus, PCR = post corona radiate.

Region	Location (x y z)			Size in mm³
L IFG (ant SLF)	-45	22	17	96
L vent PCG (SLF)	-45	-1	27	194
L dors PCG (SLF)	-32	-18	35	144
L cent STG (ILF)	-43	-18	1	497
L post STG (SLF, ILF)	-49	-28	12	82
L int capsule (genu of IC)	-13	-3	6	204
L int capsule (post-vent IC)	-15	-28	6	165
L SMA (CC)	-14	-2	54	91
R vent postcent gyrus (SLF)	47	-13	35	78
R vent PCG (SLF)	44	-4	34	83
R inf pariet lobule (SLF)	29	-35	32	86
R cent STG (ILF)	38	-10	-6	156
R post STG (SLF, ILF)	46	-25	9	372
R dors PCG (CST)	18	-21	59	114
R dors postcent gyrus (CST)	24	-33	60	96
R post MFG (ACR)	25	13	43	85
R precuneus (PCR)	8	-56	36	136
R dors cuneus (PCR, PTR)	11	-82	29	100
R cingulum (cingulum)	8	-7	31	363
R tapetum (PCR)	22	-45	25	174
R CC (genu of CC)	11	25	2	138

5.2.1.2 Tractography of white matter fiber pathways

Probabilistic fiber tracking was obtained from normalized and averaged DTI images to reveal single pathways of the language networks in adults and children. The three most important fiber pathways of the perisylvian region connecting inferior frontal and superior temporal areas were tracked, i.e., SLF, IFO, and UNC. Results for all three fasciculi and both groups are shown in Figure 5.2.

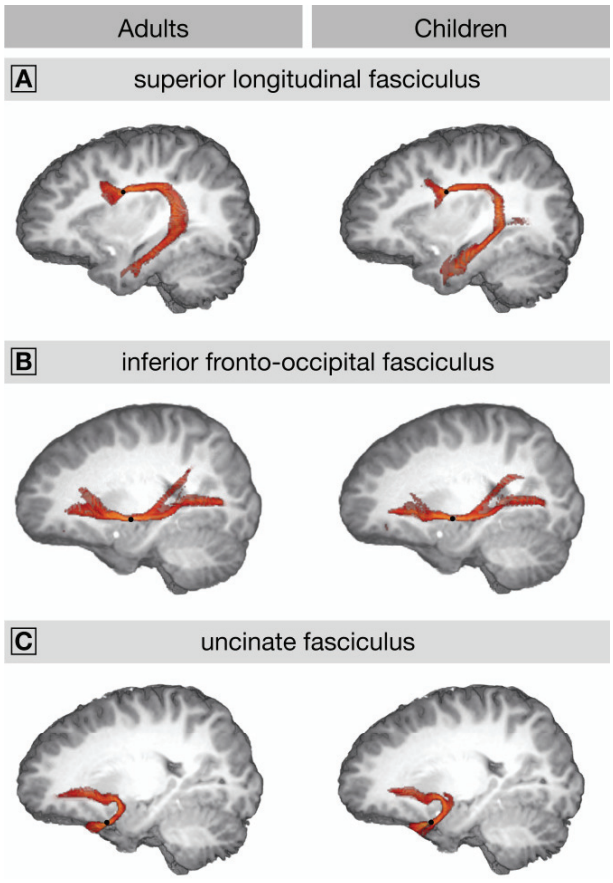

Figure 5.2 The figure shows the results of probabilistic fiber tracking ($p > 0.6$) for three main fiber pathways of the perisylvian region in the left hemisphere for adults and children. The superior longitudinal fasciculus (SLF) connects lateral temporal and inferior frontal areas via a dorsal projection that arcs just around the sylvian fissure extending into the inferior longitudinal fasciculus

(ILF) (A), while the inferior fronto-occipital fasciculus (IFO) connects the frontal and the occipital cortex via a temporal connection where it is accompanied by accompanying temporal projections via the extreme capsule and the ILF (B). Finally, the uncinate faciculus (UNC) connects the deep ventral part of the inferior frontal cortex with the anterior temporal cortex on a direct route (C). Black dots indicate the seed points for tractography with the following Talairach coordinates: SLF -37, -6, 28, IFO -30, -10, -4, and UNC -35, 7, -21. Tracking results are projected onto a 3D rendered anatomical brain sliced at -28 for the SLF and at -20 for the IFO and the UNC.

Children's tractogram data showed weaker pathways compared to adults in the tractograms. The fasciculi comprised volumes of 2032 voxels for the SLF in adults and 1887 in children, 1992 voxels for the IFO in adults and 1654 in children, and 1387 for the UNC in adults, 1193 in children. In both groups, the SLF is the largest fasciculus, followed by the IFO, and the UNC is the smallest. Adults showed overall stronger fasciluli than children.

5.2.1.3 Lateralization of perisylvian fasciculi

In order to test for maturational effects of fiber anisotropy in selected perisylvian pathways, we statistically investigated FA values in SLF, IFO, and UNC bilaterally. The pathways were tracked on the basis of a whole group map to generate tract masks. Tracking results (probability 0.6) were then restricted to a target region in order to prevent branching or crossing fibers to be included in the tract mask and to constrain the result to the core fiber pathway. The SLF was tracked from seed points at -37, -6, 28 for the left and at 34, -5, 28 for the right SLF (coordinates in Talairach space). SLF tractograms were restricted in y direction to a target region of > -50. The IFO was tracked from seed points at -30, -10, -4 for the left and 29, -12, -6 for the right IFO. The target regions were restricted to $-50 \leq y \leq 20$ and to $-10 \leq z \leq 10$. The UNC was tracked originating in -35, 7, -21 for the left and in 35, 7, -21 for the right UNC. Target regions were restricted to $18 \leq x \leq -18$ and to $-6 \leq y \leq 20$. Out of these fiber tracking results, brain masks were constructed and applied to each individual FA map. Hence, six clusters of FA values were extracted for each participant, for three fibers and two hemispheres.

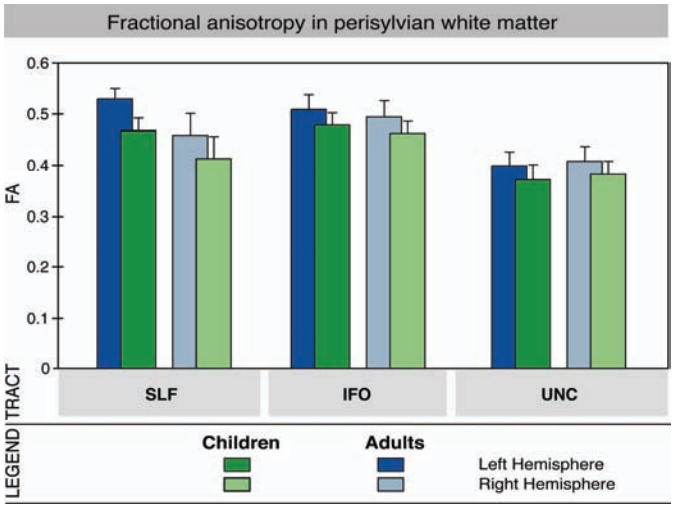

Figure 5.3 Fractional anisotropy (FA) of three perisylvian fiber pathways bilaterally in adults and children, namely superior longitudinal fasciculus (SLF), inferior-occipital fasciculus (IFO), and uncinate fasciculus (UNC). Statistical comparison revealed higher FA for adults than children and for the left than for the right hemisphere. Furthermore, there were significant interactions of tracts with group as well as hemisphere. For further information, see the text.

Masked FA values were entered in a 3 (Tract) × 2 (Hemisphere) × 2 (Group) repeated-measures GLM. Analysis revealed a significant main effect for Group with FA mean values (incl. SD) of 0.466 (0.021) for adults and 0.429 (0.025) for children. There were also significant main effects for Hemisphere, LH: 0.459 (0.022), RH: 0.436 (0.023), and for Tract with highest FA in the IFO: 0.486 (0.028) and lowest FA in the UNC: 0.390 (0.028), while the SLF showed FA values of 0.467 (0.039). Interactions were found for Group × Tract and for Tract × Hemisphere (see Figure 5.3 and Table 5.2).

Table 5.2 Repeated-measures GLM results for FA in selected fiber tracts. Factors are between-subject factor Group (adults, children) and within-subject factors Tract (SLF, IFO, UNC) and Hemisphere (left, right).

Effect	***df***	***F*-value**	***p*-value**
Group	1,18	13.55	$p < .01$
Tract	2,36	189.07	$p < .001$
Hemisphere	1,18	43.39	$p < .001$
Group × Tract	2,36	3.93	$p < .05$
Group × Hemisphere	1,18	< 1	
Tract × Hemisphere	2,36	63.14	$p < .001$
Group × Tract × Hemisphere	2,36	1.06	$p = .34$

Post-hoc analyses were run to more profoundly investigate significant interactions. In order to evaluate which level of the factor Tract was responsible for the Tract × Group and the Tract × Hemisphere interaction, a post-hoc analysis was run for each level. Results revealed that particularly the SLF exhibited larger FA for adults: 0.494 (0.028) than for children: 0.440 (0.030), while differences between groups were less pronounced but still significant in IFO [adults: 0.501 (0.028), children: 0.470 (0.020)]. However, no significant differences but a tendency ($p < .1$) was observed for the UNC [adults: 0.404 (0.025), children: 0.377 (0.025)]. Corresponding effect size for the SLF was $\eta_p^2 = .49$, while effect sizes for IFO ($\eta_p^2 = .31$) was much lower. The hemispheric effect for the three tracts was as follows. FA for the left SLF was 0.498 (0.038) and FA for the right SLF was 0.436 (0.047). IFO showed values of 0.493 (0.029) for the left and 0.479 (0.030) for the right hemisphere. For the UNC, corresponding values were 0.386 (0.030) for the left and 0.395 (0.029) for the right. Again, the strongest effect was observed in SLF ($\eta_p^2 = .82$), while IFO showed weaker, but still significant results: effect size for IFO was $\eta_p^2 = .47$. For UNC, no significant effect was observed (see Figure 5.4 and Table 5.3).

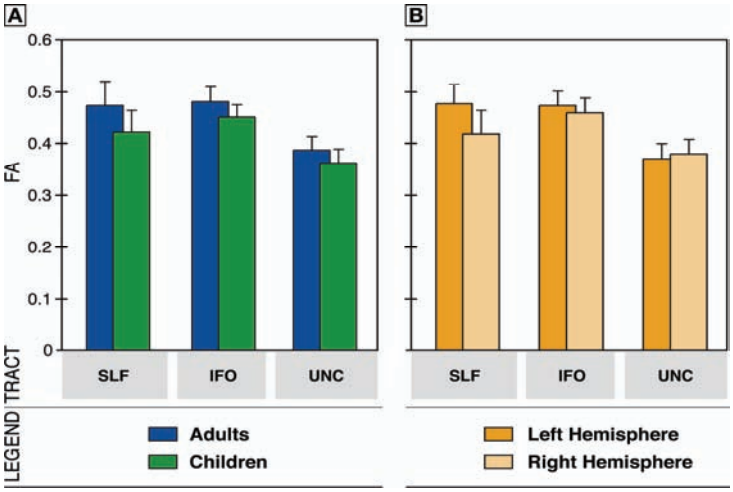

Figure 5.4 Post-hoc analysis of fractional anisotropy (FA) of the results shown in the previous figure. The interactions of tract with group (A) and with hemisphere (B) are displayed on a 2 × 2 basis. Effect sizes indicate that the tract interactions with group and with hemisphere are particularly grounded on effects in the SLF tract where children show largest differences to adults and where also hemispheric effects are most pronounced. See text for further information.

Table 5.3 Post-hoc repeated-measures GLM results for FA for each level of factor Tract. Factors are between-subject factor Group (adults, children) and within-subject factor Hemisphere (left, right). SLF = superior longitudinal fasciculus, IFO = inferior fronto-occipital fasciculus, UNC = uncinate fasciculus.

		SLF		**IFO**		**UNC**	
Effect	*df*	*F*-value	*p*-value	*F*-value	*p*-value	*F*-value	*p*-value
Group	1,18	16.98	$p < .001$	8.04	$p < .05$	5.71	$p = .06$
Hemisphere	1,18	81.32	$p < .001$	15.68	$p < .001$	5.60	$p = .06$

5.2.2 Structure-to-function comparison

In the following, results of a combined investigation of functional and structural data will be presented. Behavioral results of sentence comprehension during functional measurement are followed by functional MRI data. Afterwards, structural tractography based on functional activation areas will inspect the white matter underpinnings of sentence comprehension.

5.2.2.1 Behavioral results

Behavioral data for the acceptability judgment were statistically compared with respect to response correctness and reaction times. Data from one child were not available due to technical error. Results revealed that children and adults did not differ statistically significant in response correctness, though they did differ in reaction times.

Response correctness for children was 90.9 (8.1) percent, while adults had a response correctness of 96.4 (2.0) percent. Statistical comparison yielded no statistically significant group effect $t(1, 17) = 1.97$, $p < .10$. Participants were not required to answer as fast as possible. Still, reaction times were evaluated. They differed significantly between groups. Children produced reactions times of 1093.49 ms (561.06), while adults produced reaction times of 538.38 ms (439.18), $t(1, 17) = 21.30$, $p < .001$.

5.2.2.2 Functional language network

For functional imaging results, BOLD contrast main effects of increased activation for sentence comprehension vs. resting baseline (null events) are reported for the adults' and the children's group in succession. Subsequently, in a ROI analysis a direct statistical group comparison is provided to scrutinize group differences in Broca's area in the IFG more closely.

Adults

The BOLD main effect of sentence comprehension for adults is presented in Figure 5.5A (left). As in the studies reported in the previous chapters, enhanced activation in the perisylvian cortex bilaterally was found. Adults activated the STG, the IFG, and precentral gyrus. In Broca's area in the left IFG, adults showed activation in BA 44 (Talairach coordinate -53, 13, 15).

Further activation was found in cingulate cortex (CC), basal ganglia (BG), and cerebellum. A comprehensive list of activation areas in adults is provided in Table 5.4.

Table 5.4 Gray matter brain regions reliably activated in adults listed with Brodmann areas (BAs), location in Talairach coordinates (x, y, z), and maximum z-value for the main contrast of sentence comprehension against resting baseline (null events). IFG = inferior frontal gyrus, FO = frontal operculum, STG = superior temporal gyrus, BG = basal ganglia, CC = cingulate cortex.

Region	Left Hemisphere				Right Hemisphere			
	BA	Location			BA	Location		
IFG	44	-53	13	15	4.25				
IFG	47	-47	22	-3	4.29				
FO	47	-32	25	6	5.48				
FO		-23	16	18	4.29		31	16	3	5.14
STG	41	-56	-20	6	6.06	41	49	-26	9	6.02
STG						38	52	4	-6	4.75
Precentral Gyrus	6	-50	-2	48	3.76	6	25	-14	57	4.04
Precentral Gyrus						6	43	-2	42	3.62
Postcentral Gyrus	2	-53	-23	33	3.98				
Sup Front Gyrus	6	-2	13	51	5.01	10	28	46	24	3.92
Med Front Gyrus						6	10	-5	54	3.75
Insula	13	-32	-35	24	5.00				
Inf Pariet Cort	40	-53	-35	54	3.64				
Cuneus	19	-2	-95	24	4.30				
Cuneus	17	-11	-77	9	4.18				
Precuneus	7	-5	-74	54	4.14	7	7	-83	48	4.43
CC	30	-23	-62	9	4.31				
CC	32	-8	19	36	4.99	32	10	19	33	4.41
BG		-20	-8	6	4.25		25	-11	-6	4.59
BG							7	10	0	4.19
Fusiform Gyrus	37	-38	-53	-9	4.12				
Claustrum		-35	-8	-9	4.62		28	1	21	4.84
Cerebellum		-11	-44	-21	4.52		13	-65	-15	4.77
Cerebellum		-38	-62	-18	5.13				
Cerebellum		-11	-68	-24	4.08				

Children

Figure 5.5A (right) shows the BOLD main effect for sentence comprehension in children. Comparable to previous findings (cf. chapter 3 and 4), they activated the perisylvian cortex bilaterally, mainly the STG and the IFG. In Broca's area in the left IFG, the primary activation was found in BA 45 at -53, 22, 12. Further activation was found in BG, CC, and cerebellum. Table 5.5 provides a comprehensive list of activation areas in children.

Table 5.5 Gray matter brain regions reliably activated in children listed with Brodmann areas (BAs), location in Talairach coordinates (x, y, z), and maximum z-value for the main contrast of sentence comprehension against resting baseline (null events). IFG = inferior frontal gyrus, FO = frontal operculum, STG = superior temporal gyrus, BG = basal ganglia, CC = cingulate cortex.

Region	Left Hemisphere			Right Hemisphere		
	BA	Location	Z-max	BA	Location	Z-max
IFG	45	-53 22 12	3.99	44	58 13 15	4.56
IFG	47	-50 22 -9	4.17	47	22 10 -21	4.20
FO		-23 19 -6	4.02		31 16 0	4.55
SFG	10	-14 61 24	3.49			
SFG	6	-11 13 48	4.59			
STG	38	-32 13 -21	3.69	38	46 19 -12	4.39
STG				22	46 -23 0	5.13
MTG	22	-62 -41 6	4.97			
ITG				20	49 -2 -33	4.39
Middle FG	9	-38 10 24	3.83	46	55 34 15	4.18
Precentral Gyrus	6	-59 4 21	4.79			
Precentral Gyrus	6	-44 -5 48	4.12	6	34 -8 51	3.94
Postcentral Gyrus	3	-38 -20 45	3.84	3	34 -23 45	4.41
Paracentral Cortex	31	-5 -17 48	3.85			
Sup Pariet Cortex	7	-29 -59 42	3.73			
Inf Pariet Cortex	40	-38 -44 45	3.67	40	43 -35 39	4.22
BG		-8 -2 15	3.68			
CC				31	19 -29 39	4.23
CC				32	4 28 24	3.61
CC				24	7 13 27	3.94

Region	Left Hemisphere			Right Hemisphere		
Precuneus				7	13 -68 39	4.27
Lingual Gyrus	17	-11 -92 -3	4.19	19	16 -62 0	4.38
Fusiform Gyrus	20	-35 -38 -18	3.49			
Fusiform Gyrus	20	-38 -26 -27	4.82	20	52 -23 -24	3.80
Uncus				28	25 -11 -30	4.07
Cerebellum		-8 -29 -18	3.77		43 -56 -39	3.65
Cerebellum		-44 -62 -45	4.15		16 -77 -45	4.30

Direct group comparison

Direct statistical comparison was conducted in order to evaluate group differences for sentence comprehension statistically. Broca's area was selected as the primary ROI for group differences in this comparison. Differences between groups in loci of peak activation in this ROI were expected to indicate differences in the neural network underlying sentence comprehension. The result of this analysis revealed only a single spot of stronger activation, i.e., in children's BA 45 (-53, 22, 12) of Broca's area (see Figure 5.5A, middle). There was no activation in the ROI that was significantly stronger for adults than for children.

5.2.2.3 Structural language network

In order to identify those perisylvian white matter pathways that participate in the fronto-temporal network of language comprehension, functional and tractography data were combined with each other for a conjoined investigation. Voxel addresses of functional activation in Broca's area were applied to define seed points for a tractography analysis. The seed point for the adult's activation in Broca's area at -53, 13, 15 was set to nearby white matter at -51, 12, 15. The seed point for children's activation in Broca's area at -53, 22, 12 was set to nearby white matter at -44, 24, 10. These seed point served as starting points for fiber tracking analyses. The tractography results are shown in Figure 5.5B. Results show that tractography clearly differentiates between both activation regions in Broca's area. The adults' seed point starting in BA 44 notably hits the SLF in both groups, while the children's seed point in BA 45 hits the ventral fronto-temporal connection via the IFO.

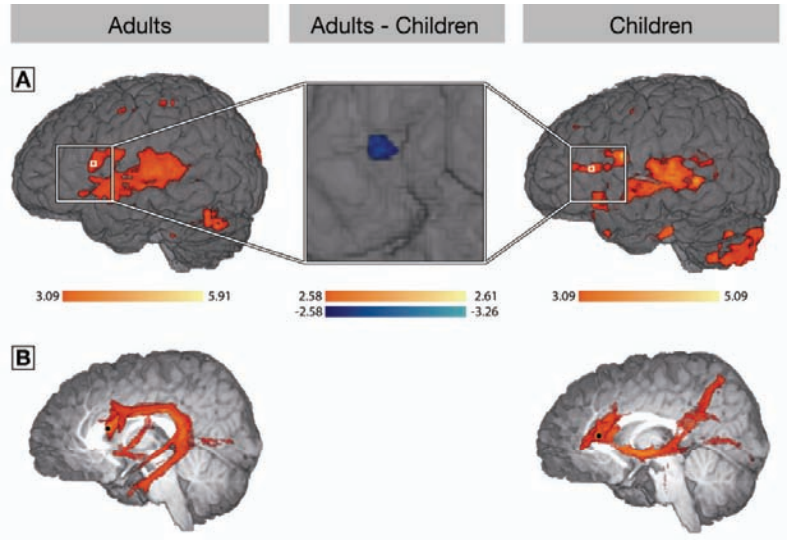

Figure 5.5 BOLD contrast main effects for sentence comprehension in adults and in children, mapped on a 3D rendered reference brain in sagittal view from left (A). Both groups show activation of IFG and STG. In IFG, activation is most pronounced for adults in BA 44 at Talairach coordinates -53, 13, 15, indicated by a white mark (A, left). For children, activation in the IFG is most pronounced in BA 45 at -53, 22, 12 (white mark), slightly extending into BA 46 (A, right). Furthermore, direct statistical comparison for the activation in the IFG at Broca's area revealed significant group differences with stronger activation for children in BA 45 at -53, 22, 12 (A, middle). No cluster of stronger activation for adults than for children was found (blue = children > adults, red = adults > children).

Probabilistic fiber tracking (B) seeded in white matter closely located to cortical activation maxima. The seed point for adults' maximum -53, 13, 15 was set to nearby white matter at -51, 12, 15. The seed point for children's activation maximum at -53, 22, 12 was set to nearby white matter at -44, 24, 10.

In order to point out that these differences of pathway connections in children and adults are truly based on different pathways being recruited rather than on a different wiring of the tracts in the IFG cortex, seed points for the structural-functional tractographies were applied across groups. Results are shown in Figure 5.6. They clearly indicate that in adults and children the same fiber pathways are tracked from the two seed points obtained from functional activation maxima in both groups.

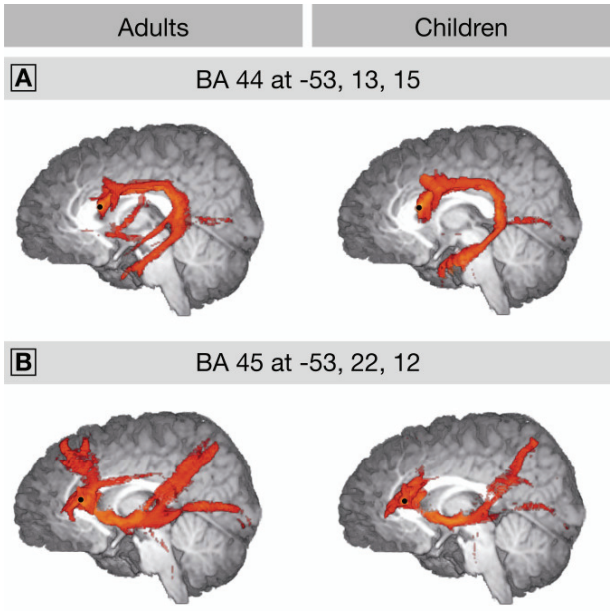

Figure 5.6. Tractograms for seed points according to functional activation maxima in adults (Figure 5.6A, BA 44 cortical activation maximum at -53, 13, 15, seed point -51, 12, 15) and children (Figure 5.6B, BA 45 cortical activation maximum at -53, 22, 12, seed point -44, 24, 10) applied across groups. Results show that in children and adults both seed points generated similar tracking results that catched the same fiber tracts.

5.3 Discussion

This study investigated the structural white matter underpinnings of the perisylvian language network in adults and children. Results revealed group differences for FA in important fiber pathways that indicate ongoing maturation in the brain's white matter of 7-year-olds. Particularly pathways within the perisylvian region comprising important language areas showed an immature state at this age.

A whole brain white matter comparison revealed lower FA in the immature brain of children compared to the mature brain of adults. This result is consistent with previous findings of white matter diffusivity changes in response to brain maturation across infancy and early childhood to adulthood (Dubois, et al., 2008; Hermoye, et al., 2006; Lebel, et al., 2008). Changes in fractional anisotropy were seen as an indicator of ongoing maturation and myelination of fiber bundles (Dubois, Hertz-Pannier, Dehaene-Lambertz, Cointepas, & Le Bihan, 2006).

The present study was able to demonstrate differences in FA between 7-year-old children and adults on a statistical direct comparison basis. White matter differences in the perisylvian region in superior temporal and left inferior frontal areas are of special interest with respect to the language network. Tractography analyses of perisylvian fiber pathways indicated higher FA values in the left than in the right hemisphere for both groups. These results are supported by an earlier study on FA lateralization in adults (Büchel, et al., 2004). That time, they implemented a voxel-based approach to identify the SLF. We could replicate their finding on leftward asymmetry in the SLF with an advanced method to identify fiber tracts via tractography. The results of the present study also suggest a particular importance of the SLF for group differences in FA between adults and children. This is in line with reported findings of ongoing changes in SLF FA until adulthood (Giorgio, et al., 2008).

Classical methods such as voxel-wise analysis of DTI data can suffer from sever limitations, specifically in the context of investigations in brain maturation. Registration might be restricted in its accuracy by low dimensional transformations and the heterogeneity of signal intensities in FA maps. Image smoothing and statistical thresholding are further sources of artifacts (Derek K. Jones, et al., 2005). In the present study, the TBSS

method was applied which allows to register datasets on the core white matter of one common target image (Stephen M. Smith, et al., 2006). Compared with e.g., gyrification of the cortex, the main white matter tract anatomy is much less variant across humans. Therefore, by mainly restricting the registration method on the regions of interest in DTI data, i.e., the white matter tracts, a group comparison even across different age groups such as children and adults was feasible.

Adults and children differed in functional activation during auditory language comprehension, particularly in the IFG. While adults showed maximum activation in BA 44 of Broca's area, children's activation maximum was observed in BA 45 of Broca's area. Direct comparison revealed children's stronger involvement of this area. Combined analysis of functional and structural brain data suggests that children put a different emphasis on subparts of the language network with a stronger involvement of the IFO. Both groups, however, where not entirely equal in behavioral data. Differences in reaction times where expected according to previous results. Response correctness did not show statistical differences, but a marginal tendency. It is known that stronger functional activation can be caused by higher task demands (Burgund, Lugar, Schlaggar, & Petersen, 2005). However, a stronger and more extended involvement of Broca's area in children was already observed in previous studies with equal response correctness data for both groups (cf. Study 1). Therefore, it is unlikely that functional differences between groups in the present study are due to unequal behavioral engagement.

A limitation of the present study is its group size of N = 10 per group. While this is a sufficient number of participants for TBSS and tractography and even for reliable fMRI statistics, further investigations were limited. An interesting analysis would have been to acquire correlation statistics of behavioral or diagnostic data with FA or other white matter indices. However, no reliable correlation statistic was obtainable because of the rather small group sizes.

Concerning tractography, adults showed in general stronger fasciluli than children, a result endorsed by their higher FA values. Fiber tracking is typically applied to single subject data. However, since in the present study single subject white matter anatomies were normalized on one average white matter skeleton, it was possible to obtain probabilistic white matter

tractography on a group data basis for adults and children. The present data revealed clearly identifiable tractography results obtained from normalized group data. This shows that fiber tracking is possible at the group level which might be more appropriate for many studies than the common method of presenting tractograms of representative single subjects. Furthermore, data indicate very similar tractograms across groups for all three fasciculi which implies that probabilistic tractography is able to produce reliable results even in young children.

Study 3 was able to demonstrate that functional processing differences between adults and children for language comprehension as reported in Studies 1 and 2 rely on a distinct neuroanatomical basis. Children involve a broader network of cortical areas that participate in distinct neural pathways within the language network.

6 General discussion

The current work has investigated a developmental perspective on the brain basis of the human faculty of language. The studies that were presented have highlighted the role of perisylvian brain circuits for the processing of auditory language comprehension. Functional imaging data have introduced brain mechanisms of the processing of syntactic and semantic aspects of language. The cortical regions involved in the brain's language network have been explored thoroughly for their activation and on the basis of their fundamental neurophysiology of functioning within that network. Their subcortical inter-lobule connections have been investigated concerning their role properties as the underpinning groundwork of that network.

The last chapter of the current work will conjointly discuss the results and findings presented so far and present an outline of a requisite future research agenda in the field of developmental neuropsychology on the neural basis of language in the human brain.

6.1 The functional neural network of auditory sentence comprehension

The processing of semantic and syntactic aspects of auditory language comprehension was investigated by functional brain imaging in the first study. In adults and 6-year-old children, broadly the same perisylvian brain regions were found to be involved. However, also age-specific effects and developmental differences were observed.

Auditory language comprehension elicited condition specific activation patterns in adults for syntactic and semantic conditions in temporal and frontal cortices. Syntactic processes elicited activation in left aFO, left lateralized activation in ant STG and bilateral activation in post STG. For semantic processes, in contrast, we found no activation in ant STG, but activation in post STG was clearly lateralized. The observed temporal lobe activation for all conditions in and around Heschl's gyrus in mid STG bilaterally was expected given that the sentence material was presented

auditorily (for a review see Scott, 2005). The pattern of STG activation for the different conditions is in general agreement with earlier studies tested with a similar paradigm, though with material not particularly constructed for children (Friederici, Rüschemeyer, Hahne, & Fiebach, 2003; Rüschemeyer, et al., 2005). These studies showed ant STG to be particularly involved in a syntactic violation condition, and post STG in both syntactic and semantic violation conditions. The selective activation in the aFO during on-line processing of syntactic violation as observed in the present study is compatible with previous findings. The FO area reported by Friederici, Bahlmann et al. (2006) at -36, 16, 0 for local syntactic violations in an artificial grammar is closely located to the aFO area activated for local phrase structure violations in the present study (-32, 27, 0). Within the left frontal cortex, the FO is seen to participate in the processing of local syntactic dependencies (Friederici, Bahlmann, et al., 2006; Friederici, Meyer, & von Cramon, 2000), whereas BA 44 holds responsible for the processing of hierarchical dependencies (Grodzinsky and Friederici, 2006; Stromswold et al., 1996) if not for the sequential realization of hierarchical interpretative dependencies in general (Bornkessel, et al., 2005).

The pFO region observed for semantic processing was less anterior and more medially located than the activation observed for syntactic processing. In contrast to the syntactic aFO area, the semantic pFO area, however, was only statistically dissociable in its activation from the correct sentence condition, but not from the syntactic violation condition**.** Rather, it even appears to be a subpart of the syntactic FO activation. On the basis of the present results, it remains open whether the pFO region is responsible for semantic processing or for the processing of both syntactic and semantic violations. Activation in this area during the processing of a syntactic violation as in the present study, could have been evoked by semantic processes in search to fill the gap in the incomplete prepositional phrase (*in-the_*) as this phrase is not only syntactically violated but moreover conceptually incomplete. The preposition not only asks for a noun phrase as a syntactically licensed confirmation, but it conceptually requires a noun that refers to a location.

Children, in contrast to adults, showed an overall broader activation during on-line language processing. This could be attributed to higher processing demands, an argument endorsed by the fact that children produced longer

reaction times than adults. The observed Group effect for reaction times corresponds to an overall broader cortical activation in children.

The children's group, in contrast to the adult sample, showed extended activation of inferior and middle frontal cortex bilaterally. Their STG did not show specific activation of particular subregions for semantic and syntactic processes as found in adults, rather all conditions involved left post STG as well as ant STG and mid STG bilaterally. Either these areas are not yet specialized in their processing function, or higher processing demands required their assistance in all conditions. Furthermore, children did not demonstrate a selective involvement of the FO for a particular condition. Rather, the FO was activated during the processing of correct, syntactically incorrect, and semantically incongruous sentences. Children, unlike adults, additionally recruited inferior and middle frontal gyri when processing correct sentences. Interestingly, children engaged left BA 44 in Broca's area (-50, 17, 21) selectively during the processing of a syntactic phrase structure violation. This activation pattern resembles that of second language learners who, similarly to our children, showed activation in BA 44/45 when processing phrase structure violations in passive sentences (Rüschemeyer, et al., 2005). Given that left BA 44/45 activation during language processing in native adults is observed with augmented syntactic processing (Bornkessel, et al., 2005; Friederici, Bahlmann, et al., 2006; Stromswold, et al., 1996), we interpret enhanced BA 44 activation for syntactically incorrect sentences observed for children as a reflection of increased syntactic processing demands. These may become necessary due to a smaller amount of automaticity of syntactic processes in children compared to adults.

The present fMRI data indicate a large overlap of the brain activation for semantic and syntactic processes in 6-year-old children. Such a pattern of activation is in line with the view that at this developmental stage semantic and syntactic processes are highly interdependent. Behavioral studies using on-line methods have shown that syntactic processes become independent of semantic processes gradually over early childhood, demonstrating an interaction of these processes around 5 years of age and an independence around 10 years (Friederici, 1983).

The data, however, are not directly comparable with ERP data collected in 2 and 2.8-year-olds with comparable sentences material. When semantically

and syntactically incorrect sentences are presented in separate experiments, 2-year-olds demonstrate a semantic N400 effect similarly to adults though longer lasting (Friedrich & Friederici, 2005), and 2.8-year-olds show a syntactic ERP pattern similarly to adults consisting of an ELAN and a P600 (Oberecker, et al., 2005) this suggests some specialization of brain systems for semantic and syntactic processes, at least when presented in separate sessions.

A crucial difference between these ERP studies and the present fMRI-study is that in the present study semantically incorrect sentences and syntactically incorrect sentences were presented together in one experiment in a randomized order. This may have affected children's processing strategies. Attentional demands on both syntactic and semantic violations at the same time may have led to an overlap in activation for the different conditions. Such an interpretation would be compatible with the view that the child's processing system on the one hand can treat semantic and syntactic aspects differently as demonstrated by the ERP data and by the specific activation of Broca's area in the syntactic fMRI data, but on the other hand attentional and resource demanding processes lead to a larger overlap in the brain activation in children than in adults.

The adult network of auditory language comprehension demonstrates a left hemispheric dominance, especially in the FO, but also in the STG with its anterior part and to some extent its mid-portion and posterior part. In adults, no region in the right hemisphere was significantly more involved than its left hemispheric equivalent.

The network of language comprehension in children is less left-lateralized than in adults. While in adults 67 % of contrasted language-related brain areas showed a left hemispheric dominance and none showed a right hemispheric dominance in their activation, in children only 44 % of contrasted areas were left-hemispherically and 11 % were right-hemispherically dominant. These data correspond to the assumption of an age-related increase in the degree of language lateralization in children (Holland et al., 2001; Szaflarski et al., 2006). A stronger involvement of the right hemisphere in children is also illustrated by lateralization indices, with five children being lateralized to the right and only one to the left.

While adults did not activate the lateral IFG at the more restrictive threshold, but only the left FO for the processing of local phrase structure

violations, IFG activation was present in children bilaterally. In adults, right hemispheric activation in the FO together with a right hemispheric involvement of the posterior STG and the cingulate gyrus has been reported for the processing of prosodic aspects during auditory language perception (Meyer, et al., 2002; 2004). The present findings for children, revealing a particular right hemispheric involvement of the FO and the SMG for the syntactic violation condition, may thus either reflect a stronger reliance on prosodic aspects of the language input or a different functional organization in children and adults. For the present material, reliance on prosodic information could have been helpful, as the sentence's final word is not only syntactically inadequate (verb instead of a noun in the prepositional phrase), it is also prosodically unexpected, as the expected word in the prepositional phrase should be a noun and not a verb carrying a sentence final prosody. This interpretation is in line with the view that young children rely on prosodic information to process syntactic structure during early language development (Pannekamp et al., 2006; Weissenborn and Höhle, 2001).

6.2 On temporal features of the perisylvian language network

Hemodynamic BOLD response properties in language-related perisylvian brain areas were investigated more closely in the second study for adults and children. While the brain regions being activated in sentence comprehension are similar in both groups, i.e., inferior frontal and superior temporal cortices bilaterally, the temporal pattern of BOLD latencies revealed some crucial differences.

For BOLD response latencies, a systematic progression was observed along the STG with fastest BOLD responses in the mid-portion around Heschl's gyrus and longer latencies in anterior and posterior directions, suggesting initial processing of sensory information in primary auditory cortex and later involvement of anterior and posterior STG and the IFG. This pattern was in general equivalent for both groups and represents a finding that is in line with earlier studies in infants (Dehaene-Lambertz, Hertz-Pannier et al., 2006) and adults (Dehaene-Lambertz et al., 2006a; Thierry et al.,

1999). Direct comparison between age groups revealed that children showed overall longer BOLD latencies than adults.

Besides the overall longer BOLD latencies in children compared to adults, time-to-peak latencies were observed to be longer in IFG than in STG for both groups. However, in children this effect was much more pronounced, as pointed out by the significant interaction in a region analysis. But children did not only show a stronger temporal-frontal regional effect, they, moreover, demonstrated a significant effect across hemispheres with slower left and faster right-hemispheric BOLD responses, a finding which was absent in adults. Particularly these group by area and group by hemisphere effects require some more profound discussion.

In two previous studies, BOLD timing properties in perisylvian areas during sentence comprehension were reported for adults and for 3-month-old infants. These studies suggested similar patterns in the temporal organizations of superior temporal and inferior frontal cortices when considering the infants' data (Dehaene-Lambertz, Hertz-Pannier, et al., 2006) and those referred for adults (Dehaene-Lambertz et al., 2006a). They did not report a quantitative comparison between infants and adults, but their conclusion of a qualitatively similar temporal organization in the developing and the mature brain seems to confirm the results of the present study. However, in absence of a direct comparison between infants and adults, an evaluation of temporal dynamics between the two groups in these areas on the basis of the Dehaene-Lambertz et al. data remains difficult. The present data of 6-year-old children and adults rather argue for a developmental effect of these contributions to sentence comprehension with later BOLD responses in inferior frontal areas and a hemispheric effect with earlier right than left hemispheric hemodynamic responses in the developing language system.

Differences between children and adults in the present study might reflect processing differences between age groups in a way that higher cognitive processing demands may cause delayed BOLD responses, particularly in the left inferior frontal region. The present study cannot yield such conclusions by itself. However, studies in adults have shown that the hemodynamic timing of brain responses can be influenced by experimental manipulation (Dehaene-Lambertz, Dehaene, et al., 2006; Heim & Friederici, 2003; Henson, Price, Rugg, Turner, & Friston, 2002; Thierry, et al., 2003).

For instance, the latency of BOLD peaks for language processing has been shown to be delayed by additional verbal working memory requirements (Thierry, et al., 2003). They demonstrated that evoked hemodynamic responses in inferior prefrontal cortex including Broca's area depended on experimental manipulation with varying demands for verbal working memory. The finding that in this previous study no such sensitivity of BOLD time course was observed in the superior temporal gyrus argues for region-specific effects based on varying cognitive demands. Accordingly, our data suggest higher cognitive processing demands for the processing of sentences in the developing brain as opposed to the adult brain. More automatic and thereby faster language processing in the mature as compared to the developing brain might account for the differences in BOLD time courses in IFG between children and adults.

The interpretation of quantitatively different processes in language processing in adults and children is supported by results from electrophysiological studies. ERP brain responses related to sentence comprehension processes have been reported to be delayed in children compared to adults (Hahne, et al., 2004; Holcomb, Coffey, & Neville, 1992; Oberecker, et al., 2005). In the semantic domain, this delay has been interpreted to reflect increasing demands on contextual integration processes (Holcomb, et al., 1992), and in the syntactic domain component delay has been interpreted to reflect slower processes. The absence of a particular ERP component indexing automatic syntactic processes has been argued to indicate that the automaticity of syntactic processes only develops slowly during childhood (Hahne, et al., 2004; Oberecker & Friederici, 2006; Oberecker, et al., 2005).

We observed equal overall hemodynamic time-to-peak values in adults for both hemispheres, but smaller values for RH in children, based particularly on the right FO. The right-hemispheric FO has been shown to be sensitive to suprasegmental, prosodic information in functional imaging studies in adults (Dehaene-Lambertz, Dehaene, et al., 2006; Friederici & Alter, 2004; Meyer, et al., 2004). A right hemispheric involvement for prosodic processes was also reported for 4-year-old children (Wartenburger, et al., 2007) and for infants (Homae, et al., 2006), both by means of near-infrared spectroscopy (NIRS). Moreover, ERP data have demonstrated that in adults prosodic information influences syntactic parsing very fast, that is in a very early

phase during speech comprehension (Eckstein & Friederici, 2006) and that the brain's sensitivity to prosodic features is present not only in adults (Pannekamp, Toepel, Alter, Hahne, & Friederici, 2005), but also in infants (Pannekamp, et al., 2006). Psycholinguistic studies in adults (Marslen-Wilson, Tyler, Warren, Grenier, & Lee, 1992; Warren, Grabe, & Nolan, 1995) have provided evidence for an interaction of prosodic and syntactic processes during auditory language comprehension (Frazier, Carlson, & Clifton, 2006), and psycholinguistic models of language acquisition state stronger reliance on prosodic information during early language processing (Weissenborn & Höhle, 2001). The shorter right than left BOLD latencies for children in our study seem to match these electrophysiological data and, moreover, are consistent with the psycholinguistic models. The present data indicate a temporal hemodynamic primacy of the right hemisphere in the developing brain, particularly the right FO, possibly reflecting the intense use of prosodic information during language processing.

However, a direct comparison of hemodynamic and electrophysiological event-related responses should be interpreted with caution. Although the BOLD contrast mechanism is considered to reflect neural responses to a stimulus (Logothetis, et al., 2001), the neurovascular interrelation of delay in neural activity and temporal properties of hemodynamic processes is in need for further clarification. It is still an open question whether observed BOLD response latency differences reflect a hemodynamic or neuronal origin or a synthesis of both. Hemodynamic response timing may reflect the timing of neuronal activity, but the inverse problem regarding inferences from hemodynamic responses to underlying neural activity only starts to be addressed (Buckner, 2003).

Given the available analytic tools, it is up to now not possible to exactly evaluate to what extent observed differences in hemodynamic timing between adults and children are grounded on differences in local vasculature and on differences in functional recruitment of involved brain areas. A factor to be considered for an interpretation of the present findings might also be the potential influence of cerebral blood flow (CBF). The BOLD signal reflects changes in CBF relative to changes in cerebral metabolic rate of oxygen ($CMRO_2$) (Richard B. Buxton, et al., 2004). By implementing a vascular model of the hemodynamic response, Vazquez et al. (2006) have suggested that changes in baseline CBF might influence latency and

amplitude parameters of the BOLD signal. Concerning development, global cortical CBF was shown to increase during early childhood, peaking at about age 5 to 6, and then to decline, reaching an adult level in late adolescence (Chiron et al., 1992; Takahashi, Shirane, Sato, & Yoshimoto, 1999). Moreover, developmental changes in regional CBF were argued to be related to cognitive development and higher order functions such as language (Chiron et al., 1992; Devous et al., 2006). Thus, a potential influence of CBF differences between adults and children must be conceived to contribute to the present findings. There are still too many open questions in our current understanding of CBF development and its relation to induced BOLD responses to agree upon robust conclusions at present.

In addition to functional and physiological aspects of the observed hemodynamic differences between adults and children, structural aspects of brain maturation must be considered. Our observation of overall longer BOLD latencies in children agrees with the assumption of ongoing maturational changes within language relevant brain areas and the structural connections between them. Regarding the developmental courses of white matter myelination in language-related temporal and frontal brain regions, Pujol et al. (2006) described temporal and frontal regions to coincide during rather early stages of maturation, and differences in FA between children and adults have been described in Study 3 of the present work. Structural maturation of white matter tracts in those fronto-temporal pathways which support language functions is even reported to continue until late childhood and adolescence (Paus, et al., 1999). Relations between the maturation of brain structure and cognitive functions have been reported for gray and white matter. Nagy et al. (2004), for example, have shown that cognitive functions are related to maturation of white matter for children older than 8 years of age. Moreover, the frontal cortex is among the last brain regions to fully mature (Sowell, Thompson, Holmes, Jernigan, & Toga, 1999). Changes in gray matter maturation are known to continue until adulthood (Toga, et al., 2006) and are correlated with changes in cognitive abilities such as vocabulary (Sowell, et al., 2004). The relationship between maturation of brain structure and development of cognitive function so far, however, is correlative only and has to be investigated more thoroughly before specific causal inferences from synchronous brain maturation and progress in cognitive functions can be drawn (Aslin & Schlaggar, 2006). Nonetheless, maturation of gray and white matter must be considered as

one aspect in the explanation for the apparent changes of BOLD time courses during development, even though the precise impact of brain maturation on the present results remains an open issue.

Taken together, a combination of neurophysiological and structural factors might account for differences in the temporal dynamics of brain responses between children and adults as it was observed in our second study. Moreover, a functional account can help to better understand the present findings. A possible scenario regarding functional and structural contributions to the development of language comprehension might be that the overall time course differences of hemodynamic responses between adults and children exist mainly due to ongoing maturational changes in children, whereas specific age differences between particular brain areas might be mainly based on differences in functional processing with structural properties contributing less. A case of almost purely functional influences might be the hemispheric age differences which most likely results from different processing strategies in children and adults with children relying more on right hemispheric prosodic processes than adults. In general, this might suggest that as long as children's brains do not possess mature structural means, they need to compensate that disadvantage by strategy and/or effort. Progressing with further brain development (through maturation and experience), more effective information transmission and processing become possible.

6.3 The structural language network basis

These structural means of white matter underpinnings in the brain were the research focus in our third study. Whole brain white matter comparison revealed differences in fractional anisotropy between adults and children, especially in the perisylvian region in superior temporal and left inferior frontal areas. White matter pathways within that region where found to show higher FA in the left than in the right hemisphere, and in adults than in children. Combined analysis of fMRI and DTI data suggests children to rely on a broader basis within the language network. They included additional cortical areas within the IFG in functional language processing which are connected within the language network mainly via a ventral connection between frontal and temporal regions, namely the IFO.

FA differences between groups in the perisylvian region extended into ventral premotor (vPM) area in BA6. This area has been argued to participate in sequencing, speech, and phonological processing (Bahlmann, Schubotz, & Friederici, 2008; Bookheimer, 2002; Wise, Greene, Buchel, & Scott, 1999). Moreover, Broca's area is sometimes viewed as an anterior extension of vPM, since both of them share a prominent anatomical characteristic, that is a lack of a fully-developed granular layer IV (Fiebach & Schubotz, 2006). Hence, FA differences in the Broca/vPM region are likely to be attributed to affect language processing.

Asynchrony of maturation of fiber bundles belonging to different functional systems was shown for the infant brain (Dubois, et al., 2008). These differences are, furthermore, known to persist during young childhood (Pujol, et al., 2006) and even into adolescence (Paus, et al., 1999). It can be hypothesized that the additional use of connections as observed in our study could be due to insufficient information exchange within the language network via the prominent but at this age still immature SLF. Very late maturation of the SLF during development was reported to last until early adulthood which makes the SLF one of the latest fiber tracts in the human brain to fully mature (Giorgio, et al., 2008). Slow axonal and/or myelin maturation of the SLF was suggested in a DTI study comparing children with a broad age range (neonates to age 10 years) and adults (Zhang, et al., 2007). In a study that investigated boys only, increased FA was reported for older adolescents (age 18) compared to younger adolescents (age 14), particularly for the left arcuate fasciculus, a subregion of the SLF (Ashtari, et al., 2007), arguing for the late maturation of the SLF.

The slow maturation of the SLF compared to other fiber bundles can be assumed to support the view of the SLF being involved in high-level processing. The SLF is the main fiber pathway connecting the important language centers Broca's area in the IFG and Wernicke's area in the STG via the arcuate fasciculus. If language is regarded to be a uniquely sophisticated faculty that developed during human evolution, the hardware brain basis of such evolutionary development might be expected to have undergone equivalent changes. Phylogenetic development during evolution could be reflected in ontogenetic development, that is, a very late maturation of fiber bundles that fulfill higher functions as the phylogenetically very recently emerged faculty of language. As was shown by comparative DTI,

the prominent temporal projections of the SLF via the arcuate fasciculus as observed in humans is absent or at least reduced in nonhuman primates (Rilling, et al., 2008).

Previous studies on structural lateralization have mainly focused on certain brain structures, such as particular areas of the cerebral cortex (Geschwind & Levitsky, 1968) or certain white matter bundles (Büchel et al., 2004; Powell et al., 2006). In fact, even referred findings on structural lateralization reported for the cortex can be actually based on underlying white matter instead of the cortex itself. In a postmortem study, Anderson et al. (1999) could verify that the repeatedly reported result of larger superior posterior temporal lobe volumes, e.g., Geschwind and Levitsky (1968), is mainly grounded on white matter differences with thicker myelin sheaths on axons in this area.

Functional cortical and structural white matter lateralization was shown to coincide in adults for functional activation during a language task and underlying structure as indicated by mean FA in the SLF (Powell, et al., 2006). Activation was stronger leftward lateralized in those subjects who also showed higher lateralized FA values. In our study, we could show that lateralization of white matter structures are a broader phenomenon than identified so far, even already in the immature brain of children. Besides the SLF, lateralization was shown for the IFO as well, consistent with previous findings in adults (Parker, et al., 2005). However, we did not observe lateralization for the UNC. The missing leftward lateralization of the UNC is inconsistent with earlier reports on fiber lateralization in children and adolescents (6-17 years) (Eluvathingal, Hasan, Kramer, Fletcher, & Ewing-Cobbs, 2007). The contradictory findings might be based on different methods for fiber identification. While our study masked obtained tractography results in order to restrict pathways to their clean core structure, the study cited above included all voxels obtained from fiber tracking. This might have caused the inclusion of branching or crossing fibers of nearby tracts in the analysis which do show actual stronger leftward asymmetry. The UNC is a ventrally located fasciculus connecting the ventral part of the IFG including the FO with the anterior part of the STG. As discussed in the previous section, the ventral IFG, particularly the FO, was shown to be sensitive to suprasegmental, prosodic information during auditory language comprehension with a strong right-hemispheric

lateralization (Friederici & Alter, 2004; Meyer, et al., 2004). This hemispheric lateralization was also observed in young children (Homae, et al., 2006; Wartenburger, et al., 2007). A possible explanation for stronger right-hemispheric connections via the UNC compared to other language-related perisylvian pathways with leftward asymmetry (SLF, IFO) could be assumed to point on the UNC's commitment to cortical areas that subserve prosodic processes. This hypothesis is to be addressed in further studies.

It is not yet determined whether the ventral connection between frontal and temporal regions comprises only the rigid single IFO that finally extends into the occipital region. DTI data from fiber connections in the monkey brain suggest that the inferior fronto-temporal connection includes the extreme capsule (Schmahmann, et al., 2007). So far, limitations in current imaging resolution for DTI hamper a sufficient resolution of the extreme as much as the external capsule (Susumu Mori, et al., 2008). Future advances in imaging techniques will certainly help to gain better discrimination.

We were able to conduct direct statistical comparison for functional data between groups, since anatomical data allowed joint nonlinear registration on one template. In the first study of the present work, no such joint registration between children and adults was possible. This is probably due to the fact, that children in Study 3 were older (mean age 7.1 years) than in the preceding functional Study 1 (mean age 6.2 years). A common stereotactic space for adults and children at 7 years of age is supported by a feasibility study on this issue (Kang, et al., 2003). For functional sentence processing, we observed involvement of superior temporal and inferior frontal areas in both adults and children. In Broca's area in the left IFG, both groups activated BA 44, but only children involved BA 45. BA 44 in Broca's area holds responsible for syntactic and structural processing (Grodzinsky & Friederici, 2006; Hoen, Pachot-Clouard, Segebarth, & Dominey, 2006), while BA 45 is involved in processing semantic and thematic aspects of language (S. D. Newman, Just, Keller, Roth, & Carpenter, 2003). This differentiation between certain aspects of language within the IFG is in line with neurocognitive models of language processing (Friederici, 2002; Ullman, 2006). Extended involvement of BA 45 in children might indicate their stronger reliance on semantic content in order to facilitate language comprehension processes. It was shown that children gain an independence of particular aspects of language processing such as

syntax and semantics only late during language development (Friederici, 1983).

A dissociated involvement of cortical areas was observed for the processing of two types of artificial grammar, a simpler linear finite state grammar (FSG) and a more advanced hierarchical phrase structure grammar (FSG) (Friederici, Bahlmann, et al., 2006). While FSG processing involved brain areas connected via IFO and UNC, the more demanding PSG involved the SLF. The presumed additional use of the ventral fronto-temporal connection in children compared to adults for sentence comprehension in our study could be interpreted as assisting action in order to support the not yet fully matured SLF.

6.4 Conclusion

The research presented in this work was able to demonstrate specific characteristics of the developing language network in children. The interaction of functional development of language on the one hand and brain development and maturation on the other was scrutinized by a variety of approaches.

Functional MRI data on semantic and syntactic processing in 6-year-old children indicated that the neural networks supporting these different aspects of language processing are not yet fully specified. Stronger and less specific activation, as observed in children, suggests higher processing demands in the developing language system. These data are not only in line with findings from on-line behavioral studies demonstrating that syntactic processes only start to gain their independence from semantic processes after the age of 5 years, but also with ERP results indicating that ERP patterns for syntactic processes in syntactically complex sentences are not yet identical to adults in 6-year-olds. The developing brain must acknowledge syntactic information in a specific way. These specific processes may be based on Broca's area, as this brain area was recruited by children for the processing of syntactic information, while adults based local phrase structure building processes within the IFG on the frontal operculum.

Analysis of temporal hemodynamics demonstrated distinct time courses of the BOLD response in the perisylvian language cortex of children and adults during language comprehension. Children’s BOLD responses

showed overall longer latencies when compared to adults. Moreover, a temporal primacy of right over left hemispheric activation was found, especially for the children's FO. While in adults, inferior frontal activation showed peak latencies later than – but close to – superior temporal activation, children's IFG activation peaked much later than STG activation. Combined data from Study 1 and 2 promote the view of a specific role of the IFG in language processing. Latency differences between children and adults in the functional BOLD response during language comprehension are in line with our current understanding of maturational changes in language-related brain areas and the structural connections between them. These data also support the view that developmental changes evolve from higher processing costs in the developing brain to faster and more automatic language processing in the mature brain.

An examination of the brain's white matter revealed overall smaller fractional anisotropy in children than in adults. This is probably due to less myelination of immature pathway connections. Particularly differences in the perisylvian language region were observed between children and adults in superior temporal and left inferior frontal areas. As indicated by FA, main fiber pathways that presumably participate in the language network, such as the superior longitudinal fasciculus and the inferior fronto-occipital fasciculus, were found to be left-lateralized in both groups. The SLF was fond to be particularly immature in children and, moreover, showing the largest differences between hemispheres. Comparison of functional activation revealed distinct involvement of Broca's area in children compared to adults. While adults recruited the opercular part (BA 44) of Broca's area in the IFG for sentence comprehension, children additionally recruited its triangular part (BA 45). These differences in functional organization were mirrored in a dissociation of associated fiber pathways connecting BA 44 and BA 45 to the temporal region, as indicated by activation-guided probabilistic tractography. Children apparently employed additional exchange of information via the IFO within the neural network of language processing. Presumably, the functional development of language comprehension in the human brain is supported by a broader network of white matter fiber tracts.

However, we are still away from a comprehensive understanding about the variety of underlying processes and mechanisms in the human brain that

concede language. We don't know yet the concrete mechanisms of brain maturation and language development that specifically enable humans to acquire the unique faculty of language within just a few years of ontogenesis. However, functional and structural brain imaging will certainly improve our knowledge on the brain implementation of language development. First steps have been done to gather DTI data for pediatric populations across broad age ranges and to make them available for researchers (Evans, 2006; Hermoye, et al., 2006). This will certainly help to achieve further insight in development and maturation of the human brain. An upcoming question to answer remains the causal direction of the interrelation between development of function and maturation of structure.

The work presented in this thesis specified the underlying brain mechanisms of auditory language comprehension in the developing brain. Augmented processing demands in children compared to adults are reflected in cortical activation patterns and underlying physiology within specified language areas. Although so far, no causal inferences can be drawn for the interaction of structure and function, the present studies point to the need of a joint view on development of function and maturation of structure.

7 References

Ahmad, Z., Balsamo, L. M., Sachs, B. C., Xu, B., & Gaillard, W. D. (2003). Auditory comprehension of language in young children - Neural networks identified with fMRI. *Neurology, 60*(10), 1598-1605.

Anderson, B., Southern, B. D., & Powers, R. E. (1999). Anatomic asymmetries of the posterior superior temporal lobes: A postmortem study. *Neuropsychiatry, Neuropsychology, & Behavioral Neurology, 12*(4), 247-254.

Anwander, A., Tittgemeyer, M., von Cramon, D. Y., Friederici, A. D., & Knosche, T. R. (2007). Connectivity-based parcellation of Broca's area. *Cerebral Cortex, 17*(4), 816-825.

Ashburner, J., & Friston, K. J. (2000). Voxel-Based Morphometry - The Methods. *NeuroImage, 11*(6), 805-821.

Ashburner, J., & Friston, K. J. (2001). Why Voxel-Based Morphometry Should Be Used. *NeuroImage, 14*(6), 1238-1243.

Ashtari, M., Cervellione, K. L., Hasan, K. M., Wu, J., McIlree, C., Kester, H., et al. (2007). White matter development during late adolescence in healthy males: A cross-sectional diffusion tensor imaging study. *NeuroImage, 35*(2), 501-510.

Aslin, R. N., & Schlaggar, B. L. (2006). Is myelination the precipitating neural event for language development in infants and toddlers? *Neurology, 66*(3), 304-305.

Assaf, Y., & Pasternak, O. (2008). Diffusion tensor imaging (DTI)-based white matter mapping in brain research: A review. *Journal of Molecular Neuroscience, 34*(1), 51-61.

Augustine, J. R. (1996). Circuitry and Functional Aspects of the Insular Lobe in Primates Including Humans. *Brain Research Reviews, 22*(3), 229-244.

Bahlmann, J., Schubotz, R. I., & Friederici, A. D. (2008). Hierarchical sequencing engages Broca's area. *NeuroImage, 42*, 525-534.

Balsamo, L. M., Xu, B., & Gaillard, W. D. (2006). Language lateralization and the role of the fusiform gyrus in semantic processing in young children. *NeuroImage, 31*(3), 1306-1314.

Balsamo, L. M., Xu, B., Grandin, C. B., Petrella, J. R., Braniecki, S. H., Elliott, T. K., et al. (2002). A functional magnetic resonance Imaging study of left hemisphere language dominance in children. *Archives of Neurology, 59*(7), 1168-1174.

Barnea-Goraly, N., Menon, V., Eckert, M., Tamm, L., Bammer, R., Karchemskiy, A., et al. (2005). White matter development during childhood and adolescence: A cross-sectional diffusion tensor imaging study. *Cerebral Cortex, 15*(12), 1848-1854.

Basser, P. J., Mattiello, J., & Lebihan, D. (1994). MR Diffusion Tenser Spectroscopy and Imaging. *Biophysical Journal, 66*(1), 259-267.

Beaulieu, C., & Allen, P. S. (1994). Determinants of anisotropic water diffusion in nerves. *Magnetic Resonance in Medicine, 31*(4), 394-400.

Behrens, T. E., Woolrich, M. W., Jenkinson, M., Johansen-Berg, H., Nunes, R. G., Clare, S., et al. (2003). Characterization and propagation of uncertainty in diffusion-weighted MR imaging. *Magnetic Resonance in Medicine, 50*(5), 1077-1088.

Ben-Shachar, M., Hendler, T., Kahn, I., Ben-Bashat, D., & Grodzinsky, Y. (2003). The neural reality of syntactic transformations: Evidence from functional magnetic resonance imaging. *Psychological Science, 14*(5), 433-440.

Bloch, F., Hansen, W. W., & Packard, M. (1946). The nuclear induction experiment. *Physical Review, 70*, 474-485.

Bookheimer, S. (2002). Functional MRI of language: New approaches to understanding the cortical organization of semantic processing. *Annual Review of Neuroscience, 25*, 151-188.

Bookstein, F. L. (2001). "Voxel-Based Morphometry" Should Not Be Used with Imperfectly Registered Images. *NeuroImage, 14*(6), 1454-1462.

Bornkessel, I., Zysset, S., Friederici, A. D., von Cramon, D. Y., & Schlesewsky, M. (2005). Who did what to whom? The neural basis of argument hierarchies during language comprehension. *Neuroimage, 26*(1), 221-233.

Bosch, V. (2000). Statistical analysis of multi-subject fMRI data: Assessment of focal activations. *JMRI-Journal of Magnetic Resonance Imaging, 11*(1), 61-64.

Brauer, J., & Friederici, A. D. (2007). Functional neural networks of semantic and syntactic processes in the developing brain. *Journal of Cognitive Neuroscience, 19*(10), 1609-1623.

Brauer, J., Neumann, J., & Friederici, A. D. (2008). Temporal dynamics of perisylvian activation during language processing in children and adults. *NeuroImage*.

Broca, P. (1863). Localisation des fonctions cérébrales: Siège du langage articulé. *Bulletin de la Société d' Anthropologie de Paris, 4*, 200-204.

Büchel, C., Raedler, T., Sommer, M., Sach, M., Weiller, C., & Koch, M. A. (2004). White matter asymmetry in the human brain: A diffusion tensor MRI study. *Cerebral Cortex, 14*(9), 945-951.

Buckner, R. L. (2003). The hemodynamic inverse problem: Making inferences about neural activity from measured MRI signals. *Proceedings of the National Academy of Sciences of the United States of America, 100*(5), 2177-2179.

Buckner, R. L., Bandettini, P. A., Ocraven, K. M., Savoy, R. L., Petersen, S. E., Raichle, M. E., et al. (1996). Detection of Cortical Activation During Averaged Single Trials of a Cognitive Task Using Functional Magnetic Resonance Imaging. *Proceedings of the National Academy of Sciences of the United States of America, 93*(25), 14878-14883.

Burgund, D. E., Lugar, H. M., Schlaggar, B. L., & Petersen, S. E. (2005). Task demands modulate sustained and transient neural activity during visual-matching tasks. *NeuroImage, 25*(2), 511-519.

Burock, M. A., Buckner, R. L., Woldorff, M. G., Rosen, B. R., & Dale, A. M. (1998). Randomized event-related experimental designs allow for extremely rapid presentation rates using functional MRI. *Neuroreport, 9*(16), 3735-3739.

Buxton, R. B., & Frank, L. R. (1997). A model for the coupling between cerebral blood flow and oxygen metabolism during neural stimulation. *Journal of Cerebral Blood Flow & Metabolism, 17*(1), 64-72.

Buxton, R. B., Uludag, K., Dubowitz, D. J., & Liu, T. T. (2004). Modeling the hemodynamic response to brain activation. *NeuroImage, 23*(Supplement 1), S220-S233.

Catani, M., Howard, R. J., Pajevic, S., & Jones, D. K. (2002). Virtual in vivo interactive dissection of white matter fasciculi in the human brain. *Neuroimage, 17*(1), 77-94.

CBCL (1998). *Arbeitsgruppe Deutsche Child Behavior Checklist CBCL/4-18 Elternfragebogen über das Verhalten von Kindern und Jugendlichen, Child Behavior Checklist/4-18 (CBCL/4-18, Achenbach, T.M., 1991) - German version.*

Chou, T. L., Booth, J. R., Burman, D. D., Bitan, T., Bigio, J. D., Lu, D., et al. (2006). Developmental changes in the neural correlates of semantic processing. *Neuroimage, 29*(4), 1141-1149.

Collins, D. L., Neelin, P., Peters, T. M., & Evans, A. C. (1994). Automatic 3d Intersubject Registration of Mr Volumetric Data in Standardized Talairach Space. *Journal of Computer Assisted Tomography, 18*(2), 192-205.

Conturo, T. E., Lori, N. F., Cull, T. S., Akbudak, E., Snyder, A. Z., Shimony, J. S., et al. (1999). Tracking neuronal fiber pathways in the living human brain. *Proceedings of the National Academy of Sciences of the United States of America, 96*(18), 10422-10427.

Dale, A. M., & Buckner, R. L. (1997). Selective Averaging of Rapidly Presented Individual Trials Using Fmri. *Human Brain Mapping, 5*(5), 329-340.

de Graaf-Peters, V. B., & Hadders-Algra, M. (2006). Ontogeny of the human central nervous system: What is happening when? *Early Human Development, 82*(4), 257-266.

Dehaene-Lambertz, G., Dehaene, S., Anton, J. L., Campagne, A., Ciuciu, P., Dehaene, G. P., et al. (2006). Functional segregation of cortical language areas by sentence repetition. *Human Brain Mapping, 27*(5), 360-371.

Dehaene-Lambertz, G., Dehaene, S., & Hertz-Pannier, L. (2002). Functional neuroimaging of speech perception in infants. *Science, 298*(5600), 2013-2015.

Dehaene-Lambertz, G., Hertz-Pannier, L., Dubois, J., Meriaux, S., Roche, A., Sigman, M., et al. (2006). Functional organization of perisylvian activation during presentation of sentences in preverbal infants. *Proceedings of the National Academy of Sciences of the United States of America, 103*(38), 14240-14245.

Douek, P., Turner, R., Pekar, J., Patronas, N., & Le Bihan, D. (1991). MR color mapping of myelin fiber orientation. *Journal of Computer Assisted Tomography, 15*(6), 923-929.

Dubois, J., Dehaene-Lambertz, G., Perrin, M., Mangin, J. F., Cointepas, Y., Duchesnay, E., et al. (2008). Asynchrony of the early maturation of white matter bundles in healthy infants: Quantitative landmarks revealed noninvasively by diffusion tensor imaging. *Human Brain Mapping, 29*(1), 14-27.

Dubois, J., Hertz-Pannier, L., Dehaene-Lambertz, G., Cointepas, Y., & Le Bihan, D. (2006). Assessment of the early organization and maturation of infants' cerebral white matter fiber bundles: A feasibility study using quantitative diffusion tensor imaging and tractography. *NeuroImage, 30*(4), 1121-1132.

Eckstein, K., & Friederici, A. D. (2006). It's early: Event-related potential evidence for initial interaction of syntax and prosody in speech comprehension. *Journal of Cognitive Neuroscience, 18*(10), 1696-1711.

Ellis, C. M., Simmons, A., Jones, D. K., Bland, J., Dawson, J. M., Horsfield, M. A., et al. (1999). Diffusion tensor MRI assesses corticospinal tract damage in ALS. *Neurology, 53*(5), 1051-1058.

Eluvathingal, T. J., Hasan, K. M., Kramer, L., Fletcher, J. M., & Ewing-Cobbs, L. (2007). Quantitative diffusion tensor tractography of association and projection fibers in normally developing children and adolescents. *Cerebral Cortex, 17*(12), 2760-2768.

Embick, D., Marantz, A., Miyashita, Y., O'Neil, W., & Sakai, K. L. (2000). A syntactic specialization for Broca's area. *Proceedings of the National Academy of Sciences of the United States of America, 97*(11), 6150-6154.

Evans, A. C. (2006). The NIH MRI study of normal brain development. *Neuroimage, 30*(1), 184-202.

Ferstl, E. C., Rinck, M., & von Cramon, D. Y. (2005). Emotional and temporal aspects of situation model processing during text comprehension: An event-related fMRI study. *Journal of Cognitive Neuroscience, 17*(5), 724-739.

Fiebach, C. J., Schlesewsky, M., & Friederici, A. D. (2001). Syntactic working memory and the establishment of filler-gap dependencies: Insights from ERPs and fMRI. *Journal of Psycholinguistic Research, 30*(3), 321-338.

Fiebach, C. J., & Schubotz, R. I. (2006). Dynamic anticipatory processing of hierarchical sequential events: A common role for Broca's area and ventral premotor cortex across domains? *Cortex, 42*(4), 499-502.

Fiez, J. A. (1997). Phonology, semantics, and the role of the left inferior prefrontal cortex. *Human Brain Mapping, 5*(2), 79-83.

Forman, S. D., Cohen, J. D., Fitzgerald, M., Eddy, W. F., Mintun, M. A., & Noll, D. C. (1995). Improved assessment of significant activation in functional magnetic resonance imaging (fMRI) - use of a cluster-size threshold. *Magnetic Resonance in Medicine, 33*(5), 636-647.

Frank, L. R. (2001). Anisotropy in high angular resolution diffusion-weighted MRI. *Magnetic Resonance in Medicine, 45*(6), 935-939.

Frazier, L., Carlson, K., & Clifton, C. (2006). Prosodic phrasing is central to language comprehension. *Trends in Cognitive Sciences, 10*(6), 244-249.

Friederici, A. D. (1983). Children's sensitivity to function words during sentence comprehension. *Linguistics 21*, 717-739.

Friederici, A. D. (2002). Towards a neural basis of auditory sentence processing. *Trends in Cognitive Sciences, 6*(2), 78-84.

Friederici, A. D., & Alter, K. (2004). Lateralization of auditory language functions: A dynamic dual pathway model. *Brain and Language, 89*(2), 267-276.

Friederici, A. D., Bahlmann, J., Heim, S., Schubotz, R. I., & Anwander, A. (2006). The brain differentiates human and non-human grammars: Functional localization and structural connectivity. *PNAS, 103*(7), 2458-2463.

Friederici, A. D., Fiebach, C. J., Schlesewsky, M., Bornkessel, I. D., & von Cramon, D. Y. (2006). Processing Linguistic Complexity and Grammaticality in the Left Frontal Cortex. *Cereb. Cortex*, 1709-1717.

Friederici, A. D., Meyer, M., & von Cramon, D. Y. (2000). Auditory language comprehension: An event-related fMRI study on the processing of syntactic and lexical information. *Brain & Language, 74*(2), 289-300.

Friederici, A. D., Rüschemeyer, S. A., Hahne, A., & Fiebach, C. J. (2003). The role of left inferior frontal and superior temporal cortex in sen-

tence comprehension: Localizing syntactic and semantic processes. *Cerebral Cortex, 13*(2), 170-177.

Friedrich, M., & Friederici, A. D. (2005). Semantic sentence processing reflected in the event-related potentials of one- and two-year-old children. *Neuroreport, 16*(16), 1801-1804.

Friston, K. J. (1994). Statistical parametric mapping. In R. W. Thatcher, M. Hallet, T. Zeffiro, E. R. John & M. Huerta (Eds.), *Functional neuroimaging: technical foundations* (pp. 79-93). San Diego: Academic Press.

Friston, K. J., Fletcher, P., Josephs, O., Holmes, A., Rugg, M. D., & Turner, R. (1998). Event-related fMRI: characterizing differential responses. *Neuroimage, 7*(1), 30-40.

Friston, K. J., Frith, C. D., Turner, R., & Frackowiak, R. S. J. (1995). Characterizing Evoked Hemodynamics with fMRI. *NeuroImage, 2*(2, Part 1), 157-165.

Friston, K. J., Holmes, A. P., Worsley, K. J., Poline, J. P., Frith, C. D., & Frackowiak, R. S. J. (1994). Statistical parametric maps in functional imaging: A general linear approach. *Human Brain Mapping, 2*(4), 189-210.

Friston, K. J., Holmes, A. P., Worsley, K. J., Poline, J. P., Frith, C. D., & Frackowiak, R. S. J. (1995). Statistical parametric maps in functional imaging: a general linear approach. *Human Brain Mapping, 2*, 189-210.

Friston, K. J., Williams, S., Howard, R., Frackowiak, R. S., & Turner, R. (1996). Movement-related effects in fMRI time-series. *Magnetic Resonance in Medicine, 35*(3), 346-355.

Geschwind, N., & Levitsky, W. (1968). Human brain: left-right asymmetries in temporal speech region. *Science, 161*(837), 186-187.

Gibson, E. (1998). Linguistic Complexity - Locality of Syntactic Dependencies. *Cognition, 68*(1), 1-76.

Giedd, J. N., Blumenthal, J., Jeffries, N. O., Castellanos, F. X., Liu, H., Zijdenbos, A., et al. (1999). Brain development during childhood and adolescence: a longitudinal MRI study. *Nature Neuroscience, 2*(10), 861-863.

Ginsberg, M. D., Dietrich, W. D., & Busto, R. (1987). Coupled forebrain increases of local cerebral glucose utilization and blood flow during physiologic stimulation of a somatosensory pathway in the rat: Demonstration by double-label autoradiography. *Neurology, 37*(1), 11-13.

Giorgio, A., Watkins, K. E., Douaud, G., James, A. C., James, S., De Stefano, N., et al. (2008). Changes in white matter microstructure during adolescence. *NeuroImage, 39*(1), 52-61.

Gleitman, L. R., & Wanner, E. (1982). Language acquisition: The state of the state of the art. In E. Wanner & L. R. Gleitman (Eds.), *Language acquisition: The state of the art* (pp. 3-48). Cambridge: Cambridge University Press.

Greenhouse, S. W., & Geisser, S. (1959). On methods in the analysis of profile data. *Psychometrika, 24*, 95-112.

Grodzinsky, Y., & Friederici, A. D. (2006). Neuroimaging of syntax and syntactic processing. *Current Opinion in Neurobiology, 16*(2), 240-246.

Hahne, A., Eckstein, K., & Friederici, A. D. (2004). Brain signatures of syntactic and semantic processes during children's language development. *Journal of Cognitive Neuroscience, 16*(7), 1302-1318.

Haier, R. J., Jung, R. E., Yeo, R. A., Head, K., & Alkire, M. T. (2004). Structural brain variation and general intelligence. *Neuroimage, 23*(1), 425-433.

Haller, S., Klarhoefer, M., Schwarzbach, J., Radue, E. W., & Indefrey, P. (2007). Spatial and temporal analysis of fMRI data on word and sentence reading. *European Journal of Neuroscience, 26*(7), 2074-2084.

Hallett, T., & Proctor, A. (1996). Maturation of the central nervous system as related to communication and cognitive development. *Infants & Young Children, 8*(4), 1-15.

Heim, S. C. A., & Friederici, A. D. (2003). Phonological processing in language production: time course of brain activity. *Neuroreport, 14*(16), 2031-2033.

Henson, R. N. A., Price, C. J., Rugg, M. D., Turner, R., & Friston, K. J. (2002). Detecting latency differences in event-related BOLD responses: Application to words versus nonwords and initial versus repeated face presentations. *Neuroimage, 15*(1), 83-97.

Hermoye, L., Saint-Martin, C., Cosnard, G., Lee, S.-K., Kim, J., Nassogne, M.-C., et al. (2006). Pediatric diffusion tensor imaging: Normal database and observation of the white matter maturation in early childhood. *NeuroImage, 29*(2), 493-504.

Hoen, M., Pachot-Clouard, M., Segebarth, C., & Dominey, P. F. (2006). When Broca experiences the Janus syndrome: An ER-fMRI study comparing sentence comprehension and cognitive sequence processing. *Cortex, 42*(4), 605-623.

Holcomb, P. J., Coffey, S. A., & Neville, H. J. (1992). Visual and auditory sentence processing: A developmental analysis using event-related brain potentials. *Developmental Neuropsychology, 8*(2,3), 203-241.

Homae, F., Watanabe, H., Nakano, T., Asakawa, K., & Taga, G. (2006). The right hemisphere of sleeping infant perceives sentential prosody. *Neuroscience Research, 54*(4), 276-280.

Huettel, S. A., Song, A. W., & McCarthy, G. (2005). Decisions under Uncertainty: Probabilistic Context Influences Activation of Prefrontal and Parietal Cortices. *J. Neurosci., 25*(13), 3304-3311.

Jenkinson, M., Bannister, P., Brady, M., & Smith, S. (2002). Improved optimization for the robust and accurate linear registration and motion correction of brain images. *Neuroimage, 17*(2), 825-841.

Jezzard, P., Meatthews, P. M., & Smith, S. M. (2001). *Functional MRI: An Introduction to Methods*. Oxford: Oxford University Press.

Johansen-Berg, H., Behrens, T. E. J., Robson, M. D., Drobnjak, I., Rushworth, M. F. S., Brady, J. M., et al. (2004). Changes in connectivity profiles define functionally distinct regions in human medial frontal cortex. *Proceedings of the National Academy of Sciences of the United States of America, 101*(36), 13335-13340.

Jones, D. K., & Pierpaoli, C. (2005). Confidence mapping in diffusion tensor magnetic resonance imaging tractography using a bootstrap approach. *Magnetic Resonance in Medicine, 53*(5), 1143-1149.

Jones, D. K., Symms, M. R., Cercignani, M., & Howard, R. J. (2005). The effect of filter size on VBM analyses of DT-MRI data. *NeuroImage, 26*(2), 546-554.

Josephs, O., Turner, R., & Friston, K. (1997). Event-related fMRI. *Human Brain Mapping, 5*, 243-248.

Jusczyk, P. W. (2002). How infants adapt speech-processing capacities to native-language structure. *Current Directions in Psychological Science, 11*(1), 15-18.

Kang, H. C., Burgund, E. D., Lugar, H. M., Petersen, S. E., & Schlaggar, B. L. (2003). Comparison of functional activation foci in children and adults using a common stereotactic space. *Neuroimage, 19*(1), 16-28.

Kiehl, K. A., Laurens, K. R., & Liddle, P. F. (2002). Reading Anomalous Sentences: An Event-Related fMRI Study of Semantic Processing. *NeuroImage, 17*(2), 842-850.

Klein, J. C., Behrens, T. E. J., Robson, M. D., Mackay, C. E., Higham, D. J., & Johansen-Berg, H. (2007). Connectivity-based parcellation of human cortex using diffusion MRI: Establishing reproducibility, validity and observer independence in BA 44/45 and SMA/pre-SMA. *Neuroimage, 34*(1), 204-211.

Klingler, J., & Gloor, P. (1960). The connections of the amygdala and of the anterior temporal cortex in the human brain. *Journal of Comparative Neurology, 115*, 333-369.

Koch, M. A., Norris, D. G., & Hund-Georgiadis, M. (2002). An investigation of functional and anatomical connectivity using magnetic resonance imaging. *Neuroimage, 16*(1), 241-250.

Kraus, M. F., Susmaras, T., Caughlin, B. P., Walker, C. J., Sweeney, J. A., & Little, D. M. (2007). White matter integrity and cognition in chronic traumatic brain injury: a diffusion tensor imaging study. *Brain, 130*(Part 10), 2508-2519.

Kruggel, F., & von Cramon, D. Y. (2001). Nonlinear regression analysis of the hemodynamic response in functional MRI. *Pattern Recognition Letters, 22*(11), 1247-1252.

Lange, N. (1996). Statistical approaches to human brain mapping by functional magnetic resonance imaging. *Statistics in Medicine, 15*(4), 389-428.

Lauterbur, P. C. (1973). Image formation by induced local interactions: examples employing nuclear magnetic resonance. *Nature, 242*, 190-191.

Lebel, C., Walker, L., Leemans, A., Phillips, L., & Beaulieu, C. (2008). Microstructural maturation of the human brain from childhood to adulthood. *NeuroImage, 40*(3), 1044-1055.

Levitt, M. H. (2008). *Spin Dynamics: Basics of Nuclear Magnetic Resonance* (2nd ed.). Chichester: John Wiley and Sons.

Logothetis, N. K. (2002). The neural basis of the blood-oxygen-level-dependent functional magnetic resonance imaging signal. *Philosophical Transactions of the Royal Society of London - Series B: Biological Sciences, 357*(1424), 1003-1037.

Logothetis, N. K., Pauls, J., Augath, M., Trinath, T., & Oeltermann, A. (2001). Neurophysiological investigation of the basis of the fMRI signal. *Nature, 412*(6843), 150-157.

Lohmann, G., Müller, K., Bosch, V., Mentzel, H., Hessler, S., Chen, L., et al. (2001). LIPSIA - a new software system for the evaluation of functional magnetic resonance images of the human brain. *Computerized Medical Imaging and Graphics, 25*(6), 449-457.

Madden, D. J., Whiting, W. L., Huettel, S. A., White, L. E., MacFall, J. R., & Provenzale, J. M. (2004). Diffusion tensor imaging of adult age differences in cerebral white matter: relation to response time. *Neuroimage, 21*(3), 1174-1181.

Mansfield, P. (1977). Multi-planar image formation using NMR spin echoes. *Journal of Physics C: Solid State Physics*(3), L55.

Marslen-Wilson, W. D., Tyler, L. K., Warren, P., Grenier, P., & Lee, C. S. (1992). Prosodic effects in minimal attachment. *Quarterly Journal of Experimental Psychology, 45*(1), 73-87.

McKeown, M. J., Makeig, S., Brown, G. G., Jung, T. P., Kindermann, S. S., Bell, A. J., et al. (1998). Analysis of fMRI data by blind separation into independent spatial components. *Human Brain Mapping, 6*(3), 160-188.

Menon, R. S., & Kim, S.-G. (1999). Spatial and temporal limits in cognitive neuroimaging with fMRI. *Trends in Cognitive Sciences, 3*(6), 207-216.

Menon, R. S., Luknowsky, D. C., & Gati, J. S. (1998). Mental Chronometry Using Latency-Resolved Functional Mri. *Proceedings of the National Academy of Sciences of the United States of America, 95*(18), 10902-10907.

Meyer, M., Alter, K., Friederici, A. D., Lohmann, G., & von Cramon, D. Y. (2002). FMRI reveals brain regions mediating slow prosodic modulations in spoken sentences. *Human Brain Mapping, 17*(2), 73-88.

Meyer, M., Steinhauer, K., Alter, K., Friederici, A. D., & von Cramon, D. Y. (2004). Brain activity varies with modulation of dynamic pitch variance in sentence melody. *Brain & Language, 89*(2), 277-289.

Miezin, F. M., Maccotta, L., Ollinger, J. M., Petersen, S. E., & Buckner, R. L. (2000). Characterizing the hemodynamic response: effects of presentation rate, sampling procedure, and the possibility of ordering brain activity based on relative timing. *NeuroImage, 11*(6), 735-759.

Mori, S. (2007). *Introduction to Diffusion Tensor Imaging*: Elsevier Science.

Mori, S., Crain, B. J., Chacko, V. P., & van Zijl, P. C. M. (1999). Three-dimensional tracking of axonal projections in the brain by magnetic resonance imaging. *Annals of Neurology, 45*(2), 265-269.

Mori, S., Kaufmann, W. E., Davatzikos, C., Stieltjes, B., Amodei, L., Fredericksen, K., et al. (2002). Imaging cortical association using diffusion-tensor-based tracts in the human brain axonal tracking. *Magnetic Resonance in Medicine, 47*(2), 215-223.

Mori, S., Oishi, K., Jiang, H., Jiang, L., Li, X., Akhter, K., et al. (2008). Stereotaxic white matter atlas based on diffusion tensor imaging in an ICBM template. *NeuroImage, 40*(2), 570-582.

Mori, S., & van Zijl, P. C. M. (2002). Fiber tracking: principles and strategies - a technical review. *NMR in Biomedicine, 15*(7-8), 468-480.

Mori, S., & Zhang, J. Y. (2006). Principles of diffusion tensor imaging and its applications to basic neuroscience research. *Neuron, 51*(5), 527-539.

Moro, A., Tettamanti, M., Perani, D., Donati, C., Cappa, S. F., & Fazio, F. (2001). Syntax and the brain: Disentangling grammar by selective anomalies. *Neuroimage, 13*(1), 110-118.

Moseley, M. E., Cohen, Y., Kucharczyk, J., Mintorovitch, J., Asgari, H. S., Wendland, M. F., et al. (1990). Diffusion-weighted MR imaging of anisotropic water diffusion in cat central nervous system. *Radiology, 176*(2), 439-445.

Mufson, E. J., Brady, D. R., & Kordower, J. H. (1990). Tracing neuronal connections in postmortem human hippocampal complex with the carbocyanine dye DiI. *Neurobiology of Aging, 11*(6), 649-653.

Mugler, J. P., & Brookeman, J. R. (1990). 3-dimensional magnetization-prepared rapid gradient-echo imaging (3D MP-RAGE). *Magnetic Resonance in Medicine, 15*(1), 152-157.

Müller, K., Neumann, J., Lohmann, G., Mildner, T., & von Cramon, D. Y. (2005). The correlation between blood oxygenation level-dependent signal strength and latency. *Journal of Magnetic Resonance Imaging, 21*(4), 489-494.

Muzik, O., Chugani, D. C., Juhasz, C., Shen, C. G., & Chugani, H. T. (2000). Statistical parametric mapping: Assessment of application in children. *Neuroimage, 12*(5), 538-549.

Nagy, Z., Westerberg, H., & Klingberg, T. (2004). Maturation of White Matter is Associated with the Development of Cognitive Functions during Childhood. *J. Cogn. Neurosci., 16*(7), 1227-1233.

Neumann, J., Lohmann, G., Zysset, S., & von Cramon, D. Y. (2003). Within-subject variability of BOLD response dynamics. *NeuroImage, 19*(3), 784-796.

Newman, A. J., Pancheva, R., Ozawa, K., Neville, H. J., & Ullman, M. T. (2001). An Event-Related fMRI Study of Syntactic and Semantic Violations. *Journal of Psycholinguistic Research, 30*(3), 339-364.

Newman, S. D., Just, M. A., Keller, T. A., Roth, J., & Carpenter, P. A. (2003). Differential effects of syntactic and semantic processing on the subregions of Broca's area. *Cognitive Brain Research, 16*(2), 297-307.

Ni, W., Constable, R. T., Mencl, W. E., Pugh, K. R., Fulbright, R. K., Shaywitz, S. E., et al. (2000). An event-related neuroimaging study distinguishing form and content in sentence processing. *Journal of Cognitive Neuroscience, 12*(1), 120-133.

Noppeney, U., & Price, C. J. (2004). Retrieval of abstract semantics. *Neuroimage, 22*(1), 164-170.

Norris, D. G. (2000). Reduced power multislice MDEFT imaging. *JMRI-Journal of Magnetic Resonance Imaging, 11*(4), 445-451.

Oberecker, R., & Friederici, A. D. (2006). Syntactic event-related potential components in 24-month-olds' sentence comprehension. *Neuroreport, 17*(10), 1017-1021.

Oberecker, R., Friedrich, M., & Friederici, A. D. (2005). Neural correlates of syntactic processing in two-year-olds. *Journal of Cognitive Neuroscience, 17*(10), 1667-1678.

Ogawa, S., Lee, T. M., Kay, A. R., & Tank, D. W. (1990). Brain magnetic resonance imaging with contrast dependent on blood oxygenation. *Proceedings of the National Academy of Sciences of the United States of America, 87*(24), 9868-9872.

Oldfield, R. C. (1971). The assessment and analysis of handedness: the Edinburgh inventory. *Neuropsychologia, 9*(1), 97-113.

Pajevic, S., & Pierpaoli, C. (1999). Color schemes to represent the orientation of anisotropic tissues from diffusion tensor data: Application to white matter fiber tract mapping in the human brain. *Magnetic Resonance in Medicine, 42*(3), 526-540.

Pannekamp, A., Toepel, U., Alter, K., Hahne, A., & Friederici, A. D. (2005). Prosody-driven sentence processing: An event-related brain potential study. *Journal of Cognitive Neuroscience, 17*(3), 407-421.

Pannekamp, A., Weber, C., & Friederici, A. D. (2006). Prosodic processing at the sentence level in infants. *Neuroreport, 17*(6), 675-678.

Parker, G. J. M., Luzzi, S., Alexander, D. C., Wheeler-Kingshott, C. A. M., Ciccarelli, O., & Lambon Ralph, M. A. (2005). Lateralization of ventral and dorsal auditory-language pathways in the human brain. *NeuroImage, 24*(3), 656-666.

Passingham, R. E., Stephan, K. E., & Kotter, R. (2002). The anatomical basis of functional localization in the cortex. *Nature Reviews Neuroscience, 3*(8), 606-616.

Paus, T., Zijdenbos, A., Worsley, K., Collins, D. L., Blumenthal, J., Giedd, J. N., et al. (1999). Structural maturation of neural pathways in children and adolescents: In vivo study. *Science, 283*(5409), 1908-1911.

Persson, J., Nyberg, L., Lind, J., Larsson, A., Nilsson, L. G., Ingvar, M., et al. (2006). Structure-function correlates of cognitive decline in aging. *Cerebral Cortex, 16*(7), 907-915.

Pierpaoli, C., & Basser, P. J. (1996). Toward a quantitative assessment of diffusion anisotropy. *Magnetic Resonance in Medicine, 36*(6), 893-906.

Pinker, S. (1984). *Language Learnability and Language Development*. Cambrige, MA: Harvard University Press.

Plante, E., Creusere, M., & Sabin, C. (2002). Dissociating sentential prosody from sentence processing: Activation interacts with task demands. *Neuroimage, 17*(1), 401-410.

Powell, H. W. R., Parker, G. J. M., Alexander, D. C., Symms, M. R., Boulby, P. A., Wheeler-Kingshott, C. A. M., et al. (2006). Hemispheric asymmetries in language-related pathways: A combined functional MPI and tractography study. *Neuroimage, 32*(1), 388-399.

Provenzale, J. M., Liang, L., DeLong, D., & White, L. E. (2007). Diffusion tensor imaging assessment of brain white matter maturation during the first postnatal year. *American Journal of Roentgenology, 189*(2), 476-486.

Pujol, J., Soriano-Mas, C., Ortiz, H., Sebastian-Galles, N., Losilla, J. M., & Deus, J. (2006). Myelination of language-related areas in the developing brain. *Neurology, 66*(3), 339-343.

Purcell, E. M., Torrey, H. C., & Pound, R. V. (1946). Resonance absorbtion by nuclear magnetic moments in a solid. *Physical Review, 69*, 37-38.

Raettig, T., & Kotz, S. A. (2008). Auditory processing of different types of pseudo-words: An event-related fMRI study. *Neuroimage, 39*(3), 1420-1428.

Raichle, M. E., Arthur, W. T., & John, C. M. (2000). A Brief History of Human Functional Brain Mapping *Brain Mapping: The Systems* (pp. 33-75). San Diego: Academic Press.

Reese, T. G., Heid, O., Weisskoff, R. M., & Wedeen, V. J. (2003). Reduction of eddy-current-induced distortion in diffusion MRI using a twice-refocused spin echo. *Magnetic Resonance in Medicine, 49*(1), 177-182.

Richter, W., Andersen, P. M., Georgopoulos, A. P., & Kim, S. G. (1997). Sequential activity in human motor areas during a delayed cued finger movement task studied by time-resolved fMRI. *Neuroreport, 8*(5), 1257-1261.

Rilling, J. K., Glasser, M. F., Preuss, T. M., Ma, X. Y., Zhao, T. J., Hu, X. P., et al. (2008). The evolution of the arcuate fasciculus revealed with comparative DTI. *Nature Neuroscience, 11*(4), 426-428.

Rüschemeyer, S. A., Fiebach, C. J., Kempe, V., & Friederici, A. D. (2005). Processing lexical semantic and syntactic information in first and second language: fMRI evidence from German and Russian. *Human Brain Mapping, 25*(2), 266-286.

Sachs, B. C., & Gaillard, W. D. (2003). Organization of language networks in children: functional magnetic resonance imaging studies. *Current Neurology & Neuroscience Reports, 3*(2), 157-162.

Savoy, R. L., Bandettini, P. A., O'Craven, K. M., Kwong, K. K., Davis, T. L., Baker, J. R., et al. (1995). *Pushing the Temporal Resolution of fMRI: Studies of Very Brief Visual Stimuli, Onset Variability and Asynchrony, and Stimulus-Correlated Changes in Noise.* Paper presented at the Annual Meeting of the Society of Magnetic Resonance, Nice, France.

Schmahmann, J. D., Pandya, D. N., Wang, R., Dai, G., D'Arceuil, H. E., de Crespigny, A. J., et al. (2007). Association fibre pathways of the brain: parallel observations from diffusion spectrum imaging and autoradiography. *Brain, 130*(Part 3), 630-653.

Scott, S. K. (2005). Auditory processing - speech, space and auditory objects. *Current Opinion in Neurobiology, 15*(2), 197-201.

Shaffer, J. P. (1995). Multiple Hypothesis Testing. *Annual Review of Psychology, 46*(1), 561-584.

Sigman, M., Jobert, A., LeBihan, D., & Dehaene, S. (2007). Parsing a sequence of brain activations at psychological times using fMRI. *NeuroImage, 35*(2), 655-668.

Smith, S. M., Jenkinson, M., Johansen-Berg, H., Rueckert, D., Nichols, T. E., Mackay, C. E., et al. (2006). Tract-based spatial statistics: Voxelwise analysis of multi-subject diffusion data. *NeuroImage, 31*(4), 1487-1505.

Smith, S. M., Jenkinson, M., Woolrich, M. W., Beckmann, C. F., Behrens, T. E. J., Johansen-Berg, H., et al. (2004). Advances in functional and structural MR image analysis and implementation as FSL. *NeuroImage, 23*(Suppl 1), S208-S219.

Snow, D., & Balog, H. L. (2002). Do children produce the melody before the words? A review of developmental intonation research. *Lingua, 112*(12), 1025-1058.

Song, A. W., Wong, E. C., Tan, S. G., & Hyde, J. S. (1996). Diffusion weighted fMRI at 1.5 T. *Magnetic Resonance in Medicine, 35*(2), 155-158.

Song, S. K., Sun, S. W., Ramsbottom, M. J., Chang, C., Russell, J., & Cross, A. H. (2002). Dysmyelination revealed through MRI as increased radial (but unchanged axial) diffusion of water. *Neuroimage, 17*(3), 1429-1436.

Sotak, C. H. (2002). The role of diffusion tensor imaging in the evaluation of ischemic brain injury - a review. *NMR in Biomedicine, 15*(7-8), 561-569.

Sowell, E. R., Peterson, B. S., Thompson, P. M., Welcome, S. E., Henkenius, A. L., & Toga, A. W. (2003). Mapping cortical change across the human life span. *Nature Neuroscience, 6*(3), 309-315.

Sowell, E. R., Thompson, P. M., Holmes, C. J., Jernigan, T. L., & Toga, A. W. (1999). In vivo evidence for post-adolescent brain maturation in frontal and striatal regions. *Nature Neuroscience, 2*(10), 859-861.

Sowell, E. R., Thompson, P. M., Leonard, C. M., Welcome, S. E., Kan, E., & Toga, A. W. (2004). Longitudinal mapping of cortical thickness and brain growth in normal children. *Journal of Neuroscience, 24*(38), 8223-8231.

Staudt, M., Krageloh-Mann, I., & Grodd, W. (2000). Normal myelination of the child brain on MRI - A Meta-analysis. *Rofo, Fortschritte auf dem Gebiete der Rontgenstrahlen und der Neuen Bildgebenden Verfahren. 172*(10), 802-811.

Stromswold, K., Caplan, D., Alpert, N., & Rauch, S. (1996). Localization of syntactic comprehension by positron emission tomography. *Brain & Language, 52*(3), 452-473.

Talairach, J., & Tournoux, P. (1988). *Co-planar stereotactic atlas of the human brain.* New York: Thieme.

Terajima, K., Matsuzawa, H., Tanaka, K., Nishizawa, M., & Nakada, T. (2007). Cell-oriented analysis in vivo using diffusion tensor imaging for normal-appearing brain tissue in multiple sclerosis. *Neuroimage, 37*(4), 1278-1285.

Thierry, G., Ibarrola, D., Demonet, J. F., & Cardebat, D. (2003). Demand on verbal working memory delays haemodynamic response in the inferior prefrontal cortex. *Human Brain Mapping, 19*(1), 37-46.

Thirion, J. P. (1998). Image matching as a diffusion process: an analogy with Maxwell's demons. *Medical Image Analysis, 2*(3), 243-260.

Thompson-Schill, S. L., D'Esposito, M., Aguirre, G. K., & Farah, M. J. (1997). Role of left inferior prefrontal cortex in retrieval of semantic knowledge - a reevaluation. *Proceedings of the National Academy of Sciences of the United States of America, 94*(26), 14792-14797.

Tittgemeyer, M., & von Cramon, D. Y. (2004). Morphometry using magnetic resonance imaging. Present results. *Nervenarzt, 75*(12), 1172-1178.

Toga, A. W., Thompson, P. M., & Sowell, E. R. (2006). Mapping brain maturation. *Trends in Neurosciences, 29*(3), 148-159.

Tournier, J. D., Calamante, F., Gadian, D. G., & Connelly, A. (2004). Direct estimation of the fiber orientation density function from diffusion-weighted MRI data using spherical deconvolution. *NeuroImage, 23*(3), 1176-1185.

Tuch, D. S., Reese, T. G., Wiegell, M. R., & Van, J. W. (2003). Diffusion MRI of Complex Neural Architecture. *Neuron, 40*(5), 885-895.

Turner, R., Le Bihan, D., Maier, J., Vavrek, R., Hedges, L. K., & Pekar, J. (1990). Echo-planar imaging of intravoxel incoherent motion. *Radiology, 177*(2), 407-414.

Tyler, L. K., & Marslen-Wilson, W. D. (1981). Children's processing of spoken language. *Journal of Verbal Learning and Verbal Behavior, 20*, 400-416.

Ugurbil, K., Garwood, M., Ellermann, J., Hendrich, K., Hinke, R., Hu, X. P., et al. (1993). Imaging at high magnetic fields - initial experiences at 4-t. *Magnetic Resonance Quarterly, 9*(4), 259-277.

Ullman, M. T. (2006). Is Broca's area part of a basal ganglia thalamocortical circuit? *Cortex, 42*(4), 480-485.

Ulualp, S. O., Biswal, B. B., Yetkin, F. Z., & Kidder, T. M. (1998). Functional magnetic resonance imaging of auditory cortex in children. *Laryngoscope, 108*(12), 1782-1786.

Ulug, A. M., Beauchamp, N., Bryan, R. N., & Vanzijl, P. C. M. (1997). Absolute Quantitation of Diffusion Constants in Human Stroke. *Stroke, 28*(3), 483-490.

Vazquez, A. L., Cohen, E. R., Gulani, V., Hernandez-Garcia, L., Zheng, Y., Lee, G. R., et al. (2006). Vascular dynamics and BOLD fMRI: CBF

level effects and analysis considerations. *NeuroImage, 32*(4), 1642-1655.

Vlaardingerbroek, M. T., & den Boer, J. A. (2002). *Magnetic Resonance Imaging: Theory and Praxis* (3rd ed.). New York, NY: Springer.

Warren, P., Grabe, E., & Nolan, F. (1995). Prosody, phonology, and parsing in closure ambiguities. *Language and Cognitive Processes, 10*, 457-486.

Wartenburger, I., Steinbrink, J., Telkemeyer, S., Friedrich, M., Friederici, A. D., & Obrig, H. (2007). The processing of prosody: Evidence of interhemispheric specialization at the age of four. *NeuroImage, 34*(1), 416-425.

Watkins, K. E., Vargha-Khadem, F., Ashburner, J., Passingham, R. E., Connelly, A., Friston, K. J., et al. (2002). MRI analysis of an inherited speech and language disorder: structural brain abnormalities. *Brain, 125*(3), 465-478.

Wedeen, V. J., Hagmann, P., Tseng, W.-Y. I., Reese, T. G., & Weisskoff, R. M. (2005). Mapping complex tissue architecture with diffusion spectrum magnetic resonance imaging. *Magnetic Resonance in Medicine, 54*(6), 1377-1386.

Weissenborn, J., & Höhle, B. (2001). *Approaches to Bootstrapping: Phonological, Lexical, Syntactic, and Neurophysiological Aspects of Early Language Acquisition* (Vol. 1,2). Amsterdam: Benjamins.

Wernicke, C. (1874). *Der aphasische Symptomencomplex. Eine psychologische Studie auf anatomischer Basis.* Breslau: Cohn und Weigert.

Whitford, T. J., Rennie, C. J., Grieve, S. M., Clark, C. R., Gordon, E., & Williams, L. M. (2007). Brain maturation in adolescence: Concurrent changes in neuroanatomy and neurophysiology. *Human Brain Mapping, 28*(3), 228-237.

Wilke, M., Lidzba, K., Staudt, M., Buchenau, K., Grodd, W., & Krageloh-Mann, I. (2005). Comprehensive language mapping in children, using functional magnetic resonance imaging: what's missing counts. *Neuroreport, 16*(9), 915-919.

Wise, R. J. S., Greene, J., Buchel, C., & Scott, S. K. (1999). Brain regions involved in articulation. *Lancet, 353*(9158), 1057-1061.

Worsley, K. J., & Friston, K. J. (1995). Analysis of fMRI time-series revisited - again. *Neuroimage, 2*, 173-181.

Worsley, K. J., Liao, C. H., Aston, J., Petre, V., Duncan, G. H., Morales, F., et al. (2002). A General Statistical Analysis for fMRI Data. *NeuroImage, 15*(1), 1-15.

Zatorre, R. J., Belin, P., & Penhune, V. B. (2002). Structure and function of auditory cortex: music and speech. *Trends in Cognitive Sciences, 6*(1), 37-46.

Zhang, J., Evans, A., Hermoye, L., Lee, S.-K., Wakana, S., Zhang, W., et al. (2007). Evidence of slow maturation of the superior longitudinal fasciculus in early childhood by diffusion tensor imaging. *NeuroImage, 38*(2), 239-247.

Curriculum Vitae

Name	Jens Brauer
Date of Birth	20. 03. 1973
Place of Birth	Jena

Education

since 2004	PhD Student at Max Planck Institute for Human Cognitive and Brain Sciences, Leipzig
1999 – 2004	Psychology (Diploma), Friedrich Schiller University Jena

Selbständigkeitserklärung

Hiermit erkläre ich, daß die vorliegende Arbeit ohne unzulässige Hilfe und ohne Verwendung anderer als der angegebenen Hilfsmittel angefertigt wurde und daß die aus fremden Quellen direkt oder indirekt übernommenen Gedanken in der Arbeit als solche kenntlich gemacht worden sind.

Jens Brauer

Leipzig, den 12.06.2008

Bibliographic details

Jens Brauer

"Functional development and structural maturation in the brain's neural network underlying language comprehension"

University of Leipzig, Doctoral thesis

147 pages, 211 references, 18 figures, 12 tables

Abstract

The present thesis investigated language processing from a neurocognitive and neuroanatomical point of view. The focus of research was on how the unique faculty of language is implemented in the developing human brain. By means of functional brain imaging (fMRI), auditory language comprehension was investigated with a focus on syntactic and semantic processing. A deeper insight in functional processes was gained by the examination of temporal hemodynamics of the brain response during language processing. Moreover, functional activation patterns were distinguished on the basis of their underlying pathway connections within the language network. To this end, diffusion-weighted MRI was utilized for an inspection of the white matter fiber bundles within the perisylvian language region.

In adults and preschool children, processing of auditorily presented sentences was observed in perisylvian areas, particularly the superior temporal gyrus (STG) and the inferior frontal gyrus (IFG) bilaterally. Children, however, showed broader recruitment and less specification in their activation pattern. They used to activate the entire perisylvian network. Only in Broca's area within the IFG, specific activation was observed in children for syntactic processing. Adults, conversely, segregated semantic and syntactic processes in the deep left frontal operculum (FO) within the IFG and by characteristic accentuations of activation within subregions of the STG. The broader activation in children suggests higher processing demands and less linguistic specification in the developing language system.

For a deeper insight in the neurophysiologic mechanisms underlying functional processing, the blood-oxygenation dependent (BOLD) response was examined more profoundly. Specifically, temporal hemodynamic properties of the BOLD time course in the brain's language areas were examined. In general, children and adults generated similar hemodynamic response patterns with fastest responses in the mid-portion of the STG around Heschl's gyrus and longer latencies in anterior and posterior directions. However, compared to adults children showed overall longer latencies. Particularly their left inferior frontal activation was delayed. Longer latencies of the hemodynamic response in children and particularly in the left IFG correspond to functional processing differences between groups. They promote the view of a specific role of the left IFG in language processing.

Inferior frontal and superior temporal areas within the perisylvian region are connected via underlying neural pathways which complement the white matter underpinnings of the language network. These fiber tracts were investigated by diffusion tensor imaging (DTI). Direct comparison revealed differences in fractional anisotropy (FA) between adults and children. FA is a measure of water diffusion and provides information on fiber integrity and strength. Children showed lower values of FA in superior temporal, left inferior frontal, and further regions. Lower FA results probably from less myelination in the immature white matter. Especially the superior longitudinal fasciculus (SLF) in the perisylvian region was not yet fully matured in preschool children. Moreover, by means of functionally guided tractography, children were found to rely on a broader basis of connections within the language network. While adults activated Brodmann's area (BA) 44 within the IFG during language comprehension that connect to the STG predominantly via the SLF, children recruited additionally BA 45 in a region that is connected to the STG via an inferior fronto-temporal interlobule connection. That is, the functional development of language comprehension in the human brain is supported by a broader network of white matter fiber tracts.

The work presented in this thesis specified the underlying brain mechanisms of auditory language comprehension in the developing brain. Augmented processing demands in children compared to adults are reflected in cortical activation patterns and underlying physiology within specified

language areas. Although so far, no causal inferences can be drawn for the interaction of structure and function, the present studies point to the need of a joint view on development of function and maturation of structure.

Zusammenfassung

Die vorliegende Dissertation erforschte Sprachverabeitung aus neurokognitiver und neuroanatomischer Sicht. Der Fokus der Forschung lag darauf, wie die einzigartige Sprachfähigkeit des Menschen im sich entwickelnden menschlichen Gehirn implementiert wird. Anhand funktioneller Magnetresonanztomographie (fMRT) wurde auditives Sprachverstehen mit dem Hauptaugenmerk auf syntaktischen und semantischen Prozessen nachgegangen. Ein tieferer Einblick in die funktionellen Verarbeitungsprozesse wurde durch die eingehende Untersuchung der zeitlichen Hämodynamik der kortikalen Hirnreaktion auf Sprachverarbeitung gewonnen. Außerdem wurden funktionelle Aktivierungsmuster anhand ihrer zugrundeliegenden neuronalen Verschaltung innerhalb des Sprachnetzwerkes unterschieden. Zu diesem Zweck wurde diffusionsgwichtete Bidgebung zur Untersuchung neuronaler Faserbündel innerhalb der sprachrelevanten perisylvischen Hirnregion verwendet. Sowohl Erwachsene als auch Vorschulkinder zeigten bilaterale Aktivierung in perisylvischen Hirnarealen während der Verarbeitung auditorisch dargebotener Sätze, insbesondere im Gyrus temporalis superior (STG) und im Gyrus frontalis inferior (IFG). Kinder jedoch zeigten ausgedehntere Aktivität sowie geringere Spezifizierung in ihrem Aktivierungsmuster. Sie rekrutierten stattdessen das gesamte perisylvische Netzwerk, unabhängig vom speziellen syntaktischen oder semantischen Anforderungskontext. Nur im Brocareal innerhalb des IFG wurde spezifische Aktivierung bei Kindern für Syntaxverarbeitung beobachtet. Erwachsene unterschieden hingegen syntaktische von semantischen Prozessen im linken frontalen Operkulum (FO) innerhalb des IFG sowie durch charakteristische Akzentuierung der Aktivierung in Subregionen des STG. Die ausgedehntere Aktivierung bei Kindern spricht für höhere Prozessanforderungen und weniger linguistische Spezifikation im sich entwickelnden neuronalen Sprachnetzwerk. Für einen tieferen Einblick in die zugrundeliegenden Mechanismen funktioneller hirnphysiologischer Prozesse wurde eine eingehendere Analyse der blood oxygenation level dependent response (BOLD) vorgenommen. Speziell wurden zeitliche hämodynamische Eigen-

schaften des BOLD Zeitverlaufes in den sprachrelevanten Hirnarealen überprüft. Grundsätzlich wurden bei Kindern und Erwachsenen ähnliche hämodynamische Reaktionsmuster beobachtet mit früher Aktivierung im mittleren Anteil des STG um Heschl's Gyrus herum sowie längeren Latenzen in anterioren und posterioren Richtungen. Jedoch zeigten Kinder verglichen mit Erwachsenen insgesamt längere Latenz. Besonders auffällig war ihre Verzögerung links inferior-frontaler Aktivierung. Längere Latenzen der hemodynamischen Antwort bei Kindern besonders im linken IFG spricht für funktionelle Verarbeitungsunterschiede zwischen den Gruppen. Sie unterstützen die Annahme einer spezifischen Rolle des linken IFG bei der Sprachverabeitung.

Inferior-frontale und superior-temporale Areale innerhalb der perisylvischen Hirnregion sind über zugrundeliegende neuronale Faserverbindungen miteinander verbunden, die das Fundament des Sprachnetzwerkes ausmachen. Diese Faserbündel wurden durch Diffusionstensorbildgebung (DTI) nachgeforscht. Ein direkter statistischer Vergleich deckte Unterschiede hinsichtlich der fraktionalen Anisotropie (FA) zwischen Erwachsenen und Kindern auf. FA ist ein Maß für Wasserdiffusionsprozesse und gibt Auskunft über Faservollständigkeit und Faserstärke. Kinder zeigten niedrigere FA-Werte in superior-temporalen und links inferior-frontalen sowie in weiteren Hirnregionen. Niedrigere FA-Werte resultieren vermutlich aus geringerer Myelinisierung der noch nicht vollständig ausgereiften weißen Substanz bei Kindern. Besonders gilt das für den Fasciculus longitudinalis superior (SLF). Des Weiteren wurde eine traktographische Analyse auf Grundlage der funktionellen Aktivierungsdaten durchgeführt. Hier zeigte sich, dass die Sprachverarbeitung bei Kindern auf eine ausgedehntere Grundlage der Verbindungen innerhalb des Sprachennetzes zu bauen. Während Erwachsene das Brodmann-Areal (BA) 44 innerhalb der IFG während des Sprachverarbeitung aktivierten, das hauptsächlich über den SLF mit dem STG verbunden ist, wurde bei Kindern zusätzlich BA 45 mit einbezogen, das zum STG über eine inferiore fronto-temporale Verbindung angebunden ist. Das heißt, die funktionelle Entwicklung des Sprachverständnisses im menschlichen Gehirn wird durch ein ausgedehnteres Netzwerk an Faserverbindungen innerhalb der weißen Substanz unterstützt.

Die experimentellen Ergebnisse, die in dieser Dissertation dargestellt wurden, spezifizierten zugrundeliegende Mechanismen des auditiven Sprachverständnisses im sich entwickelnden Gehirn. Höhere Prozesskosten bei Kindern im Vergleich zu Erwachsenen werden in kortikalen Aktivierungsmustern und in der zugrundeliegenden Hirnphysiologie innerhalb spezifischer sprachverarbeitender Hirnareale reflektiert. Obgleich bis jetzt keine kausalen Schlußfolgerungen für die Interaktion von Struktur und Funktion gezogen werden können, deuten die vorliegenden Untersuchungen auf die Notwendigkeit einer gemeinsamen Sicht auf funktionelle Entwicklung und strukturelle Reifung hin.

MPI Series in Human Cognitive and Brain Sciences:

1 Anja Hahne
Charakteristika syntaktischer und semantischer Prozesse bei der auditiv Sprachverarbeitung: Evidenz aus ereigniskorrelierten Potentialstudien

2 Ricarda Schubotz
Erinnern kurzer Zeitdauern: Behaviorale und neurophysiologische Korrelate einer Arbeitsgedächtnisfunktion

3 Volker Bosch
Das Halten von Information im Arbeitsgedächtnis: Dissoziationen langsamer corticaler Potentiale

4 Jorge Jovicich
An investigation of the use of Gradient- and Spin-Echo (GRASE) imaging for functional MRI of the human brain

5 Rosemary C. Dymond
Spatial Specificity and Temporal Accuracy in Functional Magnetic Resonance Investigations

6 Stefan Zysset
Eine experimentalpsychologische Studie zu Gedächtnisabrufprozessen unter Verwendung der funktionellen Magnetresonanztomographie

7 Ulrich Hartmann
Ein mechanisches Finite-Elemente-Modell des menschlichen Kopfes

8 Bertram Opitz
Funktionelle Neuroanatomie der Verarbeitung einfacher und komplexer akustischer Reize: Integration haemodynamischer und elektrophysiologischer Maße

9 Gisela Müller-Plath
Formale Modellierung visueller Suchstrategien mit Anwendungen bei der Lokalisation von Hirnfunktionen und in der Diagnostik von Aufmerksamkeitsstörungen

10 Thomas Jacobsen
Characteristics of processing morphological structural and inherent case in language comprehension

11 Stefan Kölsch
Brain and Music
A contribution to the investigation of central auditory processing with a new electrophysiological approach

12 Stefan Frisch
Verb-Argument-Struktur, Kasus und thematische Interpretation beim Sprachverstehen

13 Markus Ullsperger
The role of retrieval inhibition in directed forgetting – an event-related brain potential analysis

14 Martin Koch
Measurement of the Self-Diffusion Tensor of Water in the Human Brain

15 Axel Hutt
Methoden zur Untersuchung der Dynamik raumzeitlicher Signale

16 Frithjof Kruggel
Detektion und Quantifizierung von Hirnaktivität mit der funktionellen Magnetresonanztomographie

17 Anja Dove
Lokalisierung an internen Kontrollprozessen beteiligter Hirngebiete mithilfe des Aufgabenwechselparadigmas und der ereigniskorrelierten funktionellen Magnetresonanztomographie

18 Karsten Steinhauer
Hirnphysiologische Korrelate prosodischer Satzverarbeitung bei gesprochener und geschriebener Sprache

19 Silke Urban
Verbinformationen im Satzverstehen

20 Katja Werheid
Implizites Sequenzlernen bei Morbus Parkinson

21 Doreen Nessler
Is it Memory or Illusion? Electrophysiological Characteristics of True and False Recognition

22 Christoph Herrmann
Die Bedeutung von 40-Hz-Oszillationen für kognitive Prozesse

23 Christian Fiebach
Working Memory and Syntax during Sentence Processing.
A neurocognitive investigation with event-related brain potentials and functional magnetic resonance imaging

24 Grit Hein
Lokalisation von Doppelaufgabendefiziten bei gesunden älteren Personen und neurologischen Patienten

25 Monica de Filippis
Die visuelle Verarbeitung unbeachteter Wörter.
Ein elektrophysiologischer Ansatz

26 Ulrich Müller
Die katecholaminerge Modulation präfrontaler kognitiver Funktionen beim Menschen

27 Kristina Uhl
Kontrollfunktion des Arbeitsgedächtnisses über interferierende Information

28 Ina Bornkessel
The Argument Dependency Model: A Neurocognitive Approach to Incremental Interpretation

29 Sonja Lattner
Neurophysiologische Untersuchungen zur auditorischen Verarbeitung von Stimminformationen

30 Christin Grünewald
Die Rolle motorischer Schemata bei der Objektrepräsentation: Untersuchungen mit funktioneller Magnetresonanztomographie

31 Annett Schirmer
Emotional Speech Perception: Electrophysiological Insights into the Processing of Emotional Prosody and Word Valence in Men and Women

32 André J. Szameitat
Die Funktionalität des lateral-präfrontalen Cortex für die Verarbeitung von Doppelaufgaben

33 Susanne Wagner
Verbales Arbeitsgedächtnis und die Verarbeitung ambiger Wörter in Wort- und Satzkontexten

34 Sophie Manthey
Hirn und Handlung: Untersuchung der Handlungsrepräsentation im ventralen prämotorischen Cortex mit Hilfe der funktionellen Magnet-Resonanz-Tomographie

35 Stefan Heim
Towards a Common Neural Network Model of Language Production and Comprehension: fMRI Evidence for the Processing of Phonological and Syntactic Information in Single Words

36 Claudia Friedrich
Prosody and spoken word recognition: Behavioral and ERP correlates

37 Ulrike Lex
Sprachlateralisierung bei Rechts- und Linkshändern mit funktioneller Magnetresonanztomographie

38 Thomas Arnold
Computergestützte Befundung klinischer Elektroenzephalogramme

39 Carsten H. Wolters
Influence of Tissue Conductivity Inhomogeneity and Anisotropy on EEG/MEG based Source Localization in the Human Brain

40 Ansgar Hantsch
Fisch oder Karpfen? Lexikale Aktivierung von Benennungsalternative bei der Objektbenennung

41 Peggy Bungert
Zentralnervöse Verarbeitung akustischer Informationen
Signalidentifikation, Signallateralisation und zeitgebundene Informationsverarbeitung bei Patienten mit erworbenen Hirnschädigungen

42 Daniel Senkowski
Neuronal correlates of selective attention: An investigation of electro-physiological brain responses in the EEG and MEG

43 Gert Wollny
Analysis of Changes in Temporal Series of Medical Images

44 Angelika Wolf
Sprachverstehen mit Cochlea-Implantat: EKP-Studien mit postlingual ertaubten erwachsenen CI-Trägern

45 Kirsten G. Volz
Brain correlates of uncertain decisions: Types and degrees of uncertainty

46 Hagen Huttner
Magnetresonanztomographische Untersuchungen über die anatomische Variabilität des Frontallappens des menschlichen Großhirns

47 Dirk Köster
Morphology and Spoken Word Comprehension: Electrophysiological Investigations of Internal Compound Structure

48 Claudia A. Hruska
Einflüsse kontextueller und prosodischer Informationen in der auditorischen Satzverarbeitung: Untersuchungen mit ereigniskorrelierten Hirnpotentialen

49 Hannes Ruge
Eine Analyse des raum-zeitlichen Musters neuronaler Aktivierung im Aufgabenwechselparadigma zur Untersuchung handlungssteuernder Prozesse

50 Ricarda I. Schubotz
Human premotor cortex: Beyond motor performance

51 Clemens von Zerssen
Bewusstes Erinnern und falsches Wiedererkennen:
Eine funktionelle MRT Studie neuroanatomischer Gedächtniskorrelate

52 Christiane Weber
Rhythm is gonna get you.
Electrophysiological markers of rhythmic processing in infants with and without risk for Specific Language Impairment (SLI)

53 Marc Schönwiesner
Functional Mapping of Basic Acoustic Parameters in the Human Central Auditory System

54 Katja Fiehler
Temporospatial characteristics of error correction

55 Britta Stolterfoht
Processing Word Order Variations and Ellipses: The Interplay of Syntax and Information Structure during Sentence Comprehension

56 Claudia Danielmeier
Neuronale Grundlagen der Interferenz zwischen Handlung und visueller Wahrnehmung

57 Margret Hund-Georgiadis
Die Organisation von Sprache und ihre Reorganisation bei ausgewählten, neurologischen Erkrankungen gemessen mit funktioneller Magnetresonanztomographie – Einflüsse von Händigkeit, Läsion, Performanz und Perfusion

58 Jutta L. Mueller
Mechanisms of auditory sentence comprehension in first and second language: An electrophysiological miniature grammar study

59 Franziska Biedermann
Auditorische Diskriminationsleistungen nach unilateralen Läsionen im Di- und Telenzephalon

60 Shirley-Ann Rüschemeyer
The Processing of Lexical Semantic and Syntactic Information in Spoken Sentences: Neuroimaging and Behavioral Studies of Native and Non-Native Speakers

61 Kerstin Leuckefeld
The Development of Argument Processing Mechanisms in German.
An Electrophysiological Investigation with School-Aged Children and Adults

62 Axel Christian Kühn
Bestimmung der Lateralisierung von Sprachprozessen unter besondere Berücksichtigung des temporalen Cortex, gemessen mit fMRT

63 Ann Pannekamp
Prosodische Informationsverarbeitung bei normalsprachlichem und deviantem Satzmaterial: Untersuchungen mit ereigniskorrelierten Hirnpotentialen

64 Jan Derrfuß
Functional specialization in the lateral frontal cortex: The role of the inferior frontal junction in cognitive control

65 Andrea Mona Philipp
The cognitive representation of tasks
Exploring the role of response modalities using the task-switching paradigm

66 Ulrike Toepel
Contrastive Topic and Focus Information in Discourse – Prosodic Realisation and Electrophysiological Brain Correlates

67 Karsten Müller
Die Anwendung von Spektral- und Waveletanalyse zur Untersuchung der Dynamik von BOLD-Zeitreihen verschiedener Hirnareale

68 Sonja A.Kotz
The role of the basal ganglia in auditory language processing: Evidence from ERP lesion studies and functional neuroimaging

69 Sonja Rossi
The role of proficiency in syntactic second language processing: Evidence from event-related brain potentials in German and Italian

70 Birte U. Forstmann
Behavioral and neural correlates of endogenous control processes in task switching

71 Silke Paulmann
Electrophysiological Evidence on the Processing of Emotional Prosody: Insights from Healthy and Patient Populations

72 Matthias L. Schroeter
Enlightening the Brain – Optical Imaging in Cognitive Neuroscience

73 Julia Reinholz
Interhemispheric interaction in object- and word-related visual areas

74 Evelyn C. Ferstl
The Functional Neuroanatomy of Text Comprehension

75 Miriam Gade
Aufgabeninhibition als Mechanismus der Konfliktreduktion zwischen Aufgabenrepräsentationen

76 Juliane Hofmann
Phonological, Morphological, and Semantic Aspects of Grammatical Gender Processing in German

77 Petra Augurzky
Attaching Relative Clauses in German – The Role of Implicit and Explicit Prosody in Sentence Processing

78 Uta Wolfensteller
Habituelle und arbiträre sensomotorische Verknüpfungen im lateralen prämotorischen Kortex des Menschen

79 Päivi Sivonen
Event-related brain activation in speech perception: From sensory to cognitive processes

80 Yun Nan
Music phrase structure perception: the neural basis, the effects of acculturation and musical training

81 Katrin Schulze
Neural Correlates of Working Memory for Verbal and Tonal Stimuli in Nonmusicians and Musicians With and Without Absolute Pitch

82 Korinna Eckstein
Interaktion von Syntax und Prosodie beim Sprachverstehen: Untersuchungen anhand ereigniskorrelierter Hirnpotentiale

83 Florian Th. Siebörger
Funktionelle Neuroanatomie des Textverstehens: Kohärenzbildung bei Witzen und anderen ungewöhnlichen Texten

84 Diana Böttger
Aktivität im Gamma-Frequenzbereich des EEG: Einfluss demographischer Faktoren und kognitiver Korrelate

85 Jörg Bahlmann
Neural correlates of the processing of linear and hierarchical artificial grammar rules: Electrophysiological and neuroimaging studies

86 Jan Zwickel
Specific Interference Effects Between Temporally Overlapping Action and Perception

87 Markus Ullsperger
Functional Neuroanatomy of Performance Monitoring: fMRI, ERP, and Patient Studies

88 Susanne Dietrich
Vom Brüllen zum Wort – MRT-Studien zur kognitiven Verarbeitung emotionaler Vokalisationen

89 Maren Schmidt-Kassow
What's Beat got to do with ist? The Influence of Meter on Syntactic Processing: ERP Evidence from Healthy and Patient populations

90 Monika Lück
Die Verarbeitung morphologisch komplexer Wörter bei Kindern im Schulalter: Neurophysiologische Korrelate der Entwicklung

91 Diana P. Szameitat
Perzeption und akustische Eigenschaften von Emotionen in menschlichem Lachen

92 Beate Sabisch
Mechanisms of auditory sentence comprehension in children with specific language impairment and children with developmental dyslexia:
A neurophysiological investigation

93 Regine Oberecker
Grammatikverarbeitung im Kindesalter: EKP-Studien zum auditorischen Satzverstehen

94 Şükrü Barış Demiral
Incremental Argument Interpretation in Turkish Sentence Comprehension

95 Henning Holle
The Comprehension of Co-Speech Iconic Gestures: Behavioral, Electrophysiological and Neuroimaging Studies

96 Marcel Braß
Das inferior frontale Kreuzungsareal und seine Rolle bei der kognitiven Kontrolle unseres Verhaltens

97 Anna S. Hasting
Syntax in a blink: Early and automatic processing of syntactic rules as revealed by event-related brain potentials

98 Sebastian Jentschke
Neural Correlates of Processing Syntax in Music and Language – Influences of Development, Musical Training and Language Impairment

99 Amelie Mahlstedt
The Acquisition of Case marking Information as a Cue to Argument Interpretation in German
An Electrophysiological Investigation with Pre-school Children

100 Nikolaus Steinbeis
Investigating the meaning of music using EEG and fMRI

101 Tilmann A. Klein
Learning from errors: Genetic evidence for a central role of dopamine in human performance monitoring

102 Franziska Maria Korb
Die funktionelle Spezialisierung des lateralen präfrontalen Cortex: Untersuchungen mittels funktioneller Magnetre sonanztomographie

103 Sonja Fleischhauer
Neuronale Verarbeitung emotionaler Prosodie und Syntax: die Rolle des verbalen Arbeitsgedächtnisses

104 Friederike Sophie Haupt
The component mapping problem: An investigation of grammatical function reanalysis in differing experimental contexts using event-related brain potentials